

**DYNAMIC MODELLING OF A  
HIGH RATE ANAEROBIC WASTEWATER  
TREATMENT PROCESS:**

**A PROGRESS REPORT**

**C. C. I. W.  
LIBRARY**

**R.M. Jones**

**February, 1989**

**WTC-BIO-01-1989**

## **REVIEW NOTICE**

### **DYNAMIC MODELLING OF A HIGH RATE ANAEROBIC WASTEWATER TREATMENT PROCESS: A PROGRESS REPORT**

by

**R.M. Jones**

**Environment Canada  
Conservation and Protection  
Wastewater Technology Centre**

**February 1989**

**Report WTC-BIO-01-89**

This report has been reviewed for technical content by Conservation and Protection, Environmental Protection Directorate, Technology Development and Technical Services Branch. It has been approved for distribution in the Unpublished Manuscript Series. Approval does not necessarily signify that the contents reflect the views and policies of the Environmental Protection Directorate. Mention of trade names or commercial products does not constitute recommendation or endorsement for use.

This unedited version is undergoing a limited distribution to transfer the information to people working in related studies. This distribution is not intended to signify publication and, if the report is referenced, the author should cite it an unpublished report of the Wastewater Technology Centre.

Any comments concerning its content should be directed to:

**H. Melcer  
Environment Canada  
Conservation and Protection  
Wastewater Technology Centre  
867 Lakeshore Road  
P.O. Box 5050  
Burlington, Ontario L7R 4A6**

## ABSTRACT

A pilot scale anaerobic hybrid (HYBRID) reactor was operated to investigate the dynamic behaviour of the process. Step changes in feedrate and feed concentration and pseudo-random binary sequences (PRBS) of feedrate changes were implemented to generate dynamic responses. Instantaneous changes in organic loading rate during step testing ranged from 7 to 15 kg COD/m<sup>3</sup>.d. During PRBS experiments, the reactor hydraulic retention time (HRT) was changed between 2 and 0.8 days with a constant feed concentration. Steady state data was generated between dynamic experiments.

Process responses investigated were effluent filtered COD (FCOD), volatile acid concentrations and methane production rates. Two mechanistic models were evaluated. A transfer function-noise model was identified for the gas production response to feedrate changes.

The methane production rate was observed to be the most sensitive of the variables studied following changes in feedrate and feed strength. The response of methane production was rapid, displaying a time constant in the range of 0.5 to 1.5 hours. The effluent propionic acid concentration was more sensitive to changes in loading conditions than the other measured effluent variables. The agreement between steady state plant data and predictions by both mechanistic models was reasonably good, although some model inadequacies were found at the highest loading rate studied. Both mechanistic models were found to be adequate in describing the dynamic response characteristics of effluent volatile acids and FCOD, although the same inadequacies discovered during steady state modelling were apparent. The more structured four population mechanistic model was superior in predicting the rapid response in methane production.

## **ACKNOWLEDGEMENTS**

Funding for this study is being provided by Environment Canada, the Federal Panel on Energy R&D (PERD), and the MOSST Biotechnology Fund.

## TABLE OF CONTENTS

	PAGE
ABSTRACT	i
ACKNOWLEDGEMENTS	ii
LIST OF FIGURES	v
LIST OF TABLES	vii
1. INTRODUCTION	1
2. LITERATURE REVIEW	3
2.1 Microbiology	3
2.1.1 Biochemical Stages	3
2.1.2 The Role of Hydrogen	6
2.2 Process Modelling	8
2.3 Process Control	18
2.4 State Estimation	21
3. DYNAMIC MODELLING	24
3.1 Introduction	24
3.2 Two Population Model	25
3.3 Four Population Model	28
3.4 Computational Methods	39
4. EXPERIMENTAL EQUIPMENT AND PROCEDURES	40
4.1 Pilot Plant Facilities	40
4.2 Wastewater Characteristics, Collection and Storage	43
4.3 Reactor Start Up	43
4.4 Experimental Design	44
4.5 Sampling and Analysis	47

## TABLE OF CONTENTS (continued)

	PAGE
5. EXPERIMENTAL RESULTS AND DISCUSSION	48
5.1 Reactor Start Up and Operation	48
5.2 Mechanistic Modelling of Steady State Operation	53
5.3 Dynamic Operating Results	65
5.4 Mechanistic Modelling of Dynamic Operation	73
6. SUMMARY AND CONCLUSIONS	85
7. RECOMMENDATIONS	87
8. REFERENCES	88
APPENDIX I      Example of Calculation of Four Population Model Yield Coefficients From ATP Production	94
APPENDIX II     Computer Listing of Two Population Model	96
APPENDIX III    Computer Listing of Four Population Model	105
APPENDIX IV     Modelling Nomenclature	116

## LIST OF FIGURES

FIGURE		PAGE
2.1	Schematic representation of the anaerobic decomposition of organic matter	4
2.2	Hydrogen regulated metabolic pathways inside the acid-forming bacteria	7
2.3	Oxidation-reduction reaction of the NAD carrier molecule	7
2.4	Thermodynamic favourability of reactions of acetogenic bacteria, acetoclastic methanogens, hydrogen-utilizing methanogens, and sulfur-reducing bacteria	9
2.5	Schematic of simplified models of anaerobic decomposition based on two groups of bacterial species	12
4.1	Schematic of the anaerobic pilot plant	42
5.1	Sequence of events in operation of the anaerobic pilot plant	49
5.2	Feed COD concentration for the HYBRID pilot plant	50
5.3	HRT for the HYBRID pilot plant	50
5.4	Empty bed volumetric loading rates for the HYBRID pilot plant	51
5.5	Effluent total volatile acid concentrations for the HYBRID pilot plant	51
5.6	COD removal efficiency of the HYBRID pilot plant	52
5.7	Biogas production of the HYBRID pilot plant	52
5.8	Total bed volatile solids in the HYBRID reactor	55
5.9	Measured and predicted steady state effluent FCOD	60
5.10	Measured and predicted steady state CH <sub>4</sub> production	60

# LIST OF FIGURES (continued)

FIGURE		PAGE
5.11	Measured and predicted steady state effluent total volatile acids	61
5.12	Measured and predicted steady state effluent acetic acid	61
5.13	Measured and predicted steady state effluent propionic acid	62
5.14	Measured and predicted steady state effluent butyric acid	62
5.15	Predicted steady state gas phase hydrogen concentration	64
5.16	PRBS feedrate experiment used to build a model for biogas flow using time series analysis	71
5.17	Measured and predicted response of effluent FCOD to feed step #3	75
5.18	Measured and predicted response of methane production rate to feed step #3	75
5.19	Measured and predicted responses of effluent volatile acid concentrations to feed step #3	77
5.20	Measured and predicted response of effluent FCOD to concentration step #2	78
5.21	Measured and predicted response of methane production rate to concentration step #2	78
5.22	Measured and predicted responses of effluent volatile acid concentrations to concentration step #2	79
5.23	Predicted response of gas phase hydrogen concentration to feed step #3	82
5.24	Predicted response of gas phase hydrogen concentration to concentration step #2	82
5.25	PRBS feedrate experiment used to verify 4 population model (Model 2) and transfer function model biogas predictions	83



## LIST OF TABLES

TABLE		PAGE
4.1	List of Process Variables Measured On-line	41
4.2	Summary of Step Testing Experimental Conditions	45
4.3	Steady State Operating Conditions	46
5.1	Cumulative Operating Data	54
5.2	Two Population Model Parameter Values	56
5.3	Four Population Model Parameter Values	58
5.4	Summary of Characteristics of HYBRID Response During Step Testing	66
5.5	Initial and Final COD Removal Efficiencies During Concentration Step Tests	68
5.6	Transfer Function - Noise Model of Gas production Response to Feedrate Changes	72
5.7	Summary of Characteristics of Dynamic Response of HYBRID to Feed Step #3 and Concentration Step #2 as Predicted by Two Population Model and Four Population Model	74
IV-1	TWO POPULATION MODEL NOMENCLATURE	117
IV-2	FOUR POPULATION MODEL NOMENCLATURE	118

## 1. INTRODUCTION

Advanced high rate anaerobic processes provide an economically attractive alternative for the treatment of concentrated industrial wastewaters. However, when applied to industrial effluents, treatment plants can be subject to highly variable hydraulic, organic and toxic loadings. To ensure continuous, trouble-free performance, an anaerobic process must be operated to minimize negative effects of these variations on the anaerobic microorganisms. The development of the necessary operational and process control strategies is hampered by a lack of understanding of dynamic process behaviour and by the limited availability of sensors for the on-line measurement of important process variables.

Mechanistic dynamic model development for the anaerobic process can benefit plant operation in a number of ways. The development of models can lead to an improved understanding of the phenomena governing the dynamic behaviour of the process. Simulations performed with dynamic models can be used to investigate potential operational and control strategies. Techniques are available in which dynamic models can use signals from existing sensors to provide on-line estimates of other process variables. Although a number of mechanistic models of anaerobic processes have previously been developed, few model verification studies have been conducted.

This report summarizes the results from the first phase of a study in which automated monitoring and control strategies are being developed for anaerobic treatment systems. In this phase, a pilot scale anaerobic hybrid

(HYBRID) reactor was operated at Environment Canada's Wastewater Technology Centre in Burlington, Ontario. The HYBRID was operated to investigate the dynamic behaviour of the process and to generate data for dynamic modelling.

The specific objectives of this phase of the study were as follows:

- 1) Assess the dynamic response characteristics of the HYBRID reactor under conditions of changing influent concentration and feedrate;
- 2) Compile a set of mechanistic dynamic models which could have application in on-line estimation and process control in high rate anaerobic processes;
- 3) Evaluate and compare the adequacy of the models in describing the steady state and dynamic behaviour of the HYBRID process; and,
- 4) Comment on the applicability of the models for on-line estimation and control.

## 2. LITERATURE REVIEW

Since mechanistic mathematical models of the anaerobic treatment process must represent some portion of the reactions and bacterial interactions occurring in such a system, the present knowledge of these reactions and pathways is summarized. Next, an overview of the development of mechanistic mathematical models is presented. Control strategies which have been proposed or demonstrated for anaerobic treatment processes and the use of on-line estimation techniques to observe states which are not reliably measured on-line are also reviewed. This review emphasizes both the importance of an understanding of the dynamic process behaviour and shows the potential for direct application of an appropriate mechanistic model.

### 2.1 Microbiology

#### 2.1.1 Biochemical Stages

The anaerobic digestion process consists of a complex series of reactions which result from the metabolic processes of several different groups of bacteria living in a symbiotic association. The sum of these energy yielding reactions is the conversion of a wide variety of organic substrate materials into methane and carbon dioxide.

The present state of knowledge of the anaerobic decomposition of organic matter is illustrated in Figure 2.1 (McInerney et. al., 1979; Price, 1985; Harper and Pohland, 1986). The first step in the process is the hydrolysis of large organic molecules by extracellular enzymes. Carbohydrates are hydrolysed to mono-saccharides; fats are hydrolysed to glycerol and fatty acids; proteins are hydrolysed to amino acids. The next stage in the sequence is the degradation of the products of the hydrolysis stage predominantly into hydrogen, carbon dioxide, and short chain (volatile) fatty acids consisting primarily of acetic acid, propionic

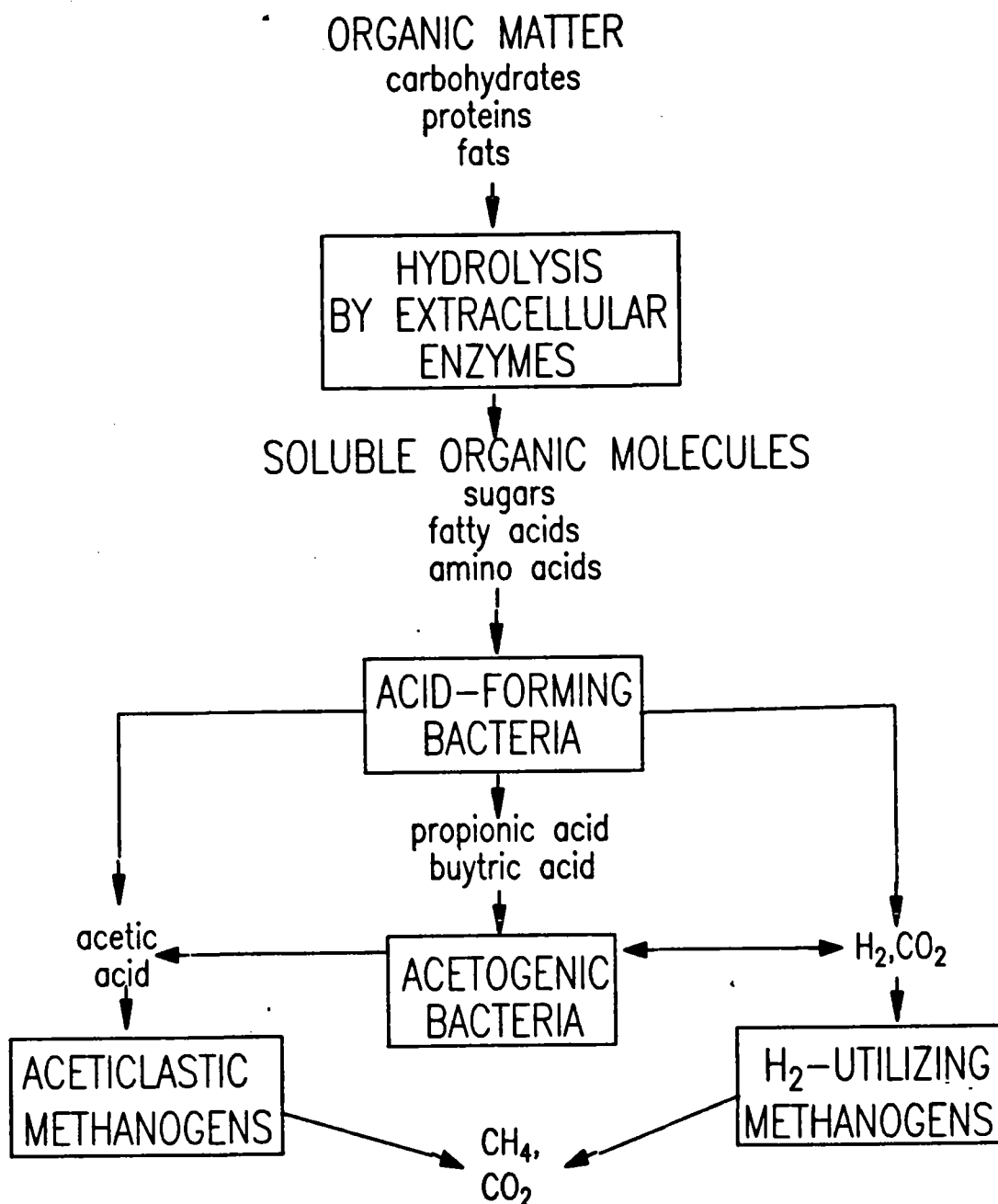


Figure 2.1

Schematic representation of the anaerobic decomposition of organic matter

acid and butyric acid. This stage is mediated by a group of bacteria often collectively referred to as the acid-forming bacteria.

The propionic and longer chain fatty acids produced in the acid-forming stage are degraded to acetic acid, carbon dioxide and hydrogen by a group of bacterial species called the hydrogen producing acetogens (McInerney et. al., 1979). Another group of bacteria referred to as the homoacetogens may metabolize carbon dioxide and hydrogen and produce acetic acid. However, their role in the anaerobic digestion process is not clear (Zeikus, 1979).

In the final stages of the reaction sequence, acetoclastic methanogens produce methane and carbon dioxide from acetic acid. This reaction is thought to produce 65-70% of the methane from the process (McInerney et. al., 1979). Methane is also produced from hydrogen and carbon dioxide by hydrogen utilizing methanogens. The specific substrates utilized vary between species of methanogens. For example, *Methanotherix soehngeni* utilizes acetic acid only, *Methanosarcina barkeri* utilizes acetic acid as well as hydrogen and carbon dioxide, and *Methanobacterium* utilizes hydrogen and carbon dioxide only (Harper and Pohland, 1986).

Sulfate-reducing bacteria can also occur in the anaerobic digestion process and compete with the previously mentioned bacterial populations for carbon and hydrogen. The result can be a reduction in methane production due to the reduced availability of methanogenic substrates (Price, 1985).

The need to maintain a balance between all bacterial populations in the anaerobic digestion process in order to maximize waste stabilization has long been recognized (McCarty, 1964). Methanogenesis has normally been thought to be the overall rate-limiting step in the treatment of soluble wastewaters and many studies have been conducted in which volatile fatty

acid accumulations have been observed during overloading or process stress (Barnes et. al., 1984; Guiot and van den Berg, 1984; Stover et. al., 1985; Kennedy et. al., 1985; Eng et. al., 1986). It is only recently, however, that the role hydrogen plays in the accumulation of intermediate products has been recognized.

### 2.1.2 The Role of Hydrogen

The most detailed illustration of the role of hydrogen in regulating the formation of acetic, propionic and butyric acids has been described for the degradation of glucose via the Embden-Meyerhof pathway (Mosey, 1983). This metabolic pathway is used by the acid-forming bacteria to obtain energy from the conversion of glucose to volatile fatty acids.

The Embden-Meyerhof pathway is shown in Figure 2.2. Hydrogen regulates the conversion process by throttling reactions at several points in the pathway. Reactions at points A and B proceed with a transfer of electrons (hydrogen) to the oxidized form of the NAD (nicotinamide-adenine dinucleotide) carrier molecule ( $\text{NAD}^+$ ). For these reactions to proceed continuously, the NADH produced must eventually be re-oxidized to  $\text{NAD}^+$ . This occurs through the reduction of protons to form hydrogen gas (Figure 2.3). The hydrogen gas is normally removed by hydrogen-utilizing methanogens and sulfate-reducing bacteria. If hydrogen gas is allowed to accumulate, the equilibrium of the oxidation-reduction reaction which regenerates  $\text{NAD}^+$  moves in a direction which reduces the amount of  $\text{NAD}^+$  available at points A and B, slowing the reactions at these points. With the subsequent increase in NADH, the rates of the reactions at points C and D increase, resulting in a diversion of intermediates to propionic and butyric acids.

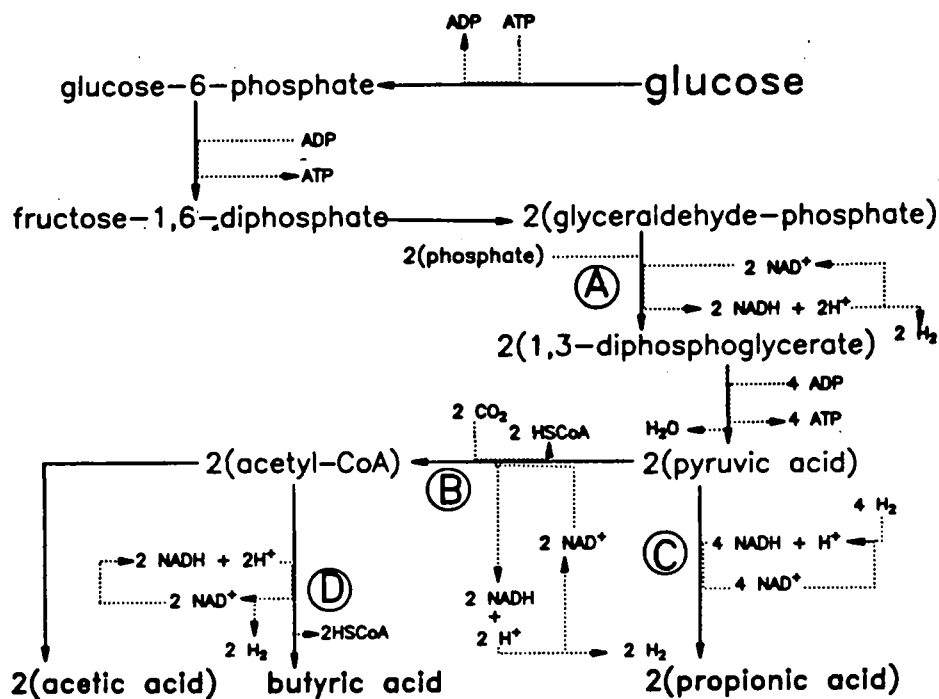


Figure 2.2 Hydrogen regulated metabolic pathways inside the acid-forming bacteria (Mosey, 1983)

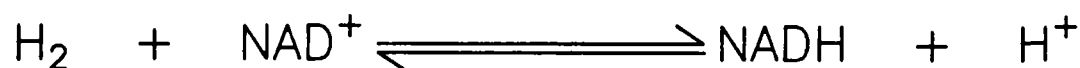


Figure 2.3 Oxidation-reduction reaction of the NAD carrier molecule



The effects of hydrogen on the hydrogen-producing acetogens, the hydrogen-utilizing methanogens and the sulfate-reducing bacteria have been expressed in terms of the hydrogen-dependent thermodynamic favourabilities of the reactions (Harper and Pohland, 1986). These relationships, which have been reproduced in Figure 2.4, are based on the assumptions of equilibrium of gas phase hydrogen with the liquid phase, free transport of dissolved molecular hydrogen across the cell membrane, and constant concentrations of other reactants in the system. It can be seen that the conversions of propionic (1) and butyric (2) acids to acetic acid by the hydrogen-producing acetogens becomes less favourable with increasing hydrogen concentrations. Also, above a certain hydrogen concentration, methane production from hydrogen and carbon dioxide (3) becomes more favourable than methane production from acetic acid (4), which is important since some methanogenic bacterial species can switch substrates. Acetate utilization by sulfate-reducing bacteria (5) is favoured over acetate utilization by methanogens at all hydrogen partial pressures.

The effects of hydrogen when other pathways are involved in the process (ie: when compounds other than glucose are being degraded) have not been illustrated mechanistically. However, experimentation by several researchers has shown similar hydrogen effects when more complex organic materials have been degraded. Harper and Pohland (1986) have reviewed these studies.

## 2.2 Process Modelling

In this overview of the major historical developments in mechanistic modelling of anaerobic treatment processes, the discussion is structured to outline the pathways considered by the particular models, the state variables predicted, and the kinetic expressions used to describe

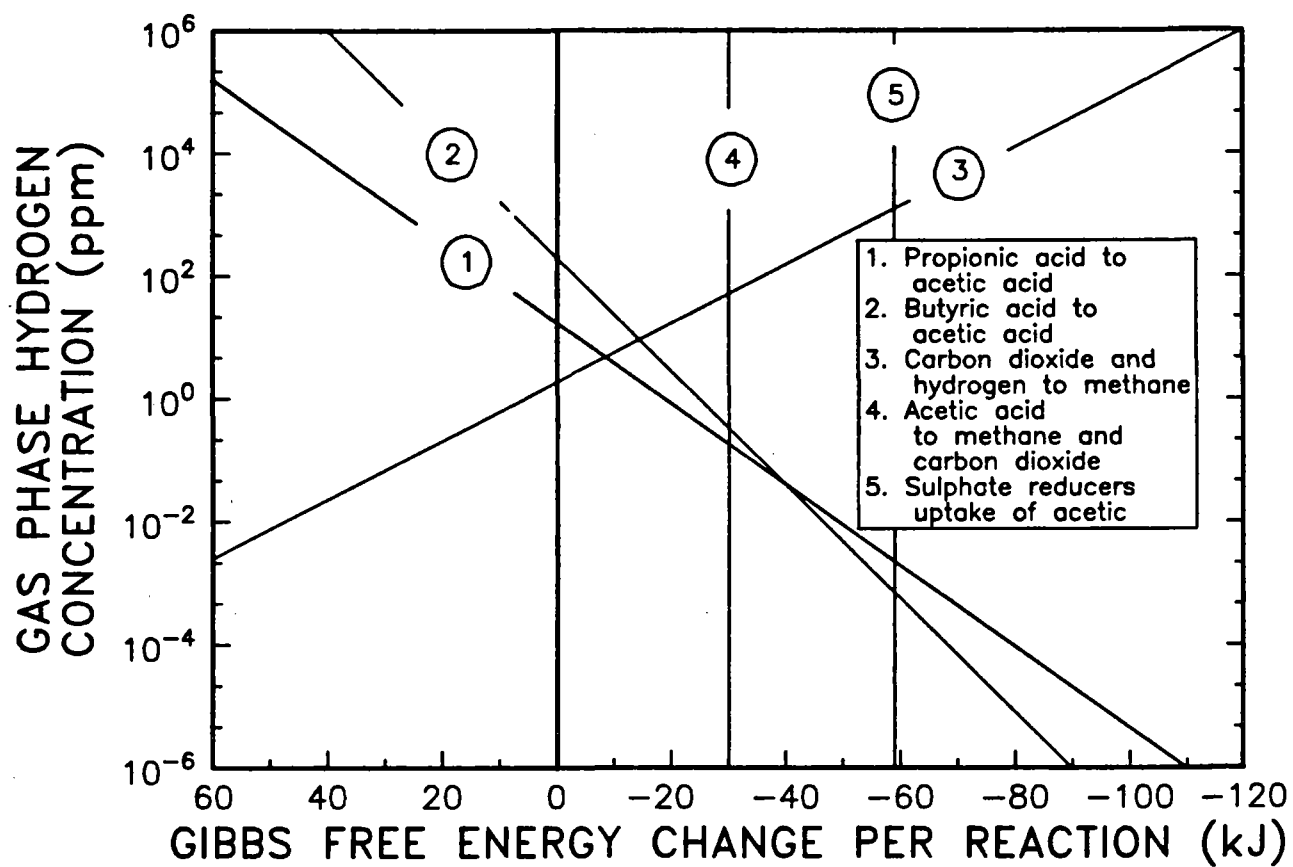


Figure 2.4 Thermodynamic favourability of reactions of acetogenic bacteria, aceticlastic methanogens, hydrogen-utilizing methanogens, and sulfur-reducing bacteria (Harper and Pohland, 1986)

biological growth and substrate utilization. The concluding paragraphs of the section discuss possible improvements to the latest mechanistic models and present some considerations which would be relevant when modelling high rate systems.

Andrews (1969) developed the first mathematical model for a continuous flow, complete-mixed anaerobic digestion process. The model included only one biological reaction for the conversion of acetic acid to methane and carbon dioxide. The justification for this simplification was that the methanogens have much lower growth rates than acid-forming bacteria, and thus the methane-producing reactions could be considered the overall rate-limiting step.

The Andrews model was comprised of dynamic mass balances for two state variables - the effluent concentrations of acetic acid and bacterial solids. The kinetics for bacterial growth and substrate utilization were described by a Monod relationship to which an inhibition term had been added. The total pool of undissociated volatile acids, expressed as acetic acid, was considered to be the growth-limiting substrate. The inhibition term described the inhibitory effect of the undissociated volatile acids at high concentrations.

The original model was subsequently extended by Andrews and Graef (1971) by incorporating interactions between volatile acids, pH, alkalinity, gas production rate and gas composition. The structure of the model which defined these interactions formed the basis for most of the later models of anaerobic treatment processes. Material balances were included for substrate, bacterial solids, dissolved carbon dioxide, cations, and gas phase carbon dioxide. Methane production was predicted as a growth related by-product and the pH was determined from equilibrium and charge balance relationships of the carbon dioxide-bicarbonate buffering

system. Values of the parameters in the model were taken from the literature or were estimated from appropriate stoichiometric relationships. Simulation studies were conducted to predict the course of reactor failure from hydraulic or organic overloading.

Later models of the anaerobic digestion process considered the kinetics of the acid-forming groups of bacteria in addition to the methanogens. In the dual-microbial community models based on the structure illustrated in Figure 2.5, complex organics in the influent were first converted to simple soluble organics by extra-cellular enzymes of the acid-forming bacteria. The acid-formers then converted the soluble organics to a product assumed to be representable by a single volatile fatty acid. In the last step, methanogenic bacteria converted this volatile acid to methane and carbon dioxide.

The first mechanistic model to include kinetics for both acid-forming and methanogenic bacteria was developed by Ghosh and Pohland (1974). A set of steady state equations was developed for a continuous flow, complete-mixed digester fed with a glucose substrate. The equations predicted steady state reactor concentrations of glucose, volatile acids and biomass. The steady state gas production rate was also predicted from a mass balance equation. The growth rates of the acid-formers and methane-formers were described by a Monod equation. No kinetic inhibition functions were included. The model was calibrated using data from laboratory scale digesters. This data showed that the maximum specific growth rate of the acid-formers was significantly higher than that of the methanogens, indicating that methane generation appeared to be the rate-limiting step in the stabilization of soluble wastes.

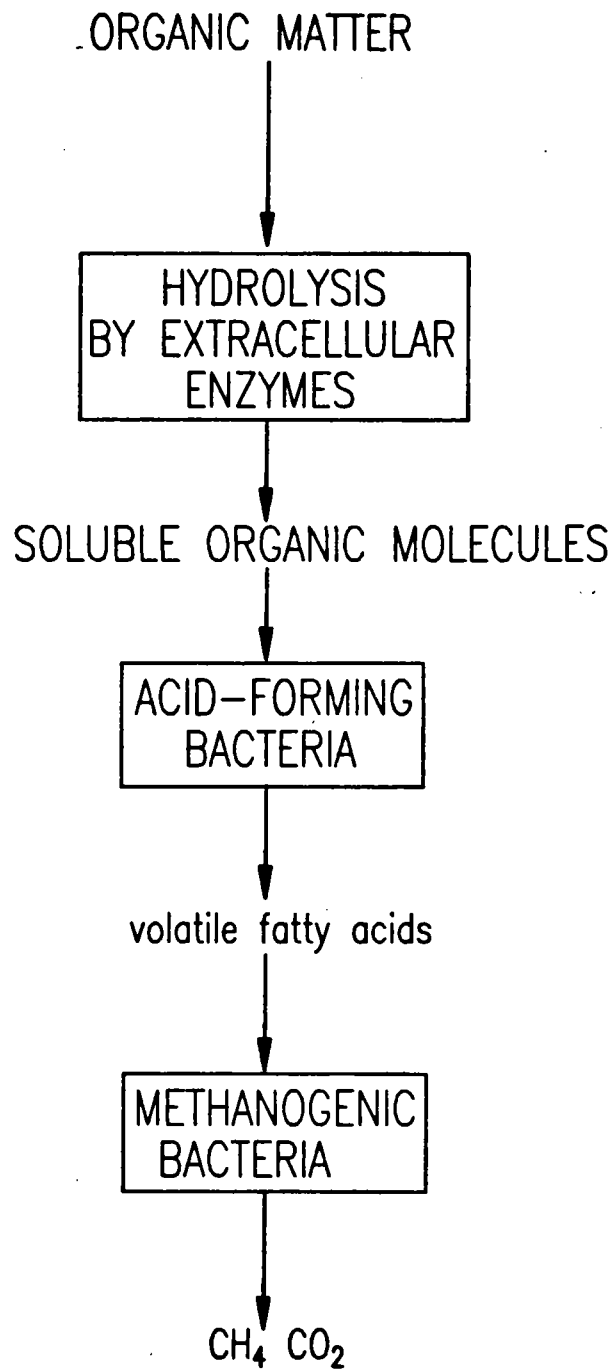


Figure 2.5

Schematic of simplified models of anaerobic decomposition based on two groups of bacterial species.

The first comprehensive dual microbial dynamic model was developed by Hill and Barth (1977). This model was similar in structure to the model of Andrews and Graef in that the interactions between the gas, liquid and biological phases of the reactor were considered. The state variables included were insoluble organic matter, soluble organics, volatile acids, acid-forming bacteria, methanogenic bacteria, dissolved carbon dioxide, gas phase carbon dioxide, cation concentration and ammonium concentration. Methane production and pH were predicted in the same way as the Andrews and Graef model. The kinetics of substrate utilization and growth were described by growth and inhibition functions in which soluble organics and un-ionized volatile acids were the growth limiting substrates for the acid-formers and methanogens respectively. The acid-formers were inhibited by undissociated volatile acids and the methanogens were inhibited by undissociated volatile acids and ammonia.

A major advantage of the Hill and Barth model over the simpler, single bacterial models was that simulations could be carried out for digesters fed with an actual wastewater containing both soluble and insoluble fractions, instead of a simplified synthetic waste consisting of a single volatile acid. The model was calibrated using literature parameter values and was verified qualitatively using data from laboratory scale digesters fed with animal waste. The model was able to predict process responses such as the accumulation of volatile acids during start-up.

The most recent theoretical models for the anaerobic digestion process are based on the four groups of bacteria and the sequence of reactions illustrated in Figure 2.1. The earliest attempts at incorporating the additional reaction sequences into a dynamic model relied on the addition of an inhibition term to the Monod growth and substrate utilization kinetics of the methanogenic bacteria (Sinechal et. al., 1979; Halme

et. al., 1984). Inhibition was assumed to increase with increasing concentrations of propionic and butyric acids.

Heyes and Hall (1981) developed one of the first dynamic models to more directly incorporate the four population reaction sequence. The effects of hydrogen on the conversion of propionate and butyrate to acetate was incorporated through a free energy availability factor based on the concentration of hydrogen in the gas phase. The free energy available for the breakdown of propionate and butyrate was calculated and compared to the free energy required for the production of one mole of ATP per mole of reaction. If insufficient free energy was available, the relevant reaction would be inhibited, with the inhibition being modelled as linearly increasing with decreasing available free energy. The uninhibited growth and substrate utilization kinetics were based on a Monod function. Heyes and Hall disputed the validity of undissociated volatile acid inhibition functions, and instead proposed a pH inhibition factor for the methanogens. The model did not include a relationship between the concentration of hydrogen and the distribution of volatile acids formed from glucose.

Another approach to incorporating the effects of hydrogen concentration into the four population reaction sequence was developed by Mosey (1983). This model was based on the conversion of glucose to organic acid through the Embden-Meyerhof pathway. Kinetic equations were presented for the rate of uptake of glucose by acid-forming bacteria, the rate of uptake of propionic and butyric acids by hydrogen-producing acetogenic bacteria, the rate of uptake of acetic acid by aceticlastic methanogens, and the rate of uptake of hydrogen by hydrogen-utilizing methanogens. The unregulated rates were expressed by Monod models. The overall rate of uptake of glucose and the rates of formation and degradation of propionate and butyrate were regulated by the relative availabilities of the reduced

(NADH) and oxidised forms ( $\text{NAD}^+$ ) of the NAD carrier molecule. The oxidation-reduction reaction of NAD and hydrogen was used to relate the oxidation state of the NAD carrier to the concentration of hydrogen in the digester gas. Regulation functions were then formulated in terms of gas phase hydrogen concentration.

Rozzi et. al. (1985) incorporated Mosey's kinetic equations into a comprehensive model which considered the interactions between the gas, liquid and biological phases of the reactor in a manner similar to earlier models (ie: Hill and Barth; Andrews and Graef). The model was developed to represent an anaerobic contact process. State variables estimated by the model included reactor concentrations of glucose, acetic acid, propionic acid, butyric acid, cations and dissolved  $\text{CO}_2$ , and the gas phase concentration of hydrogen. The gas phase  $\text{CO}_2$  was assumed to be in equilibrium with the dissolved  $\text{CO}_2$ .

This model represents the most advanced stage of development of dynamic models of anaerobic treatment processes. Further improvements could involve the incorporation of better knowledge of the metabolic pathways of the microorganisms. The ability of some methanogenic organisms to switch from carbon dioxide and hydrogen substrates to an acetic acid substrate, the effects of sulfate-reducers, and the degradation mechanisms of non-carbohydrate substrates have not been included in models described to date.

All of the models discussed to this point were developed assuming an ideal continuous stirred tank reactor (CSTR). In all of these systems, with the exception of that modelled by Rozzi et. al. (1985), the hydraulic retention time (HRT) and the bacterial solids retention time (SRT) were equal. In high rate anaerobic process designs, a variety of techniques are employed to retain the bacterial solids in the system so that HRTs can be



manipulated independently of the SRTs. The result is that much lower HRTs can be achieved than those necessary to prevent the wash-out of bacterial solids in conventional sludge digesters. In the anaerobic contact process modelled by Rozzi et. al., solids were assumed to be recycled back to a CSTR from a settler in order to maintain a constant SRT. Other designs may use media which allow the development of an attached biofilm, or they may rely on the development of granules of bacterial solids having a high settling velocity. In any case, such designs may affect the mixing and mass transfer characteristics of the reactor, subsequently affecting the dynamic response. In fixed film processes, large gradients of substrates and products within the biofilm can make it difficult to model process behaviour by considering effluent characteristics alone (McCarty and Smith, 1986). Even in conventional sludge digesters, mixing and mass transfer considerations could be important. In a dynamic study of a full scale sludge digester, Beck (1986) deduced that an instantaneous increase in digester gas production after feeding was largely due to the physical agitation of the digester contents and not to an increase in biological activity.

Several authors have incorporated the results of fluid-flow pattern studies in high rate anaerobic reactors into dynamic models. An upflow anaerobic sludge blanket (UASB) reactor has been modelled as two CSTR's in series representing the sludge bed and sludge blanket zones and a plugflow region representing the settler (Van Der Meer and Heertjes, 1983; Bolle et. al., 1986). An upflow anaerobic filter has been modelled as three CSTR's in series (Halbert and Wojtowicz, 1982)

It is apparent from this review that a large amount of research has been directed towards the development of mechanistic dynamic models of the anaerobic treatment process. However, very few studies have considered the

problem of parameter estimation and model verification using actual operating data. Carr and O'Donnell (1977) compared responses predicted by the single bacterial Andrews and Graef (1971) model to experimental step test data from laboratory scale, continuous flow, complete-mixed digestors fed with an acetic acid substrate. Model parameters were adjusted to give the best visual fit of model predictions to the experimental data collected during step changes in the influent acetic acid concentration. Reasonable agreement was observed between the simulated and the experimental data. Chalon et. al. (1982) used a least squares procedure based on the difference between actual and predicted daily gas production rates from a laboratory scale digester to calibrate a dual microbial community model similar in form to the model developed by Hill and Barth (1977). There are no published reports which consider the simultaneous fit of all state variables to actual operating data for this form of model. In addition, no reports have been published on the calibration or verification of the four population models.

In summary, dynamic models of the anaerobic treatment process have evolved from models based on a single group of bacteria converting a single substrate to methane, to models based on complex metabolic pathways mediated by several different groups of bacteria that convert degradable organic molecules to a variety of intermediate and end products. With the development of increasingly complex process models, researchers now understand more about the factors affecting anaerobic reactor stability and performance. However, more complete verification of the success of anaerobic process models in predicting actual reactor behaviour is required. The next step would be to use this improved process understanding to devise operational and control strategies which could help

maintain consistent performance under the influence of a variety of disturbances. The next section in this review defines the process control problems in anaerobic treatment processes and summarizes attempts made to solve them. In some of the studies described, dynamic models have been used directly, either to simulate operational situations or to design controllers.

### 2.3 Process Control

Two overall control objectives can be highlighted for anaerobic treatment systems: the achievement of a consistently high degree of waste stabilization; and, the highest possible conversion of waste to methane. In wastewater treatment, the first objective would be the most important. However, since the ultimate product of the stabilization process is methane, the two can be thought of as being highly related. To achieve these objectives, the environmental requirements of, and the balance between the microbial populations present in the system must be maintained. This task is complicated by the different environmental requirements and the different growth rates of the participating microbial groups.

An unbalanced condition in an anaerobic treatment process often manifests itself in an accumulation of volatile fatty acids and a decrease in pH. The control of pH in anaerobic treatment processes has therefore been a major topic in the literature. Early studies on pH control concentrated on off-line methods of calculating the required amount of alkalinity addition from titrimetric measurements of effluent volatile acids and alkalinity (Pohland and Engstrom, 1964). This method of pH control is standard practice in the operation of anaerobic sludge digesters (US EPA, 1979).

In conventional sludge digesters, where long time constants result from minimum hydraulic retention times of 15 days, such off-line techniques

may be appropriate. However, in high rate anaerobic wastewater treatment processes, conditions may change much more rapidly. On-line control of pH would be more appropriate in this case. The use of on-line feedback control of pH has been investigated extensively in simulation studies (Graef and Andrews, 1974; Collins and Gilliland, 1974). Some controversy still exists among researchers as to whether pH can be reliably measured on-line. This has prompted study into the use of bicarbonate alkalinity measured with an on-line titration device as a more appropriate feedback variable (Rozzi, 1984; Rozzi et. al., 1985).

In anaerobic treatment processes, adaptive schemes are an appropriate choice for a control structure since anaerobic processes are non-linear systems in which the dynamics of the biomass are continually changing due to changing input perturbations and a changing environment. Bastin et. al. (1982) have investigated the use of an adaptive regulator for control of the gas production rate from a sludge digester. Through simulation studies using a mechanistic dynamic model similar to that of Hill and Barth (1977), steady state values of the digester feed rate were found which maximized the gas production rate at a given influent substrate concentration while maintaining a required effluent concentration. On-line regulation of the gas production to this setpoint was achieved by manipulating the feedrate. Control actions were computed with an adaptive form of a one-step optimal controller.

Performance of the above controller was tested in simulation studies. Such an approach could be useful in situations where the feed characteristics change slowly, allowing a search for optimum setpoint values to be conducted using off-line concentration measurements. In high rate anaerobic wastewater treatment systems, application could be hindered

by a lack of suitable instrumentation for on-line substrate concentration measurements. Also, gas production may not be the most appropriate control variable in wastewater treatment situations.

The problem of regulating the effluent substrate concentration to a prescribed level was investigated in simulation studies by Dochain and Bastin (1985). An adaptive control algorithm required measurements of the influent and effluent substrate concentration, and the methane production rate. Control actions consisted solely of manipulation of the process feed rate.

Three problems in applying control to anaerobic wastewater treatment processes become apparent when reviewing the literature. First, there are no clear answers to the question of which are the most appropriate feedback variables for the exercise of control. Second, inflexible designs of anaerobic treatment processes limit the capacity to implement control actions. The magnitude of feedrate control actions would be limited by the available wastewater equalization capacities. Mosey (1983) has suggested the manipulation of the gas phase hydrogen concentration as a method of control. In the review paper by Harper and Pohland (1986), two-phase designs were proposed which could provide a means of manipulating the hydrogen concentration. Third, there is a lack of suitable on-line instrumentation. The next section describes on-line estimation techniques which have been used to overcome this common problem in biological processes.

## 2.4 State Estimation

Many of the system variables which would be useful for control in biological treatment processes can only be determined offline through time consuming analyses or are only measureable on-line using instruments which are expensive or difficult to maintain. The availability of a dynamic process model enables some of these variables to be estimated using on-line state estimation techniques. By applying these techniques, all of the information available on the process - input functions, the known process model structure and parameters, and observed process outputs - can be used for the calculation of internal system states. Some techniques can also be used to calculate unknown process parameters and evaluate the process model structure.

Investigations using on-line estimation schemes in the activated sludge process have been relatively extensive. The most commonly studied problem has been on-line state reconstruction from the dissolved oxygen (DO) dynamics. The procedure usually involves the manipulation of the DO dynamic mass balance into a linear equation form. Key variables such as the oxygen uptake rate (OUR) and oxygen transfer coefficient ( $k_{la}$ ) are estimated as parameters in the equation using a recursive estimation technique (Olsson, 1985). Once these key variables have been estimated, other important process variables on which control actions can be based such as substrate and biomass concentrations can be obtained from a combination of mechanistic and empirical model equations (Holmberg, 1982).

A simple on-line estimator has been developed (Bastin and Dochain, 1986) and demonstrated at the pilot scale (Dochain *et. al.*, 1986) for anaerobic wastewater treatment processes. The scheme was developed using a model similar in form to the single bacterial model of Andrews (1969). On-line estimates of the specific growth rate and the effluent substrate

concentration were obtained given that the feed rate and influent substrate concentration were known and a noisy measurement of the methane flow rate was available. A major drawback to this approach is that the influent substrate concentration is required for the estimator. In most applications it could be assumed that if an on-line measurement of the influent substrate concentration is available, an effluent measurement would also be available.

In situations where the structure of the mechanistic model is of interest, a significant amount of random error is associated with process measurements, and the process is affected by unmeasured random disturbances, the Kalman filter (Kalman, 1960) has been applied to estimation problems. A modification of this algorithm, the extended Kalman filter (Jazwinski, 1970) was designed for systems in which a linearized model is not adequate over the applicable range of conditions. The applicability of the techniques is in fact much wider than on-line state estimation as they have also been used to solve model identification (Beck, 1976) and sensor selection (Pollock, 1983) problems.

The use of an extended Kalman filter for state and parameter estimation in biotechnical processes has been investigated using a continuous culture model as the 'actual' process (Svrcek *et. al.*, 1974). The model was similar in form to the Andrews (1969) model for anaerobic digestion. Tracking of the reactor biomass concentration, given a noisy inlet substrate concentration measurement, illustrated the tuning of a Kalman filter to trade-off between heavily weighing new input measurements (increasing the noise in the filter prediction) and improving the filter response time to changes in the influent substrate concentration. The filter was also used to estimate the parameters in the Monod model given noisy measurements of the influent substrate concentration and the biomass

concentration. The results did not show convergence to the actual parameter values. The performance of the filter might have been improved given additional process measurements such as the reactor temperature or the effluent substrate concentration. Convergence of parameter estimates from an extended Kalman filter, when the observability of the process is carefully considered, was illustrated in another study in which this technique was applied to a continuous yeast fermentation process (Bellgardt *et. al.*, 1986).

The use of an extended Kalman filter to assist in operational control of a biological wastewater treatment plant was first investigated by Beck (1981). The filter incorporated a model for the activated sludge process developed by Poduska and Andrews (1975). The algorithm was found to give reasonable estimates of the concentrations of the two nitrifying bacterial species from measurements of the influent flow-rate and ammonium-N concentration, and the effluent concentrations of ammonium-N, nitrite-N, and nitrate-N.

Holmberg and Olsson (1985) used an extended Kalman filter to estimate the oxygen transfer rate and respiration rate in a simulation study of an activated sludge process. A non-linear oxygen mass balance equation was used in the filter. The advantage of this approach over the recursive least square estimators was that both parameters could be estimated simultaneously while taking into account the different rates of change of the parameters and the non-linearities of the process response. The Kalman filter was shown to converge to the true parameter values.



### 3. DYNAMIC MODELLING

#### 3.1 Introduction

The availability of an appropriate dynamic model would enable the initial evaluation of a number of alternative operational and control strategies without extensive pilot or full scale plant runs. A dynamic model could also be used with Kalman filtering techniques to obtain on-line estimates of anaerobic process variables such as substrate and biomass concentrations. In addition, a mechanistic dynamic model could be utilized directly in the design of advanced optimal control algorithms for the anaerobic treatment process.

Although a number of dynamic models for the anaerobic treatment process have been developed, no studies have been conducted to verify the adequacy of these models in predicting the dynamic behaviour of a high rate process applied to the treatment of a complex wastewater. A major objective of this study was to obtain and verify a model which could be used for process simulation, process control and state estimation in this application.

Two different dynamic models were compiled for this study from information available in the literature. The first was a model based on the two bacterial reaction sequence shown in Figure 2.4. This model is most similar in structure to the Hill and Barth (1977) model, although the interaction terms which define the gas-liquid and acid-base state of the reactor were omitted to simplify this initial stage of verification. This model was included in the investigation to test the substrate utilization and product formation kinetics commonly found in the literature. The

second was a comprehensive four population model, based on the work of Mosey (1983) and Rozzi et. al. (1985). Verification of this model is important in the assessment of hydrogen as a monitoring and control variable. This section summarizes the relationships in each of these models.

### 3.2 Two Population Model

The major assumptions considered in developing this model were:

- i) the reactor can be represented by a continuous stirred tank reactor (CSTR) or a set of CSTR's in series;
- ii) the biodegradable component of the incoming wastewater is completely soluble;
- iii) all intermediates in the process can be represented by a single volatile acid;
- iv) the solubility of methane in the liquid phase is negligible, so that all methane produced is released to the gas phase;
- v) substrate utilization and product formation follow Monod kinetics;
- vi) pH effects on the kinetics are negligible; and,
- vii) the bacterial concentrations are constant during any period simulated.

Assumption (vi) limits the application of the model to situations in which there is good pH control. Assumption (vii) was thought to be appropriate for modelling short term dynamic changes in high rate systems. A discussion of the mass balance equations in the model follows.

#### 1) Acid Formation from Soluble Organics

The mass balance for the conversion of soluble organics to volatile fatty acids is expressed as,

$$\frac{dS}{dt} = \frac{F}{V}(S_o - S) - \frac{1}{KXS} SR \quad (3.1)$$

where,

S = concentration of biodegradable soluble organics (measured as biodegradable COD) in the effluent, mg/L,

S<sub>0</sub> = concentration of soluble organics in the influent, mg/L,

F = reactor feedrate, L/d,

V = reactor volume, L,

KXS = acid former yield coefficient, mg acid formers/mg soluble organics,

and

SR = growth rate of acid formers, mg acid formers/L.d.

The growth rate of the acid formers is given by the Monod expression,

$$SR = \frac{S_{MAX}(S)(AF)}{KAS + S} \quad (3.2)$$

where,

S<sub>MAX</sub> = the maximum specific growth rate, 1/d,

KAS = saturation constant, mg (soluble organics)/L, and

AF = concentration of the acid formers, mg/L.

## 2) Volatile Acid Balance

The mass balance for volatile acids contains reaction terms for the production of volatile acids from soluble organics by the acid formers and the consumption by the methanogens.

$$\frac{dVA}{dt} = \frac{F}{V}(VA_0 - VA) + SR(KHAX) - \frac{1}{KXS1} MR \quad (3.3)$$

where,

VA = the effluent concentration of volatile acids, mg/L,

VA<sub>0</sub> = the influent concentration of volatile acids, mg/L,

KHAX = volatile acid yield coefficient, mg volatile acid/mg acid formers,

KXS1 = methanogen yield coefficient, mg methanogens/mg volatile acids, and

MR = growth rate of the methanogens, mg methanogens/L.d.

The growth rate of the methanogens is given by the Monod expression,

$$MR = \frac{MMAX(VA)(MF)}{KM + VA} \quad (3.4)$$

where,

MMAX = maximum specific growth rate, 1/d,

MF = concentration of methanogens, mg/L, and

KM = saturation constant, mg (volatile acids)/L.

The production of methane in the model occurs in proportion to the growth rate of the methanogens.

$$QCH4 = KCH4(SV)(V)(MR) \quad (3.5)$$

where,

QCH4 = methane production rate, L/d

KCH4 = methane yield coefficient, mmole methane/mg methanogens

SV = volume of 1 mmole of ideal gas at 1 atm, 35 °C = .0253 L

### 3) Inert Balance

This balance accounts for the portion of the incoming wastewater which is non-biodegradable but which may be measured by a test such as the chemical oxygen demand (COD).

$$\frac{dI}{dt} = \frac{F}{V}(I_0 - I) \quad (3.6)$$

where,

I = concentration of non-biodegradable material in the effluent, mg/L, and

I<sub>0</sub> = concentration of non-biodegradable material in the influent, mg/L

### 3.3 Four Population Model

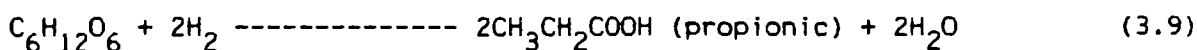
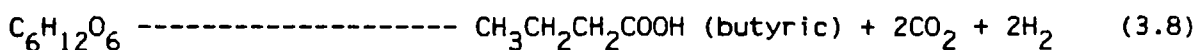
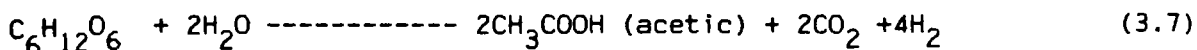
A comprehensive model was assembled to incorporate the effects of hydrogen on the response of the anaerobic treatment process. Since relationships describing interactions between the gas and the liquid phases of the system were required in writing a hydrogen balance for the model, balances for the acid-base system similar to those found in Andrews and Graef (1971) and Hill and Barth (1977) were used. This approach was also used in the four population model developed by Rozzi (1985). Simulation of variable pH and variable gas composition situations are possible with this model. All stoichiometric equations described in this section have been previously summarized by Mosey (1983).

The major assumptions considered in developing this model were:

- i) the reactor can be represented by a continuous stirred tank reactor (CSTR) or a set of CSTR's in series;
- ii) the biodegradable component of the incoming wastewater is completely soluble;
- iii) the formation of volatile acids from soluble organics by the acid-forming bacteria follows the Embden-Meyerhof pathway;
- iv) the solubility of methane and hydrogen in the liquid phase is negligible, so that all methane and hydrogen produced is released to the gas phase;
- v) substrate utilization and product formation follow Monod kinetics;
- vi) pH effects on the kinetics are negligible; and,
- vii) the bacterial concentrations are constant during any period simulated.

### 1) Acid Formation from Soluble Organics

The conversion of soluble organics to a volatile acid mixture consisting mainly of acetic, propionic and butyric acids is achieved by the relatively fast-growing acid forming bacteria. For a glucose substrate, the following reactions are involved.



The mass balance for biodegradable soluble organics (such as glucose) is expressed as,

$$\frac{dG}{dt} = \frac{F}{V}(G_o - G) - \frac{1}{KAC}(GR)(RFAC) - \frac{1}{KPR}(GR)(RFPR) - \frac{1}{KBT}(GR)(RFBT) \quad (3.10)$$

where,

$G$  = concentration of soluble organics in the effluent, mg/L,

$G_o$  = concentration of soluble organics in the influent, mg/L,

$F$  = reactor feedrate, L/d,

$V$  = reactor volume, L,

$KAC$  = biomass yield coefficient, mg organisms/mg organics to acetic,

$KPR$  = biomass yield coefficient, mg organisms/mg organics to propionic,

$KBT$  = biomass yield coefficient, mg organisms/mg organics to butyric,

$GR$  = unregulated growth rate of acid formers, mg acid formers/L.d,

$RFAC$  = regulation by hydrogen of the conversion of organics to acetic,

$RFPR$  = regulation by hydrogen of the conversion of organics to propionic,

and

$RFBT$  = regulation by hydrogen of the conversion of organics to butyric.

The unregulated rate of the acid formers is given by the Monod expression,

$$GR = \frac{G_{\max}(G)(AF)}{K_{sg} + G} \quad (3.11)$$

where,

$G_{\max}$  = the maximum unregulated specific growth, 1/d,

$K_{sg}$  = saturation constant, mg(organics)/L, and

$AF$  = concentration of acid formers, mg/L.

The hydrogen regulation functions are the expressions developed by Mosey (1983), which relate the hydrogen concentration (which is related to the relative concentrations of  $NAD^+$  and  $NADH$ ) to the relative rates of conversion of glucose to the various volatile acids following the Embden-Meyerhof pathway. The regulation functions are written in terms of hydrogen partial pressure in the gas phase as follows,

$$RFAC = \left( \frac{1}{1 + 1500(PH_2)} \right)^2 \left( 1 - \frac{2(1500)(PH_2)}{1 + 1500(PH_2)} \right) \quad (3.12)$$

$$RFPR = \left( \frac{1}{1 + 1500(PH_2)} \right) \left( \frac{1500(PH_2)}{1 + 1500(PH_2)} \right) \quad (3.13)$$

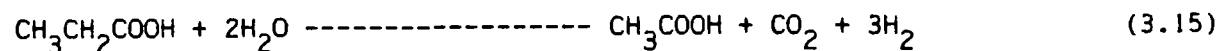
$$RFBT = \left( \frac{1}{1 + 1500(PH_2)} \right)^2 \left( \frac{1500(PH_2)}{1 + 1500(PH_2)} \right) \quad (3.14)$$

where,

$PH_2$  = partial pressure of hydrogen in the gas phase, atm.

## 2) Propionic Acid Balance

The conversion of propionic acid to acetic acid by the acetogenic bacteria is given by the reaction,



The mass balance, which contains reaction terms for the production of propionic acid from glucose (soluble organics) and the consumption of propionic acid according to the above reaction, is written as,

$$\frac{dP}{dt} = \frac{F}{V}(P_o - P) + KGP(GR)(RFPR) - \frac{1}{KPRA}(PRR)(RFPRA) \quad (3.16)$$

where,

P = concentration of propionic acid in the effluent, mg/L,

P<sub>o</sub> = concentration of propionoc acid in the influent, mg/L,

KGP = propionic acid yield coefficient, (mg propionic)/(mg organisms),

KPRA = biomass yield coefficient, mg organisms/mg propionic to acetic,

PRR = unregulated growth rate-propionic acid acetogenic bacteria, mg organisms/L.d, and

RFPRA= regulation by hydrogen of the conversion of propionic to acetic

$$= \frac{1}{1 + 1500(PH_2)} \quad (3.17)$$

The growth rate of the propionic acid utilizing acetogens is given by the following Monod expression,

$$PRR = \frac{P_{max}(P)(PA)}{K_{sp} + P} \quad (3.18)$$

where,

P<sub>max</sub> = maximum unregulated specific growth rate, 1/d,

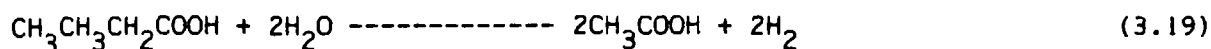
PA = concentration of propionic acid utilizing acetogens, mg/L, and

K<sub>sp</sub> = saturation constant, mg(propionic)/L.

### 3)Butyric Acid Balance

The stoichiometry of the production of acetic acid from butyric acid is given by the following equation,





The mass balance contains reaction terms for the production of butyric acid from glucose (soluble organics) and for the consumption of butyric acid in the above reaction. The balance is written as follows:

$$\frac{dB}{dt} = \frac{F}{V}(\text{Bo} - B) + \text{KGB}(\text{GR})(\text{RFBT}) - \frac{1}{\text{KBTA}}(\text{BR})(\text{RFBTA}) \quad (3.20)$$

where,

B = concentration of butyric acid in the effluent, mg/L,

Bo = concentration of butyric acid in the influent, mg/L,

KGB = butyric acid yield coefficient, (mg butyric)/(mg organisms),

KBTA = biomass yield coefficient, (mg organisms)/(mg butyric to acetic),

RFBTA = regulation by hydrogen of the conversion of butyric acid to acetic,

$$= \frac{1}{1 + 1500\text{PH}_2} \quad (3.21)$$

BR = unregulated growth rate of butyric acid utilizing acetogens,

mg organisms/L.d

$$= \frac{\text{Bmax}(B)(\text{BA})}{\text{Ksb} + B} \quad (3.22)$$

where,

Bmax = maximum specific unregulated growth rate, 1/d,

BA = concentration of butyric acid utilizing acetogens, mg/L, and

Ksb = saturation constant, mg(butyric)/L.

#### 4) Acetic Acid Balance

Methane and carbon dioxide are produced from acetic acid according to the following reaction:



The mass balance for acetic acid contains reaction terms for the production of acetic acid from glucose (soluble organics) and from propionic and butyric acids, and for the consumption of acetic acid in the above reaction. The balance is written as follows:

$$\frac{dA}{dt} = \frac{F}{V} (A_o - A) + KGA(GR)(RFAC) + KPA(PRR)(RFPRA) + KBA(BR)(RFBTA) - MR/KAM \quad (3.24)$$

where,

A = concentration of acetic acid in the effluent, mg/L,

A<sub>o</sub> = concentration of acetic acid in the influent, mg/L,

KGA = acetic acid yield coefficient, mg acetic from organics/mg organisms,

KPA = acetic acid yield coefficient, mg acetic from propionic/mg organisms,

KBA = acetic acid yield coefficient, mg acetic from butyric/mg organisms,

and

KAM = biomass yield coefficient, mg organisms/mg acetic to methane.

MR = aceticlastic methanogens growth rate, mg organisms/L.d,

$$= \frac{M_{\max}(A)(AMF)}{K_{sm} + A} \quad (3.25)$$

where,

M<sub>max</sub> = maximum specific growth rate of aceticlastic methane formers, 1/d,

K<sub>sm</sub> = saturation constant, mg(acetic)/L, and

AMF = concentration of aceticlastic methanogens, mg/L.

### 5) Gas Phase Hydrogen Balance

As shown previously in the stoichiometric equations, hydrogen is produced in the conversion steps of glucose (soluble organics) to acetic acid, glucose to butyric acid, propionic acid to acetic acid, and butyric acid to acetic acid. Hydrogen is consumed as glucose is converted to

propionic acid and as methane is produced in the following reaction:



The hydrogen balance assumes that the gas and liquid phases are in equilibrium, that the contribution of hydrogen to the total gas flow rate is negligible, and that the amount of hydrogen leaving the system dissolved in the effluent can be neglected. The resulting equation for the hydrogen balance is equivalent to that used by Rozzi (1985).

$$\begin{aligned} \frac{d\text{PH}_2}{dt} = & \frac{1}{\text{KH}_2} \left( - \frac{\text{PH}_2(\text{QM})}{\text{PT}} + \text{KHPA}(\text{PRR})(\text{RFPRA}) + \text{KHBA}(\text{BR})(\text{RFBTA}) - \text{KHP}(\text{GR})(\text{RFPR}) \right. \\ & \left. - \frac{\text{MHR}}{\text{KHCM}} + \text{KHB}(\text{GR})(\text{RFBT}) + \text{KHA}(\text{GR})(\text{RFAC}) \right) \end{aligned} \quad (3.27)$$

where,

$\text{KH}_2$  = Henry's law constant for hydrogen, mmole hydrogen /atm.L,

$\text{KHPA}$  =  $\text{H}_2$  yield coefficient, mmole  $\text{H}_2$ (propionic to acetic step)/mg organisms,

$\text{KHBA}$  =  $\text{H}_2$  yield coefficient, mmole  $\text{H}_2$ (butyric to acetic step)/mg organisms,

$\text{KHP}$  =  $\text{H}_2$  yield coefficient, mmole  $\text{H}_2$ (organics to propionic step)/mg organisms,

$\text{KHB}$  =  $\text{H}_2$  yield coefficient, mmole  $\text{H}_2$ (organics to butyric step)/mg organisms,

$\text{KHA}$  =  $\text{H}_2$  yield coefficient, mmole  $\text{H}_2$ (organics to acetic step)/mg organisms,

$\text{KHCM}$  = biomass yield coefficient, mg organisms/mmole  $\text{H}_2$  (to  $\text{CH}_4$ ),

$\text{MHR}$  = hydrogen utilizing methanogens growth rate (mg organisms/L.d),

$\text{PT}$  = total gas phase pressure, atm, and

$\text{QM}$  = total molar gas flowrate ( $\text{CH}_4 + \text{CO}_2$ ), mmole/(L.d).

The total molar gas flowrate is found by considering the production of methane from both of the methanogenic groups of bacteria and by considering the partial pressure of carbon dioxide. The method of finding the carbon dioxide partial pressure will be discussed in a later section.

$$QM = \frac{KCH4A(MR) + KCH4H(MHR)}{(1 - PCO2/PT)} \quad (3.28)$$

where,

KCH4A = methane yield coefficient (acetoclastic methane prod'n),  
mmole methane/mg acetoclastic methanogens,

KCH4H = methane yield coefficient (methane prod'n from H<sub>2</sub>),  
mmole methane/mg hydrogen-utilizing methanogens,

PCO<sub>2</sub> = carbon dioxide partial pressure, atm,

and,

$$MHR = \frac{MH_{max}(PH_2)(HMF)}{K_{sh} + PH_2} \quad (3.29)$$

where,

MH<sub>max</sub> = maximum specific growth rate of H<sub>2</sub> utilizing methane formers, 1/d,

HMF = concentration of hydrogen utilizing methane formers, mg/L,

K<sub>sh</sub> = saturation constant, atm.

## 6) Bicarbonate Equilibrium

The approach described in this section for considering the gas-liquid interactions in an anaerobic reactor was initially used in the Andrews and Graef (1971) dynamic model. The carbon dioxide and bicarbonate equilibrium is represented by equations (3.30) and (3.31).



$$\frac{(H^+)(HCO_3^-)}{CO_2d} = KH_2CO_3 \quad (3.31)$$

where,

(H<sup>+</sup>) = hydrogen ion concentration, mmole/L,

(CO<sub>2</sub>d) = dissolved carbon dioxide concentration (both CO<sub>2</sub> and H<sub>2</sub>CO<sub>3</sub>), mmole/L,

(HCO<sub>3</sub><sup>-</sup>) = bicarbonate concentration, mmole/L, and

$KH_2CO_3$  = equilibrium constant.

In the model, equation (3.31) allows calculation of the pH if the dissolved carbon dioxide and the bicarbonate concentrations are known. The bicarbonate concentration is calculated from a charge balance in the reactor. The charge balance described by Andrews and Graef was modified to include the three different volatile acid concentrations considered.

$$(H^+) + (C^+) = (HCO_3^-) + 2(CO_3^{2-}) + A/60 + P/74 + B/88 + (OH^-) + (A^-) \quad (3.32)$$

where,

$(C^+)$  = concentration of cations other than  $H^+$ , mmole/L,

$(CO_3^{2-})$  = concentration of carbonate ion, mmole/L,

$(OH^-)$  = concentration of hydroxide ion, mmole/L, and

$(A^-)$  = concentration of cations other than those shown in equation (3.32), mmole/L

For pH in the range from 5 to 8, the following assumptions are made:

$$(H^+) = (OH^-)$$

and,

$$(CO_3^{2-}) = 0$$

Also, it is assumed that the total volatile acid concentration is approximately equal to the ionized acid concentration. Note that the concentration of each volatile acid is divided by the appropriate molecular weight to get the equivalent molar concentration. Defining,

$$TVA = A/60 + P/74 + B/88 \quad (3.33)$$

= total molar volatile acid concentration, mmole/L,

and rewriting equation (3.32) gives

$$[(C^+) - (A^-)] = (HCO_3^-) + (TVA) \quad (3.34)$$

$$(HCO_3^-) = (Z) - (TVA) \quad (3.35)$$

where,

(Z) = net cation concentration in the effluent,  $[(C^+) - (A^-)]$ , mmole/L

The net cation concentration, Z, is found from a material balance. If pH control is achieved through the addition of a strong base, such as sodium hydroxide, and assuming that the volumetric addition rate of this base is negligible compared to the total flowrate in the reactor, the material balance is written,

$$\frac{dZ}{dt} = \frac{F}{V}(Z_o - Z) + \frac{F_c}{V}ZB \quad (3.36)$$

where,

$Z_o$  = Influent net cation concentration, mmole/L,

$F_c$  = addition rate of strong base for pH control, L/d, and

$ZB$  = concentration of strong base for pH control, mmole/L.

#### 7) Dissolved Carbon Dioxide Balance

This balance combines with the equations described in the previous section to completely define the carbon dioxide-bicarbonate equilibrium in the liquid phase and allows the model to predict the gas phase characteristics through interaction equations which will also be defined in this section. The balance is based on that developed by Andrews and Graef (1971) with modifications for the additional biological production taken into consideration. The material balance can be written as follows,

$$\frac{dCO_2^d}{dt} = \frac{F}{V}(CO_2^{do} - CO_2^d) + RB + RC - QMCO_2 \quad (3.37)$$

where,

$CO_2^{do}$  = influent dissolved carbon dioxide composition, mmole/L,

$RB$  = biological production of  $CO_2$ , mmole/L.d,

RC = chemical reaction term for  $\text{CO}_2$ , mmole/L.d, and

QMC02 = molar gas flow rate of  $\text{CO}_2$ , mmole/d.

The net biological production of carbon dioxide is described by the following equation,

$$\text{RB} = \text{KC02GA}(\text{GR})(\text{RFAC}) + \text{KC02GB}(\text{GR})(\text{RFBT}) + \text{KC02A}(\text{MR}) - \text{MHR}/\text{KC02H} \quad (3.38)$$

where,

KC02GA =  $\text{CO}_2$  yield coefficient (organics to acetic step), mmole  $\text{CO}_2$ /mg organisms,

KC02GB =  $\text{CO}_2$  yield coefficient (organics to butyric step), mmole  $\text{CO}_2$ /mg organism,

KC02A =  $\text{CO}_2$  yield coefficient (acetic to methane step), mmole  $\text{CO}_2$ /mg organism,

and

KC02H = biomass yield coefficient ( $\text{CO}_2 + \text{H}_2$  to methane step),  
mg organism/mmole  $\text{CO}_2$ .

The chemical reaction term accounts for the reaction of the volatile acids with bicarbonate to form carbon dioxide and the maintenance of a charge balance as the net cation concentration changes.

$$\text{RC} = \frac{F}{V}(\text{HCO}_3^- \text{ in} - \text{HCO}_3^-) + \frac{dP}{dt}/74 + \frac{dB}{dt}/88 + \frac{dA}{dt}/60 - \frac{dZ}{dt} \quad (3.39)$$

where,

$\text{HCO}_3^- \text{ in}$  = influent concentration of bicarbonate, mmole/L.

A description of the interactions between the gas and liquid phases is now required. Assuming that the carbon dioxide in the gas and liquid phases are in equilibrium,

$$\text{PCO}_2 = \text{CO}_2 \text{d}/\text{KHC02} \quad (3.40)$$

where,

KHC02 = Henry's law constant for carbon dioxide, mmole/L.atm.

With  $PCO_2$  defined, the total molar gas flowrate can be calculated from equation (3.28) and the  $CO_2$  molar gas flowrate can be calculated from,

$$Q_{MCO_2} = Q_M(PCO_2/PT) \quad (3.41)$$

#### 8) Inert Balance

As in the two population model, this balance accounts for the portion of the incoming wastewater which is non-biodegradable but that may be measured by a test such as the chemical oxygen demand (COD).

$$\frac{dI}{dt} = \frac{F}{V}(I_o - I) \quad (3.42)$$

where,

$I$  = concentration of non-biodegradable material in the effluent, mg/L, and

$I_o$  = concentration of non-biodegradable material in the influent, mg/L.

#### 9) Gas Production Rates

The volumetric gas production rates are calculated by the following equations:

$$Q_{CO_2} = SV(V)(PCO_2/PT)(Q_M) \quad (3.42)$$

and,

$$Q_{CH_4} = SV(V)(KCH_4A(MR) + KCH_4H(MHR)) \quad (3.43)$$

### 3.4 Computational Methods

Both models were programmed in FORTRAN. Computer code for the two population model and the four population model is included in Appendix II and Appendix III, respectively. The sets of non-linear differential equations in each model were solved with Gear's method for systems of stiff differential equations using the IMSL software package.



## 4. EXPERIMENTAL EQUIPMENT AND PROCEDURES

### 4.1 Pilot Plant Facilities

For this study an anaerobic hybrid (HYBRID) reactor was operated at Environment Canada's Wastewater Technology Centre (WTC) in Burlington, Ontario. The reactor, operated in an upflow mode, consisted of a cylindrical steel tank 0.76 m in diameter and 2.5 m high with 9 cm diameter Norton Actifil random plastic packing in the top 45 % of the tank volume. The lower 55 % of the reactor was left open to allow for accumulation of non-attached biomass in a sludge bed. The empty bed volume of the reactor was 1050 L, with an initial void volume of 1000 L.

The pilot plant was equipped with sensors to allow for the measurement of several process variables. The variables and the measurement sensors are listed in Table 4.1. The sensors were interfaced to a microcomputer-based data acquisition and control system consisting of a CBM 8032 microcomputer and a Control Microsystems front end. Variables measured on-line were stored on a floppy disc at 5 minute intervals.

The microcomputer system also allowed for the on-line feedback control of pH through the addition of 1 N NaOH to the reactor feed, and open-loop control of the variable speed feed and recycle pumps. A pH setpoint of 6.6 and an effluent recycle rate of 2.5 L/min were maintained throughout the study. The internal temperature of the reactor was maintained at 35 °C by thermostatically controlled resistance heating on the tank walls.

Figure 4.1 shows a schematic of the HYBRID reactor, including the sensors and control elements interfaced to the microcomputer.

Table 4.1 List of Process Variables Measured On-line

Variable	Instrument
Recycle Flow	Magnetic Flowmeter
Reactor Temperature	Resistance Temperature Detector
pH	Beckman pH probe
Biogas flow	Wet test meter
Biogas CH <sub>4</sub> content	Astro Infrared Analyser
Biogas CO <sub>2</sub> content	Beckman Infrared Analyser
Biogas H <sub>2</sub> content	GMI Hydrogen Monitor

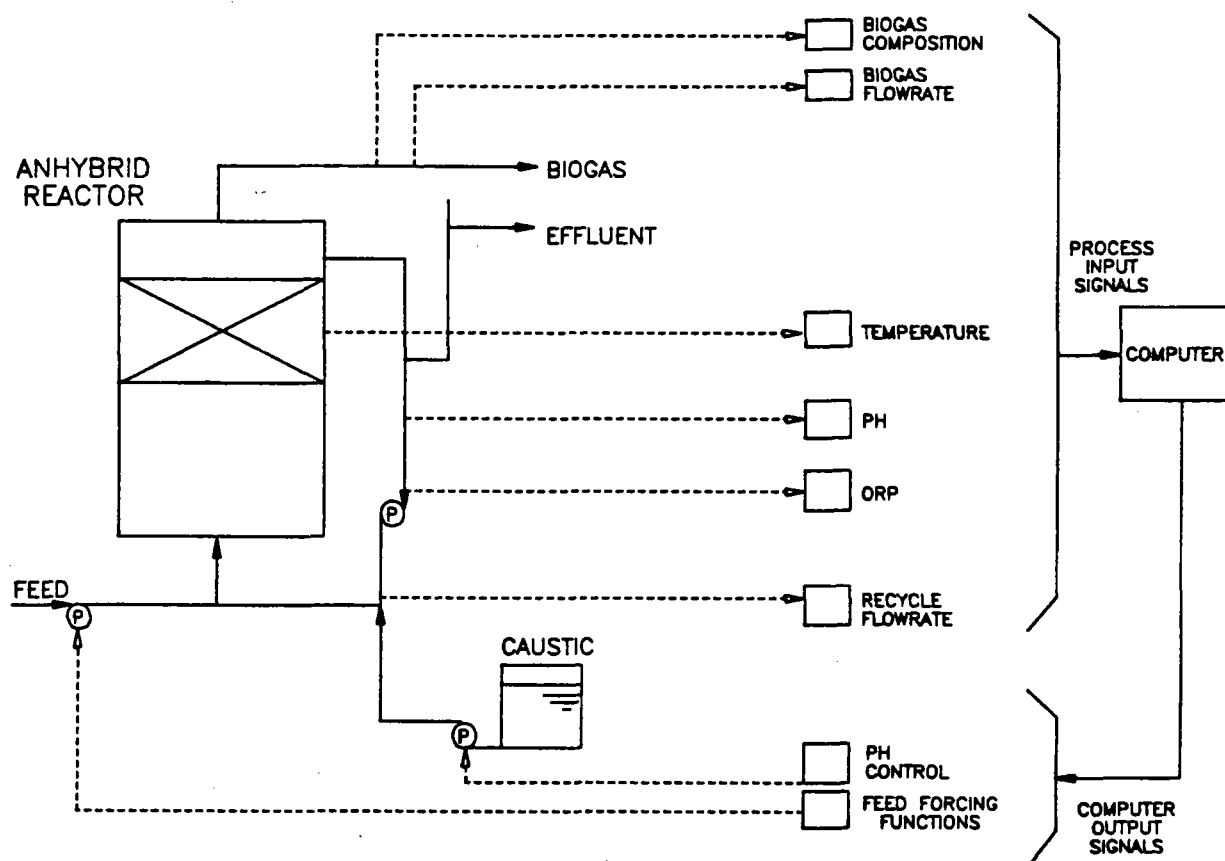


Figure 4.1 Schematic of the anaerobic pilot plant.

#### 4.2 Wastewater Characteristics, Collection and Storage

Wastewater used in the study was from a MacMillan Bloedel pulp and paper mill in Sturgeon Falls, Ontario. The wastewater was selected due to its availability during a separate study at the WTC. Details of the sources of wastewater at the mill, the shipping of the wastewater to Burlington and the characteristics of the wastewater based on grab samples at the mill have been summarized by Hall *et. al.* (1986).

At the WTC, the raw wastewater was stored in a mixed, refrigerated 5000 L feed storage tank and diluted to the desired feed concentration by the addition of tap water. Nutrients were also added at this point as required. Influent to the reactor flowed by gravity into a mixed 40 L head tank where it was heated before being pumped to the reactor.

#### 4.3 Reactor Start Up

Prior to the beginning of this study, the media in the HYBRID was used as a portion of the packing in an anaerobic filter. Biomass which had grown attached to the packing in the anaerobic filter was left attached as the media was transferred to the HYBRID. This biomass thus acted as the seed for start up of the HYBRID.

The initial feed to the HYBRID consisted of a 25% dilution of Sturgeon Falls wastewater supplemented with  $K_2HPO_4$  to provide adequate nutrient levels for biomass growth. The strategy employed during initial start up was similar to that used by Hall *et. al.* (1986). The HYBRID was operated with a dilute feedstock at HRT's of 2 days or less. When the effluent total volatile acid concentration was below 300 - 500 mg/L, the organic loading rate was raised in steps until a target loading rate of approximately  $10 \text{ kg COD/m}^3 \text{ reactor volume.day}$  was reached.

#### 4.4 Experimental Design

Step forcing functions were applied to the pilot plant to generate data on the dynamic response of the HYBRID to changes in feed rate and feed concentration. The design of the experiments was iterative, with the results from an initial set of tests being used to determine settings for a second set. The step test experimental conditions are summarized in Table 4.2.

To obtain more information on the gas production dynamics of the HYBRID, a set of experiments was conducted in which pseudo-random binary sequences (PRBS) of feedrate were run automatically under direct control of the microcomputer data acquisition and control system. The first PRBS was composed of a 1 day sequence of random changes between high and low values of feed rate, with a switching time of 60 minutes. The feed rate changed between 500 and 1300 L/d (HRT's between 2 and 0.8 days). The second PRBS used the same feed rate limits but was run for 2 days with a switching time of 30 minutes. For both PRBS experiments, the feed concentration was set at a constant level to achieve an approximate average organic loading of 8 kg COD/m<sup>3</sup>.d.

Prior to each dynamic experiment, the plant operating conditions were maintained at a constant level for a minimum of 7 days to achieve a pseudo-steady state. After a step change, the test was considered complete after a minimum of 4 HRT's. The steady state operating conditions maintained between dynamic experiments are summarized in Table 4.3.

Table 4.2 Summary of Step Testing Experimental Conditions

Step Test	Initial Conditions		Final Conditions	
	Influent COD (mg/L)	Feedrate (L/d)	Influent COD (mg/L)	Feedrate (L/d)
Feed Step #1	9600	497	9600	1200
Feed Step #2	8587	490	8510	1353
Feed Step #3	13080	420	13080	1426
Concentration Step #1	2150	774	18160	754
Concentration Step #2	6936	909	23903	896

Table 4.3 Steady State Operating Conditions

Steady State Period	Influent COD (mg/L)	Feedrate (L/d)	Loading Rate (kg COD/m <sup>3</sup> .d)	Remarks
1	9600	497	4.8	-period before feed step #1
2	8587	490	4.2	-period before feed step #2
3	8510	1353	11.5	-end of feed step #2
4	2150	774	1.7	-period before concentration step #1
5	18160	754	13.7	-end of concentration step #1
6	13080	420	5.5	-period before feed step #3
7	6936	909	6.3	-period before concentration step #2
8	23903	896	21.4	-end of concentration step #2
9	9884	503	5.0	-period before PRBS testing

#### 4.5 Sampling and Analysis

As a check of the data collected and stored on-line, local instrument readings were taken on a daily basis. Reactor feed rates were determined by collecting effluent for approximately 8 hours. Samples of biogas were taken from the exhaust system for weekly off-line checks of the on-line analysers. Grab samples of reactor influent and effluent were collected 5 days per week for analysis of volatile acids, and 3 days per week for COD analysis. Total bed (non-attached) volatile solids concentrations were determined periodically from sample profiles along the reactor. During step test experiments, an automatic sampler collected grab samples of effluent on an hourly basis for COD and volatile acid analysis.

Sample preparation and COD analyses were performed as described in Standard Methods (1980). Gas chromatography was used for volatile acids and off-line gas quality determinations.



## 5. EXPERIMENTAL RESULTS AND DISCUSSION

The sequence of events during the 413 days of reactor operation in this study is summarized in Figure 5.1. The reactor operation and performance for the entire study period is illustrated in Figures 5.2 to 5.7.

### 5.1 Reactor Start Up and Operation

For the first 10 weeks of HYBRID reactor operation, the wastewater feed concentration and the HRT were maintained at approximately 6000 mg COD/L (Figure 5.2) and 2 days (Figure 5.3), respectively, with a resulting organic loading rate of 3 kg COD/m<sup>3</sup>.d (Figure 5.4). As the loading rate was subsequently increased, the performance of the reactor declined. Effluent total volatile acid concentrations (Figure 5.5) of more than 1000 mg/L and average COD removal efficiencies (Figure 5.6) of less than 40% were observed. Investigations conducted due to similar problems experienced in the Hall *et. al.* (1986) study identified nitrogen as a limiting nutrient. As a result, a continuous addition to the reactor feed of 50 mg/L NH<sub>4</sub>-N began on operating day 190.

After the commencement of nitrogen addition, a rapid decrease in effluent volatile acid concentrations and a rapid increase in the biogas production rate (Figure 5.7) was observed. By day 216, a 60% COD removal efficiency was being achieved at an approximate loading of 10 kg COD/m<sup>3</sup>.d. At this point, the reactor was considered to be ready for experimentation.

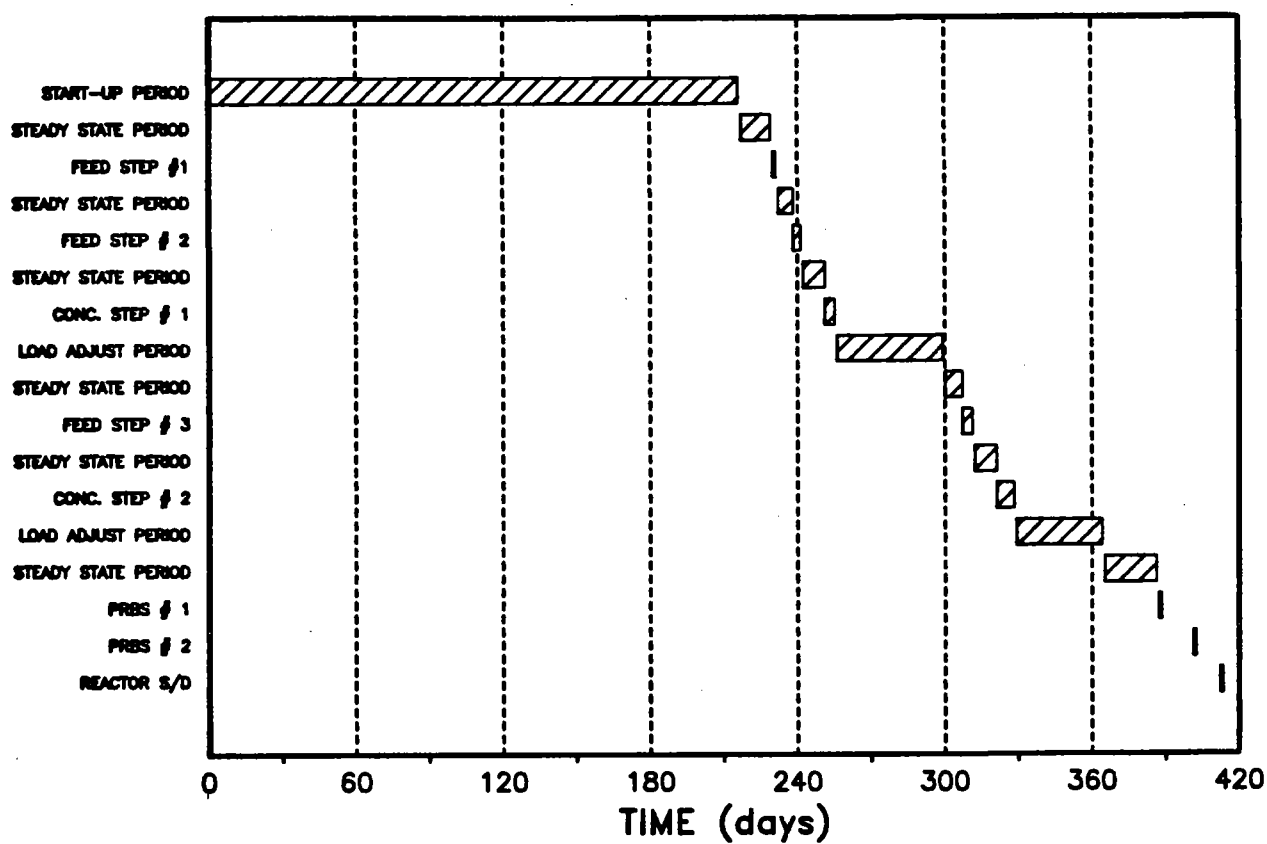


Figure 5.1 Sequence of events in operation of the anaerobic pilot plant.

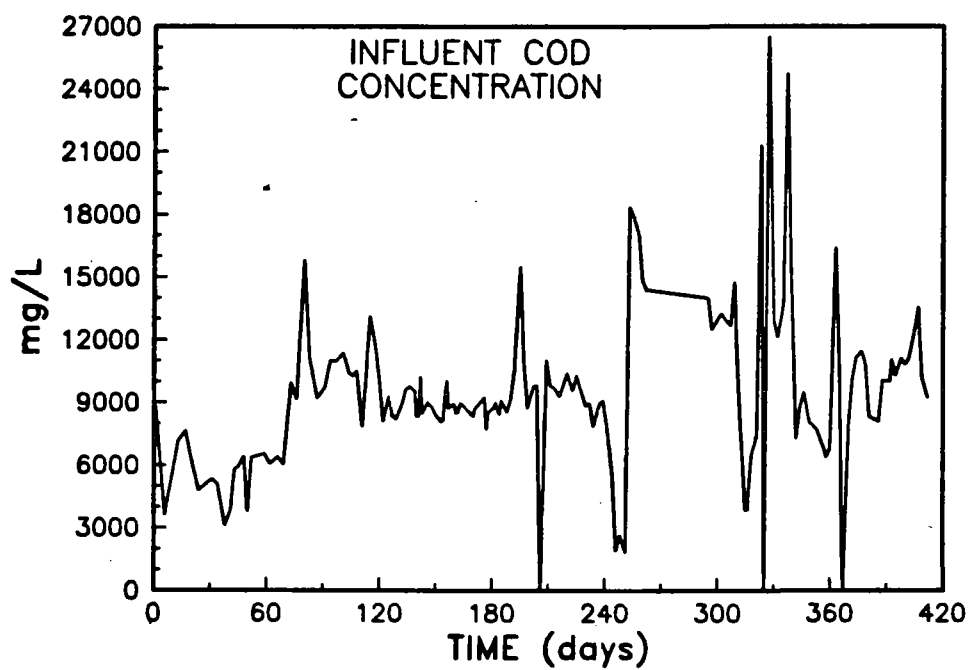


Figure 5.2 Feed COD concentration for the HYBRID pilot plant.

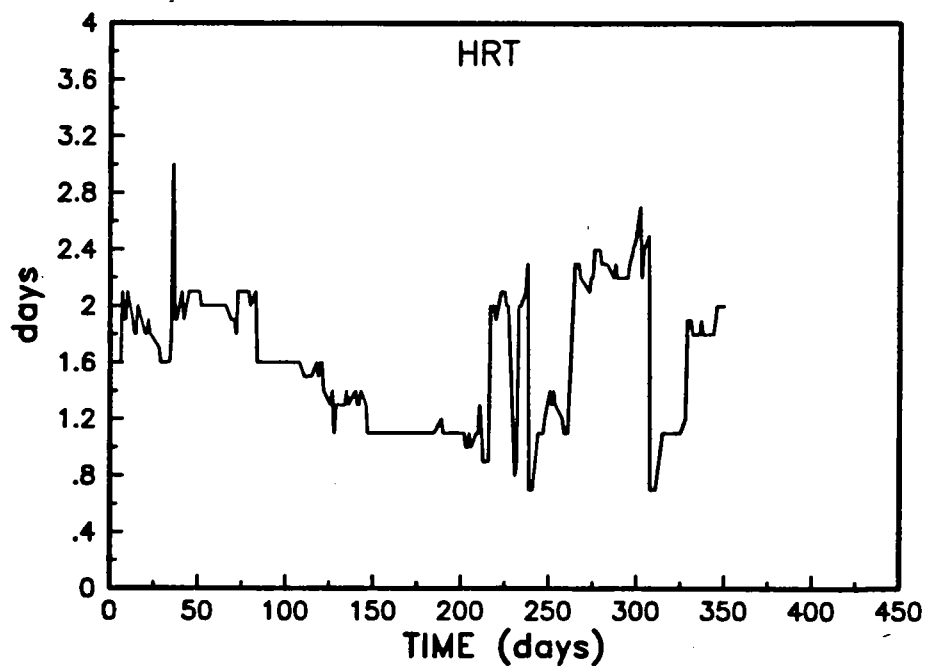


Figure 5.3 HRT for the HYBRID pilot plant.

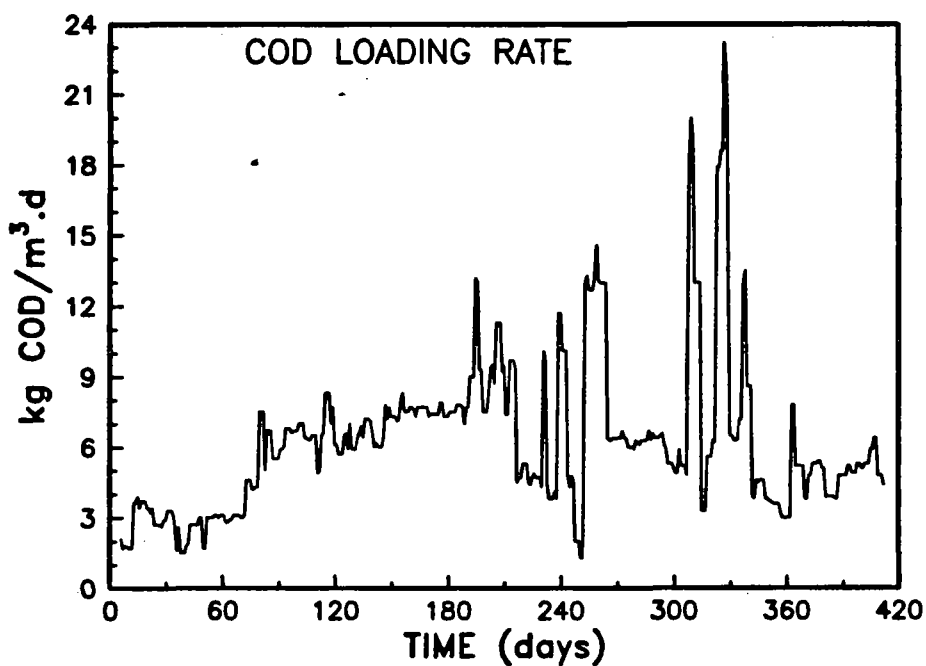


Figure 5.4 Empty bed volumetric loading rates for the HYBRID pilot plant.

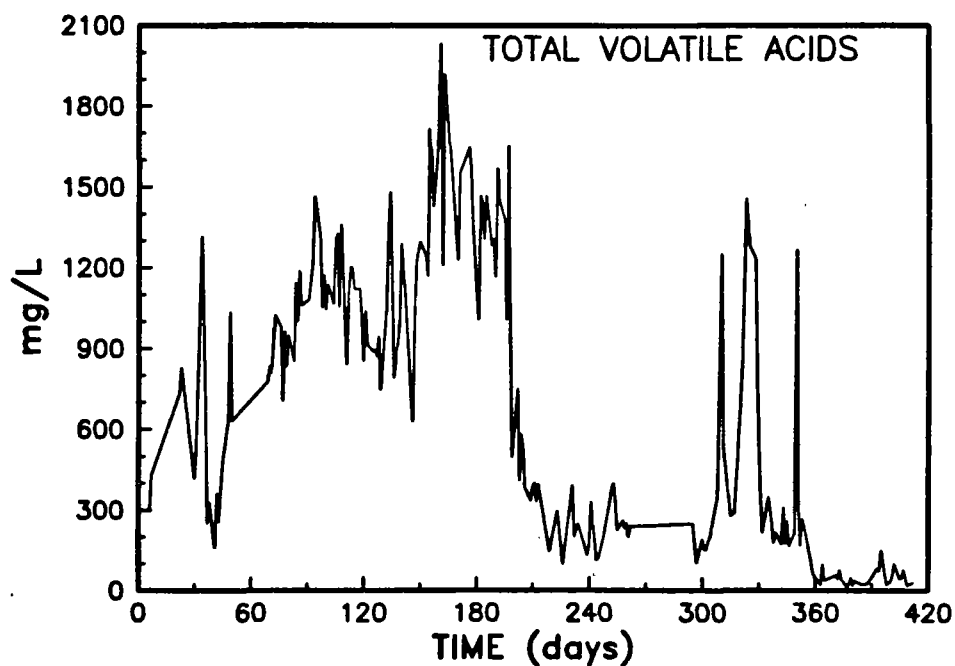


Figure 5.5 Effluent total volatile acid concentrations for the HYBRID pilot plant.

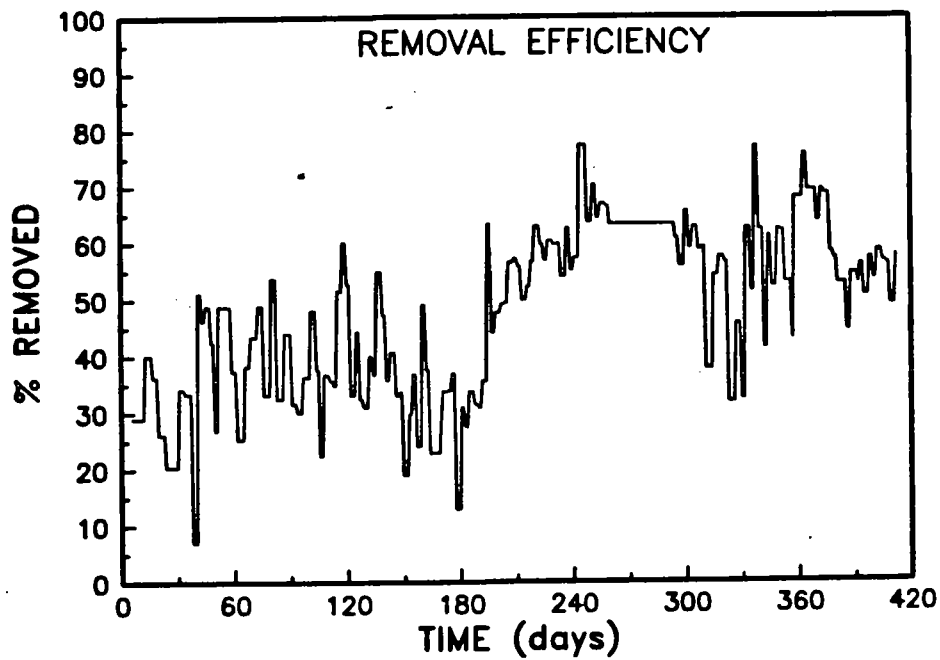


Figure 5.6 COD removal efficiency of the HYBRID pilot plant.

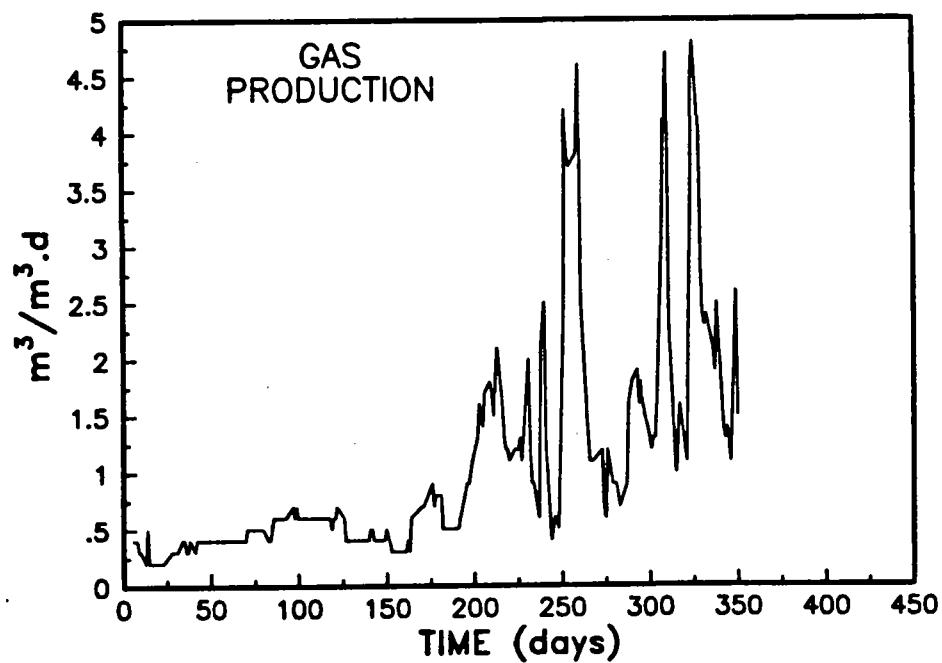


Figure 5.7 Biogas production of the HYBRID pilot plant.

Cumulative operating data for both the start up and subsequent experimental periods are summarized in Table 5.1. The low removal efficiency and biogas yields observed during start-up reflect the nutrient limitation during this period. The 57% COD removal efficiency and the methane yield of  $0.32 \text{ m}^3/\text{kg COD removed}$  observed after start up is similar to the performance observed in high rate anaerobic reactors operated with the same wastewater in the study by Hall *et. al.* (1986).

## 5.2 Mechanistic Modelling of Steady State Operation

Data collected during steady state operating periods was used to evaluate the adequacy of both the two population and four population mechanistic models in predicting steady state operation. Parameters in the models were adjusted to provide the best visual fit of the steady state model predictions to the pilot plant data. Steady state model predictions were obtained numerically by running simulations until no change in process states was observed over time for a given set of parameter values.

Total bacterial concentrations were assumed equal to the measured total bed volatile solids (Figure 5.8). The proportions of each bacterial group present were adjusted to fit the data.

An initial set of parameters in the two population model was obtained from Hill and Barth (1977) for use as the base case in the model calibration. These parameter values are summarized in the "Base Case" column of Table 5.2. For comparison, parameter values summarized in the review paper by Henze and Harremoes (1983) are included in the "Literature Values" column of Table 5.2. It has been shown previously that a parameter set found to give a good fit to experimental data when using a Monod kinetic model is not a unique parameter set and that the parameter estimates are highly sensitive to measurement noise (Holmberg and Ranta,

Table 5.1 Cumulative Operating Data

Cumulative Parameter	Start-Up* Period	Experimental** Period
COD Loaded ( $\text{kg}/\text{m}^3$ )	1322	1398
COD Removed ( $\text{kg}/\text{m}^3$ )***	517	802
Percent Removed	39	57
Biogas Produced ( $\text{m}^3/\text{m}^3$ )	133	370
Biogas Yield ( $\text{m}^3/\text{kg COD}_r$ )	0.26	0.46
Methane Produced ( $\text{m}^3/\text{m}^3$ )	93	257
Methane Yield ( $\text{m}^3/\text{kg COD}_r$ )	0.18	0.32
Methane Content (%)	70	70

\* Operating Days 1-216

\*\* Operating Days 217-413

\*\*\* Removal based on total influent COD and filtered effluent COD

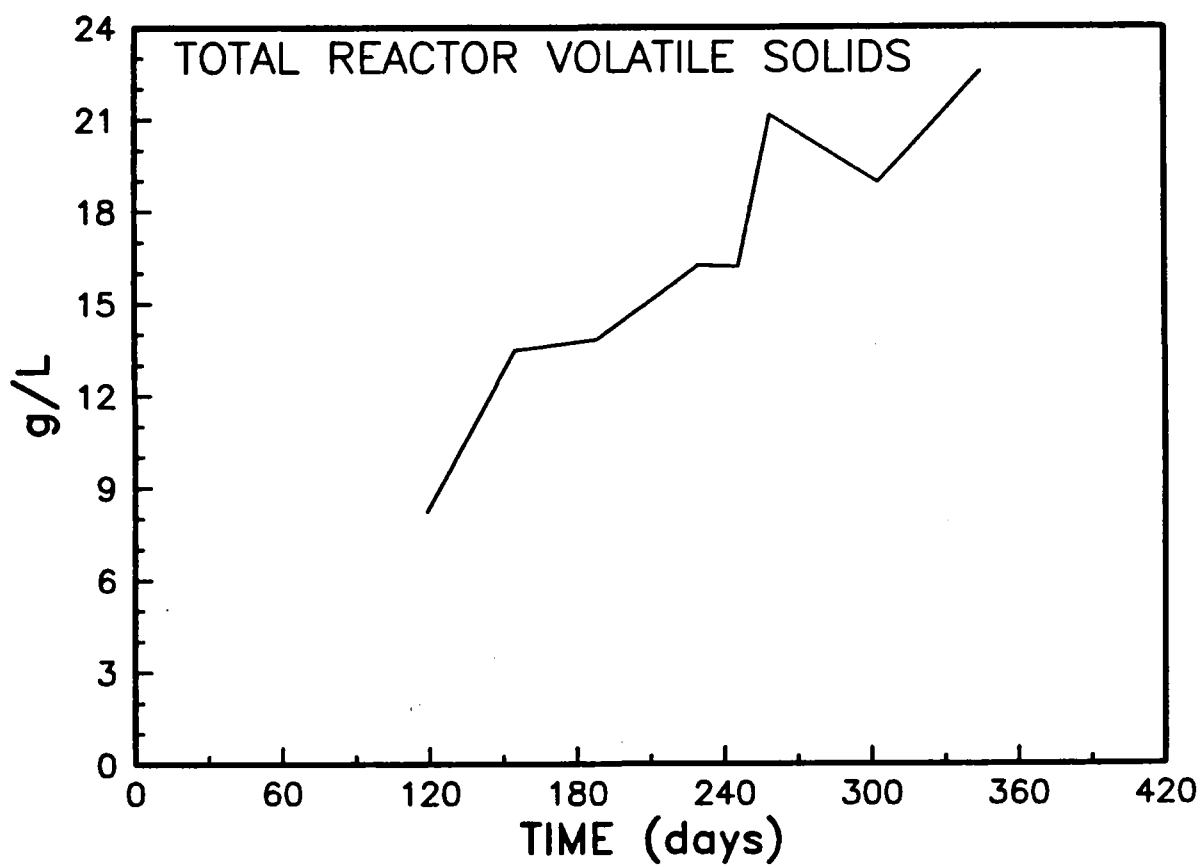


Figure 5.8 Total bed volatile solids in the HYBRID reactor



Table 5.2 Two Population Model Parameter Values

Parameter	Base Case	Steady State	Concentration Step #2	Feed Step #3	Literature* Values
KXS (mg/mg)	0.20	0.35	0.35	0.35	0.15-0.54
SMAX (1/day)	0.4	0.5	0.5	0.5	1.3-30
KAS (mg/L)	150	1880	1880	1880	23-37000
KHAX (mg/mg)	2.45	1.25	1.25	1.25	
KXS1 (mg/mg)	0.06	0.06	0.06	0.06	
MMAX (1/day)	0.4	0.25	0.25	0.4	0.08-3.4
KM (mg/L)	3100	292	292	292	2-3900
KCH4 (mmole/mg)	0.26	0.35	0.35	0.4	
BACTERIAL POPULATIONS (Mass Fractions)					
MF	0.1	0.1	0.1	0.1	
AF	0.9	0.9	0.9	0.9	

\* Henze and Harremoes (1983)

1982). This could partly explain why there is a wide range of parameter values found in the literature. The other columns in Table 5.2 contain parameter sets found when simulating the experimental data. These columns will be discussed in later sections of the report.

An initial parameter set for the four population model was obtained from information presented in the modelling study of Mosey (1983). Maximum specific growth rates and saturation constants used by Mosey were taken from previous experimental studies. Yields were calculated by Mosey from adenosine triphosphate (ATP) production based on known metabolic pathways and using the cell yield relationship established by Bauchop and Eldsen (1960) (10 g cells formed per mole of ATP generated). Considering only the uptake of substrate for energy, yields for the four population model mass balances were calculated. An example of the yield calculation is included in Appendix I. The resulting parameter values are summarized in the "Base Case" column of Table 5.3. The other columns contain parameters resulting from data fitting and will be discussed later.

Process responses investigated were effluent filtered COD (FCOD), volatile acid concentrations and methane production rates. A measurement of gas phase hydrogen concentration was not available during experimentation because attempts to operate the GMI Hydrogen Monitor were unsuccessful. The carbon dioxide balance was also omitted in an effort to simplify this initial phase of modelling.

Measured steady state values for the HYBRID reactor are compared to the fitted model predictions in Figures 5.9 to 5.14. Error bars given for the measured data are 95% confidence intervals calculated from daily or hourly pilot plant measurements. Sampling and analytical variability and process drift caused by slow biological responses are expected to be the

Table 5.3 Four Population Model Parameter Values

Parameter	Base Case	Steady State	Concentration Step #2	Feed Step #3
GMAX (1/day)	42.9	1.0	1.0	1.0
KSG (mg/L)	23	1800	1800	1800
PMAX (1/day)	0.38	0.28	0.28	0.28
KSP (mg/L)	37	37	37	37
BMAX (1/day)	0.71	0.5	0.5	0.5
KSB (mg/L)	7.3	7.3	7.3	7.3
MMAX (1/day)	0.4	0.39	0.39	0.75
KSM (mg/L)	166.8	166.8	166.8	166.8
MHMAX (1/day)	4	6.5	6.5	6.5
KSH (mg/L)	0.0133	0.0133	0.0133	0.0133
KAC (mg/mg)	0.22	0.18	0.18	0.18
KPR (mg/mg)	0.11	0.11	0.11	0.11
KBT (mg/mg)	0.11	0.11	0.11	0.11
KGP (mg/mg)	7.5	7.8	7.8	7.8
KPRA (mg/mg)	0.14	0.14	0.14	0.14
KGB (mg/mg)	4.44	7.4	7.4	7.4
KBTA (mg/mg)	0.23	0.23	0.23	0.23
KGA (mg/mg)	3.0	2.0	2.0	2.0
KPA (mg/mg)	5.8	5.8	5.8	5.8
KBA (mg/mg)	5.9	5.9	5.9	5.9
KAM (mg/mg)	0.04	0.03	0.03	0.03
KHA (mmole/mg)	0.1	0.1	0.1	0.1
KHBA (mmole/mg)	0.01	0.01	0.01	0.01
KHPA (mmole/mg)	0.3	0.3	0.3	0.3
KHCM (mg/mmole)	2.0	1.0	1.0	1.0
KCO2GA (mmole/mg)	0.05	0.05	0.05	0.05
KCO2GB (mmole/mg)	0.1	0.1	0.1	0.1
KCO2A (mmole/mg)	0.4	0.4	0.4	0.4
KCO2H (mg/mmole)	8.0	8.0	8.0	8.0
KCH4A (mmole/mg)	0.3	0.5	0.5	0.5
KCH4H (mmole/mg)	0.08	0.15	0.15	0.15
BACTERIAL POPULATIONS (Mass Fractions)				
AF	0.85	0.85	0.85	0.85
PA	0.025	0.025	0.025	0.025
BA	0.025	0.025	0.025	0.025
AMF	0.035	0.035	0.035	0.035
HMF	0.065	0.065	0.065	0.065

main factors contributing to the variability in the measurements.

The agreement between measured values and model predictions is reasonably good and demonstrates that either the two population or the four population model could describe the steady state behaviour of the variables studied under most operating conditions. Model predictions fit the measured steady state effluent FCOD concentration data (Figure 5.9) reasonably well at all conditions except steady state period #8 (representing the end of concentration step #2). Under these conditions, effluent FCOD was underestimated by both models. The predicted methane production rate (Figure 5.10) was also close to experimental values at all but steady state period #8. The models overestimated the data at this point. The total volatile acid (TVA) predictions (Figure 5.11) of both models agreed with the measured data at period #8. However, the TVA concentrations at period #3 were overestimated by both models and by the two population model at period #5. The predictions of individual volatile acids by the four population model fit the data reasonably well, with the exception of periods #3 and #5 where acetic acid (Figure 5.12) was overestimated, period #5 where propionic acid (Figure 5.13) was underestimated, and period #7 where butyric acid (Figure 5.14) was underestimated.

The inadequacy of the models in describing the response during period #8 may have been caused by an inhibition phenomena not taken into account by either model. The overestimated COD removal and gas production rates during this period would reinforce this hypothesis. If an important mechanism was missing from the models, a single parameter set would not be

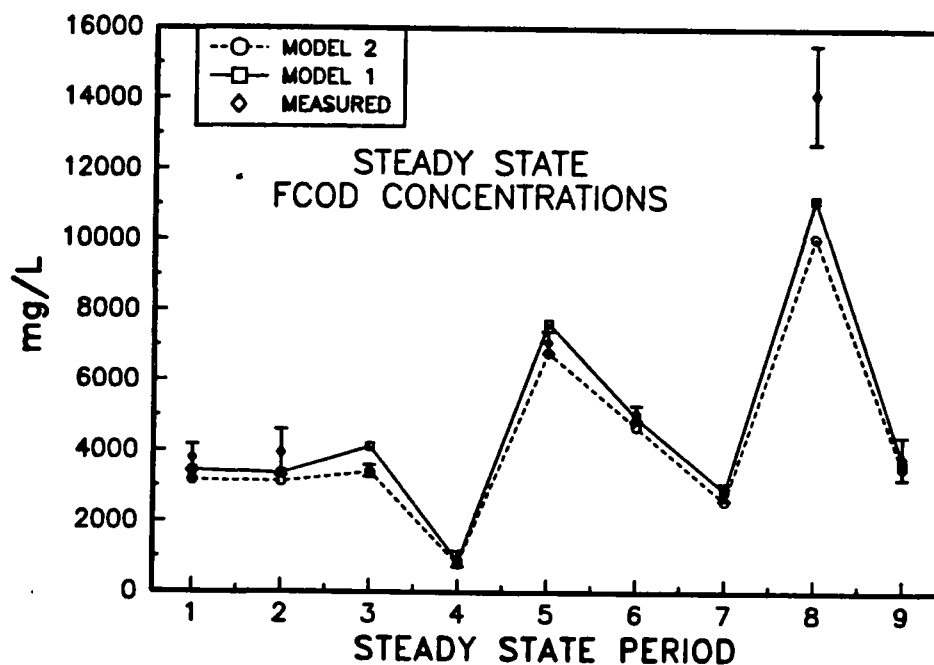


Figure 5.9 Measured and predicted steady state effluent FCOD (Model 1 = 2 population model; Model 2 = 4 population model)

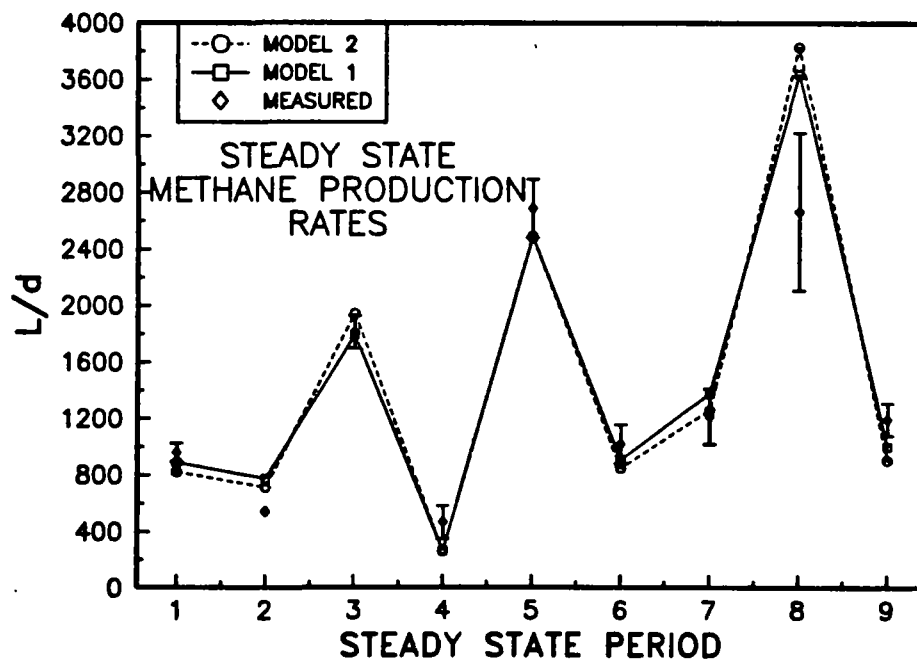


Figure 5.10 Measured and predicted steady state  $\text{CH}_4$  production (Model 1 = 2 population model; Model 2 = 4 population model)

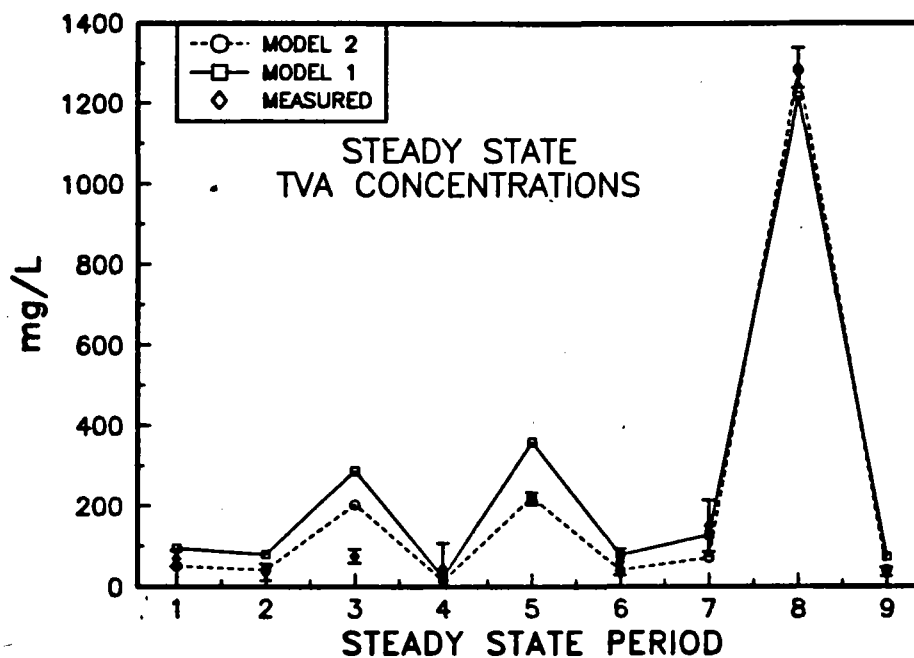


Figure 5.11 Measured and predicted steady state effluent total volatile acids (Model 1 = 2 population model; Model 2 = 4 population model)

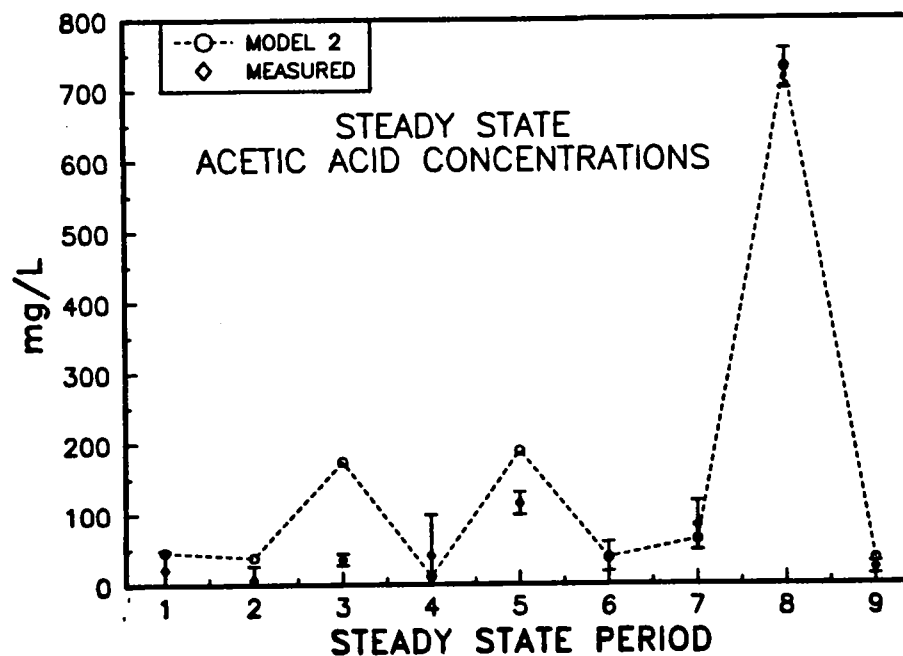


Figure 5.12 Measured and predicted steady state effluent acetic acid (Model 1 = 2 population model; Model 2 = 4 population model)

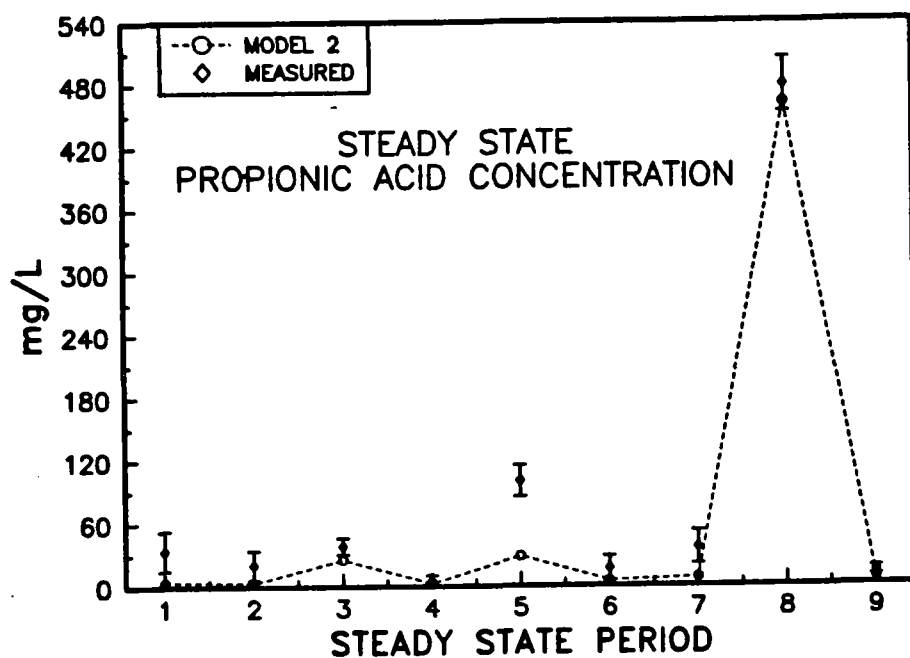


Figure 5.13 Measured and predicted steady state effluent propionic acid

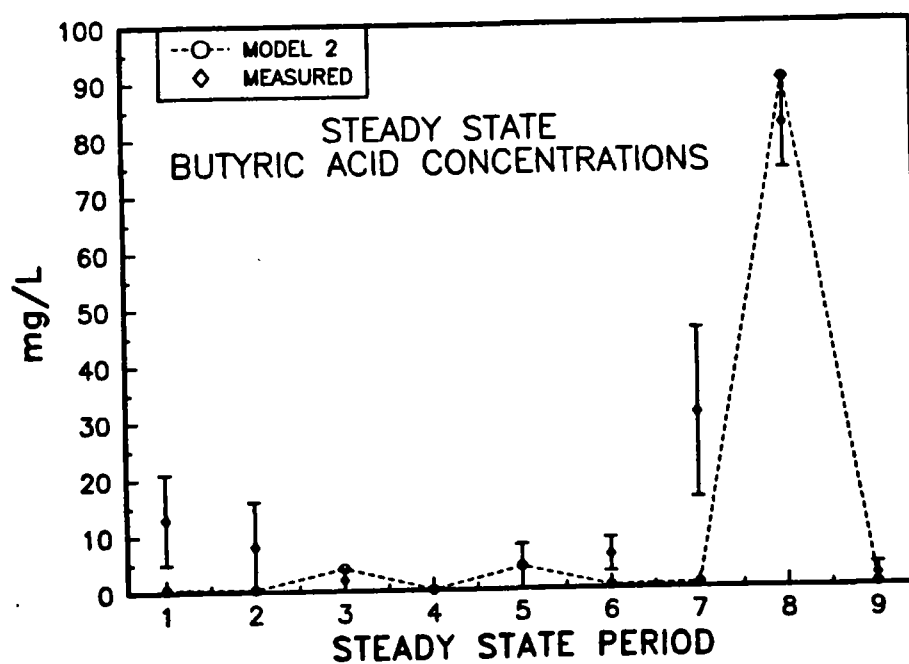


Figure 5.14 Measured and predicted steady state effluent butyric acid

adequate for all operating conditions. As a possible solution to a similar problem, the use of more than one model when considering a wide range of operating conditions has been investigated in the design of a multivariable adaptive controller for the activated sludge process (Cheruy et. al., 1982).

The predictions of the gas phase hydrogen concentration by the four population model are plotted in Figure 5.15. The range of concentrations predicted is slightly lower than the range of 40-80 ppm measured by Mosey (1983) in the gas from municipal digesters.

The parameter sets resulting from the visual fit of the two population and four population models to the steady state data are shown in the "Steady State" columns of Table 5.2 and Table 5.3, respectively. In the two population model, all fitted parameters were within an order of magnitude of the base case except for the half saturation constants of the Monod growth rate expressions. However, since the form of the growth rate expressions in the two population model was not the same as the expressions in the Hill and Barth model (where an inhibition term was added to the growth expressions), this difference in parameter values was not surprising. The only major differences from the base case in the four population model were the values of the Monod growth rate constants for the acid-formers. In the fitted parameter set, the value of the maximum specific growth rate (GMAX) was 1.0/day compared to 42.9/day in the base case. The fitted value of the saturation constant (KSG) was 1800 mg/L compared to the base case value of 23 mg/L. The physical significance of this difference is that for the system studied here, a lower rate of uptake of acid-former substrate (measured as the biodegradable portion of the FCOD in the reactor) would be expected for any concentration of substrate in the reactor. For any given HRT (all other conditions being constant), the



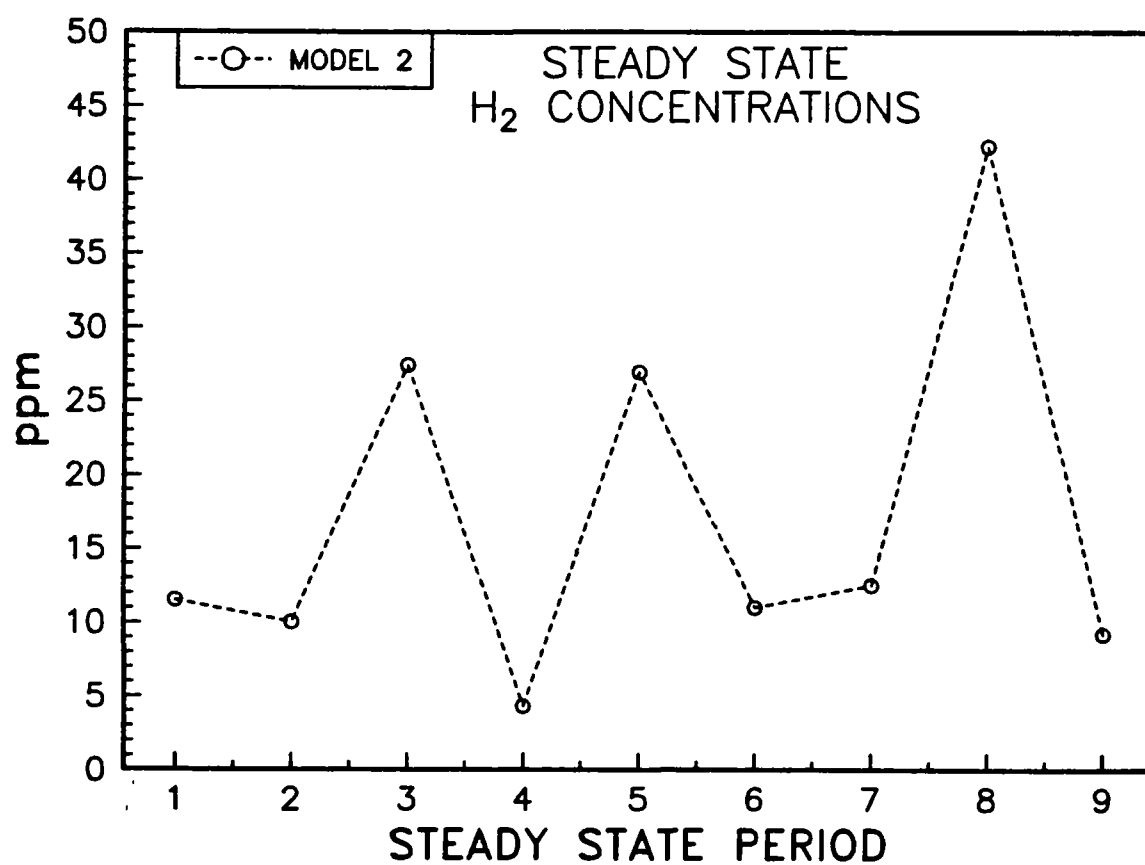


Figure 5.15 Predicted steady state gas phase hydrogen concentration  
(Model 2 = four population model)

effluent substrate concentration would therefore be higher for the present system as compared to a system represented by the base case parameter set. The base case parameters were taken from a study in which a pure glucose substrate was used (Ghosh and Pohland, 1974), whereas the acid-former substrates in the present study might have included more complex polymeric carbohydrates such as cellulose (Jurgensen *et. al.*, 1985). The additional degradation steps for these materials could explain part of the difference in the rate of uptake over a pure glucose substrate. Any differences between parameter sets should also be considered in light of the findings of Holmberg and Ranta (1982) discussed earlier. These researchers recommended that Monod expressions be considered as black-box rather than physical models, and cautioned against attributing differences in parameter values to biological phenomena. However, in comparing the parameters obtained by Ghosh and Pohland with the present parameter set, the large difference in experimental conditions would be expected to have some effect on the parameter values.

### 5.3 Dynamic Operating Results

Approximate dynamic characteristics of the response of effluent acetic, propionic, butyric, and TVA concentrations, effluent FCOD concentration and methane flow rate to step changes in the HYBRID reactor feedrate and feed concentration are summarized in Table 5.4. The response curves generated by the step tests were analysed graphically to estimate the approximate system time constants, process gains, deadtimes and response orders. With the exception of the methane flow rate response observed during concentration step #2, all of the responses appeared approximately first order. Feed step #1 was aborted due to a loss of

Table 5.4 Summary of Characteristics of HYBRID Response During Step Testing

Experiment	Response Variable	Time Constant (Hours)	Deadtime (Hours)	Gain*
Feed Step #1 (Aborted)				
Feed Step #2	FCOD	-	-	-
	Acetic Acid	-	-	-
	Propionic Acid	-	-	-
	Butyric Acid	-	-	-
	TVA	-	-	-
	Methane	0.5	0.25	1.5
Feed Step #3	FCOD	-	-	-
	Acetic Acid	3	3	0.04
	Propionic Acid	15	3	0.1
	Butyric Acid	-	-	-
	TVA	4	3	0.14
	Methane	0.5	0	1.8
Concentration Step #1	FCOD	14	1	0.4
	Acetic Acid	-	-	-
	Propionic Acid	4	4	0.01
	Butyric Acid	-	-	-
	TVA	4	4	0.01
	Methane	1.5	0.5	0.14
Concentration Step #2	FCOD	16	1	0.7
	Acetic Acid	11	8	0.04
	Propionic Acid	18	2	0.02
	Butyric Acid	14	4	0.004
	TVA	20	5	0.07
	Methane	0.5	0	0.09

\* Units for Gain:  
 Feed Steps;  
 FCOD, Acetic, Propionic and Butyric Acids, (mg/L)/(L/d)  
 Methane (L/d)/(L/d)  
 Concentration Steps;  
 FCOD, Acetic, Propionic and Butyric Acids, (mg/L)/(mg/L)  
 Methane (L/d)/(mg/L)

recycle shortly after the beginning of the experiment. Feed step #3 was terminated after only 3 HRT's because of operating problems caused by an unexpected change in feed composition. Response variables for which no time constant, deadtime or gain is recorded did not show a significant response to the forcing function.

In all tests, the methane production rate was observed to rise significantly and suddenly in response to the forcing function, illustrating that the methane production is a very sensitive indicator of changing loading conditions. However, it is difficult to deduce anything about the process efficiency with a measurement of only the methane production rate. For example, consider the change in removal efficiency during concentration step #2. The initial and final average influent COD concentrations and effluent FCOD concentrations during the concentration step tests are shown together with calculated COD removal efficiencies in Table 5.5. An examination of this data reveals that although a significant increase in the methane production rate was observed (Figure 5.10 and Table 5.4), the COD removal efficiency dropped from 59% to 40%.

Since acetic acid is considered to be the major precursor to methane formation, a relationship between the acetic acid response and the methane response would be expected. However, feed step #3 and concentration step #2 were the only step tests in which the increase in the effluent acetic acid concentration was large enough to be distinguishable from measurement noise. This is not a positive indication that there is no relationship between the effluent acetic acid concentration and methane production. It is possible that the methanogens respond to smaller concentration changes than is detectable due to the variability of the acetic acid analysis. In the tests where an acetic acid response was measured, the time constant of the response was substantially greater than the time constant of the

Table 5.5 Initial and Final COD Removal Efficiencies During Concentration Step Tests

Step Test	Initial Conditions			Final Conditions		
	Influent COD (mg/L)	Effluent FCOD (mg/L)	COD Removal (%)	Influent COD (mg/L)	Effluent FCOD (mg/L)	COD Removal (%)
Conc. Step #1	2150	945	56	18160	7095	60
Conc. Step #2	6936	2855	59	23903	14141	41

methane response. However, a difference in the time constant of the methane response and any precursor might be expected due to differences between production and consumption rates. For example, the maximum production rate of methane could be reached at a relatively low residual acetic acid concentration, while the production of acetic acid by the acid-formers could continue at a rate which would result in the effluent acetic acid continuing to climb after this maximum had been reached.

Of the soluble effluent components measured, a significant response of the propionic acid concentration to changes in loading conditions was observed most often. A significant response in acetic acid and butyric acid was only observed during the most severe tests (feed step #3 and concentration step #2). The effluent propionic acid concentration may therefore be one of the more sensitive indicators of process efficiency. Since propionic acid is a process intermediate, an increase in concentration would indicate that biodegradable components of the wastewater are not being completely stabilized. The disadvantage of propionic acid as an indicator of process efficiency is that it is not readily measurable on-line.

The effluent FCOD concentration showed no measurable response to feedrate changes. In other words, the organic removal rate increased in proportion to the increase in the organic loading rate that resulted from the feedrate changes. This would indicate that the activity of the biomass was not at a maximum before the feedrate step changes.

A significant response in the effluent FCOD concentration was observed during concentration step tests. Since the COD removal efficiency before and after the implementation of concentration step #1 was relatively constant (Table 5.5), the response in effluent FCOD concentration was

likely due to the increased feed concentration of inerts washing through the system. In contrast, the decrease in COD removal efficiency during concentration step #2 indicates that a portion of the effluent response was due to an increase in the concentration of biodegradable compounds in the effluent.

The results of the step tests illustrated some of the limitations of this approach to process identification. Due to the high level of noise in some of the responses, it was difficult to estimate some of the characteristic response parameters shown in Table 5.4. This problem was compounded by the long time periods required for the system to reach a steady state. As is evidenced by the fact that feed step #1 was aborted and feed step #3 was cut short due to operating problems, even in a controlled pilot plant setting it was difficult to keep all operating conditions constant until a new true steady state was reached.

The results from one of the PRBS experiments was used to build an empirical model for the biogas flowrate response to changes in reactor feedrate. The feedrate forcing function and the process response during this model building run are plotted in Figure 5.16. A time series analysis of the data using the Box and Jenkins (1976) approach resulted in a simple first order plus deadtime discrete transfer function with the noise represented by a second order moving average process (Table 5.6).

There were a number of advantages to using the PRBS experimental design and a time series analysis of the resulting data over the step test approach. First, it was not necessary to attain a steady state between input perturbations. This allowed much more dynamic process information to be generated within a given experimental period. Second, by using the time series analysis method, a dynamic process model and a process noise model were identified simultaneously. This minimized the difficulties in

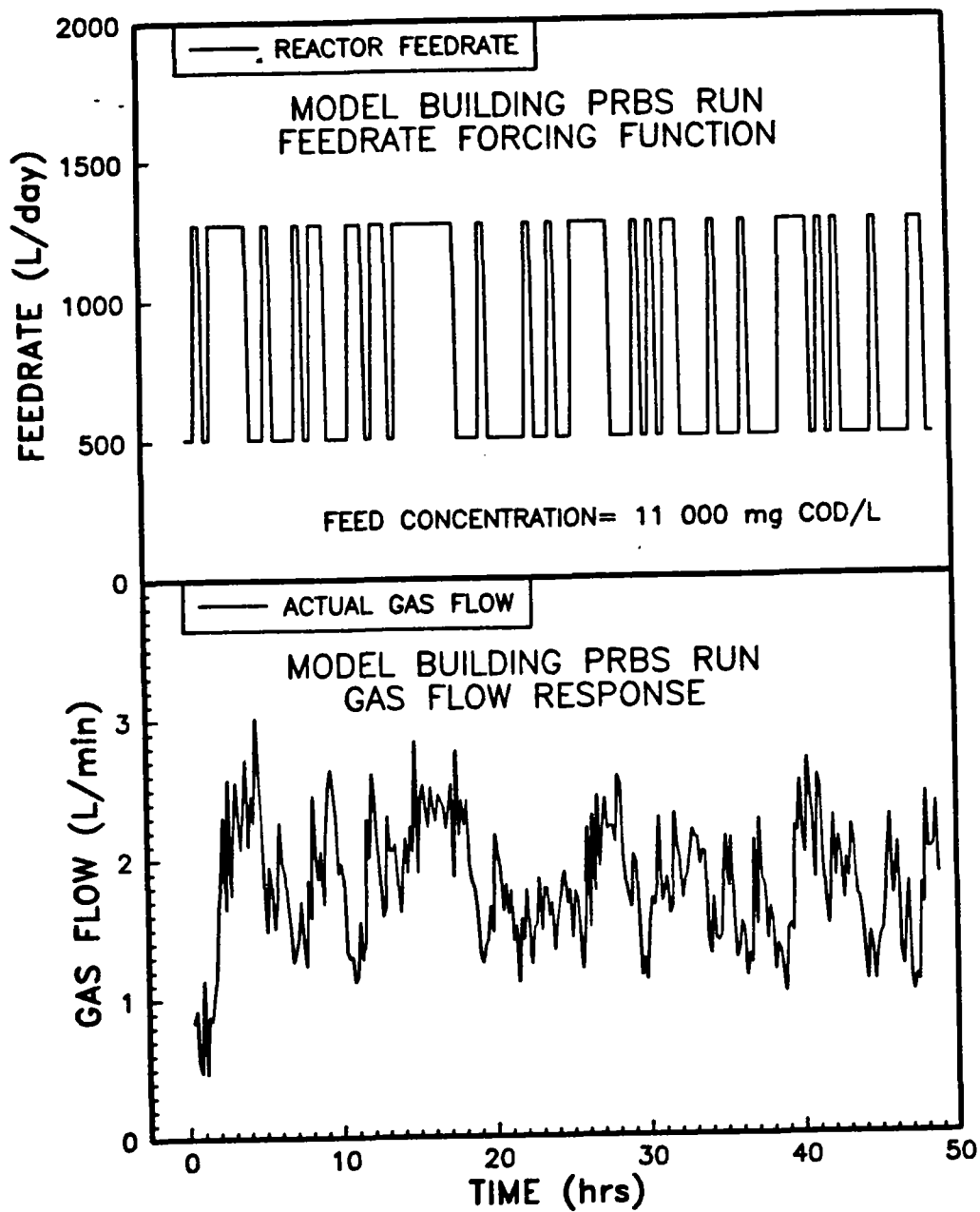


Figure 5.16 PRBS feedrate experiment used to build a model for biogas flow using time series analysis



$$Y_t = \frac{3.266 \times 10^{-4}}{1 - 0.7741 B} X_{t-2} + (1 + 0.1683 B + 0.1700 B^2) a_t$$
$$Y_t = \text{total biogas flowrate at time } t$$
$$X_t = \text{reactor feedrate at time } t$$

$a_t$  = white noise sequence of independent random variables with zero mean and constant variance

B = backward difference operator (ie:  $BY_t = Y_{t-1}$ )

**Note:**

Equivalent continuous time constant ;  $= -10/\ln(0.7741)$   
 $= 39$  minutes

identifying the process model caused by disturbances in the process output not related to the designed perturbations.

The PRBS results verified the fast gas production response observed during step testing. The equivalent continuous time constant was estimated from the discrete transfer function model to be 0.65 hours. This is within the range of 0.5 to 1.5 hours observed during step test experiments.

#### 5.4 Mechanistic Modelling of Dynamic Operation

Since the most substantial response of measured variables was observed during feed step #3 and concentration step #2, data collected during these experiments was used to evaluate the ability of the two population and four population models to predict the dynamic response of the process to changes in feedrate and feed concentration. Characteristics of the predicted response of the HYBRID in these step tests are summarized in Table 5.7. The predicted process response is compared to the actual measured response in Figures 5.17 to 5.22. In fitting the models to the concentration step, none of the parameter values were adjusted from the parameter set found to give the best visual fit to the steady state response (Tables 5.2 and 5.3). The value of the maximum specific growth rate of the aceticlastic methane-formers was adjusted to give the best visual fit of the predictions of both models to the feed step response

Both models correctly predict the effluent FCOD to remain relatively constant during feed step #3 (Figure 5.17). The two population model did not predict the fast gas response observed on the actual process while the four population model predicted a response with the same time constant as the measured response (Figure 5.18). The gain of the gas response was slightly overestimated by the four population model. With the exception of

Table 5.7 Summary of Characteristics of Dynamic Response of HYBRID to Feed Step #3 and Concentration Step #2 as Predicted by Two Population Model and Four Population Model

Experiment	Response Variable	Time Constant (Hours)	Deadtime (Hours)	Gain*
<u>Two Population Model</u>				
Feed Step #3	FCOD	4	0	1.3
	TVA	4	0	0.1
	Methane	3	0	1.9
Concentration Step #2	FCOD	19	0	0.5
	TVA	12.5	0	0.06
	Methane	5	0	0.1
<u>Four Population Model</u>				
Feed Step #3	FCOD	0.5	0	0.2
	Acetic Acid	1.0	0	0.06
	Propionic Acid	8	0	0.1
	Butyric Acid	3	0	0.02
	TVA	4	0	0.2
	Methane	0.5	0	2.0
	Hydrogen	<0.5	0	0.03
Concentration Step #2	FCOD	25	0	0.4
	Acetic Acid	6	0	0.04
	Propionic Acid	21	0	0.02
	Butyric Acid	14	0	0.005
	TVA	11	0	0.07
	Methane	1.0	0	0.15
	Hydrogen	<0.5	0	0.002

\* Units for Gain:  
 Feed Steps;  
 FCOD, Acetic, Propionic and Butyric Acids, (mg/L)/(L/d)  
 Methane (L/d)/(L/d)  
 Hydrogen (ppm)/(L/d)  
 Concentration Steps;  
 FCOD, Acetic, Propionic and Butyric Acids, (mg/L)/(mg/L)  
 Methane (L/d)/(mg/L)  
 Hydrogen (ppm)/(mg/L)

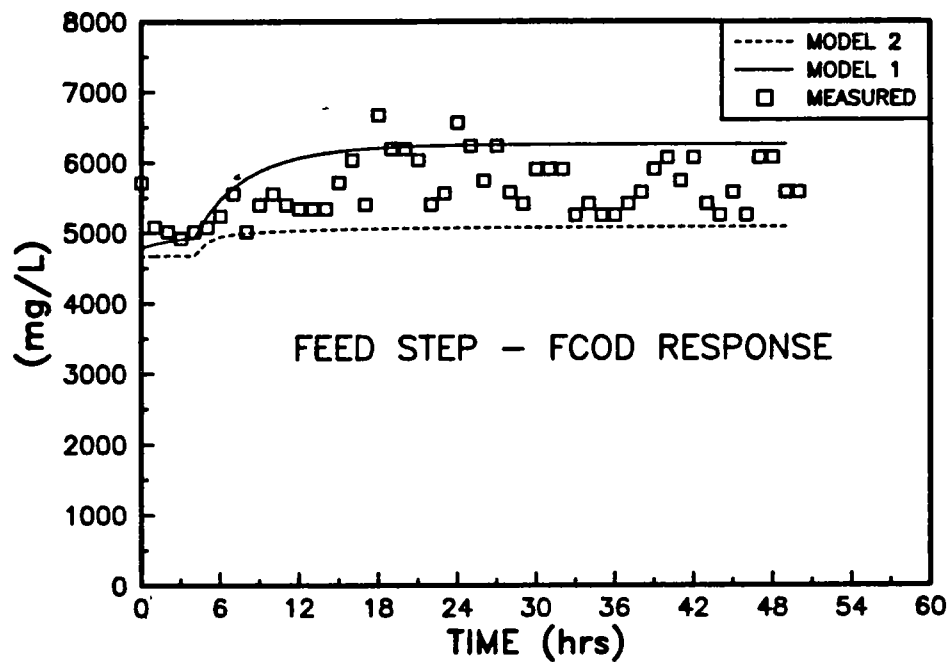


Figure 5.17 Measured and predicted response of effluent FCOD to feed step #3 (Model 1 = 2 population model; Model 2 = 4 population model)

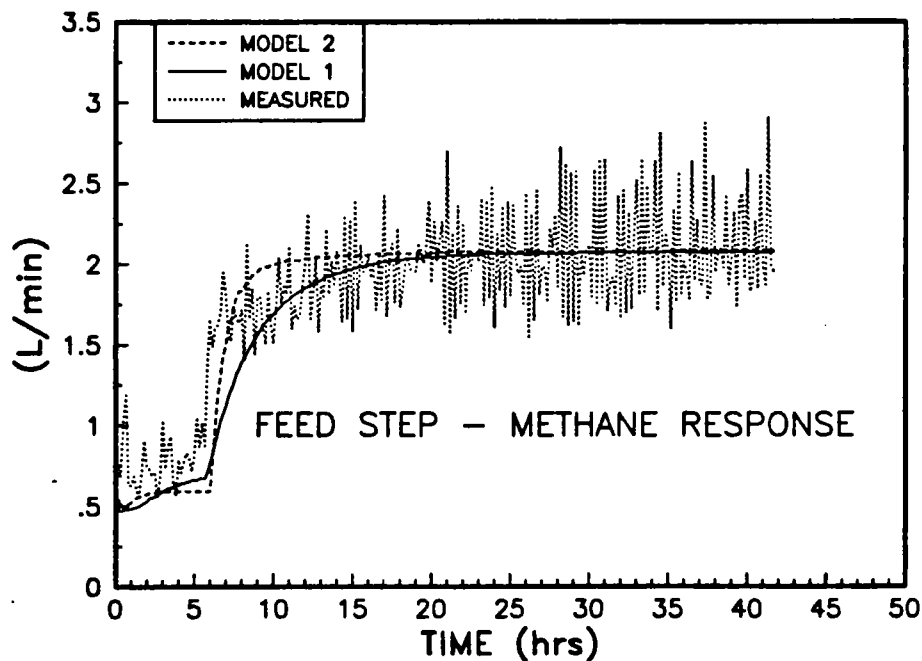


Figure 5.18 Measured and predicted response of methane production rate to feed step #3 (Model 1 = 2 population model; Model 2 = 4 population model)

the deadtime observed in the measured response of the effluent TVA, the model predictions of TVA show excellent agreement with the measured response (Figure 5.19). The predictions of individual acid responses by the four population model are also reasonable.

The difficulties in fitting the model predictions to the measured response of concentration step #2 in the steady state modelling phase, are also apparent during the dynamic response. Although the time constant of the FCOD response (Figure 5.20) is reasonably well predicted, the gain is significantly underestimated. The measured response of methane exhibits a slow decline after reaching a maximum within one hour of the step input (Figure 5.21). In contrast, both models predict a first order response. The four population model comes closer to predicting the initial rapid methane production.

The predicted dynamic response of the effluent TVA concentration of both models shows excellent agreement with the measured response during concentration step #2. As in feed step #3, the characteristic of the TVA response not satisfactorily predicted by the models, was the deadtime. In comparing the actual and predicted responses of individual volatile acids (Figure 5.22), the lags exhibited by the acids become more apparent.

The mixing characteristics of the HYBRID reactor could have contributed to the time lags in the observed volatile acid response. Well mixed conditions would result in a change in the concentration of a soluble component in the reactor being immediately dispersed throughout the reactor and appearing as a change in the effluent concentration of that component. Under plugflow mixing conditions, profiles of soluble components would be observed along the length of the reactor, and a change in concentration of a soluble component near the inlet of the reactor would not be immediately observed by measuring the outlet concentration of that component. An

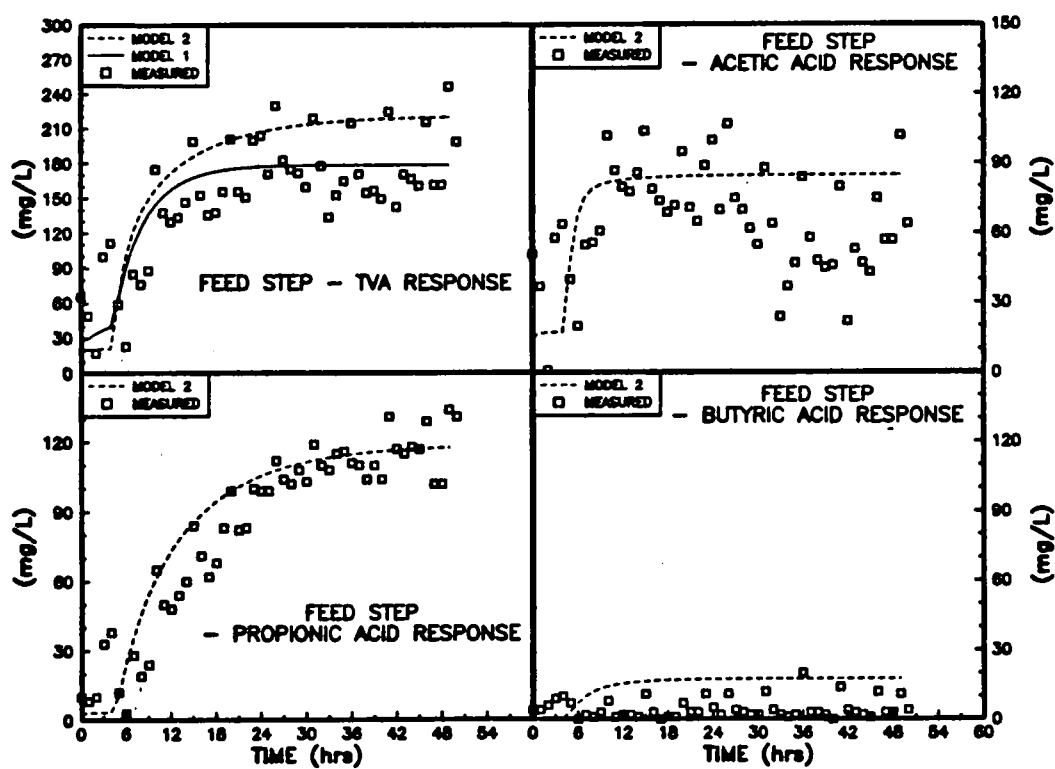


Figure 5.19 Measured and predicted responses of effluent volatile acid concentrations to feed step #3 (Model 1 = 2 population model; Model 2 = 4 population model)

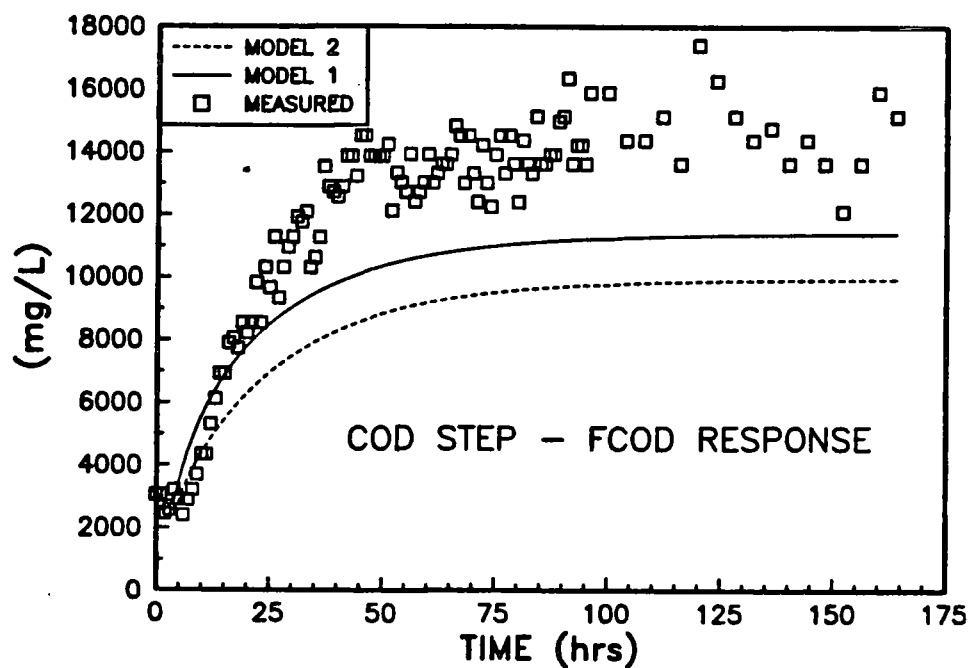


Figure 5.20 Measured and predicted response of effluent FCOD to concentration step #2 (Model 1 = 2 population model; Model 2 = 4 population model)

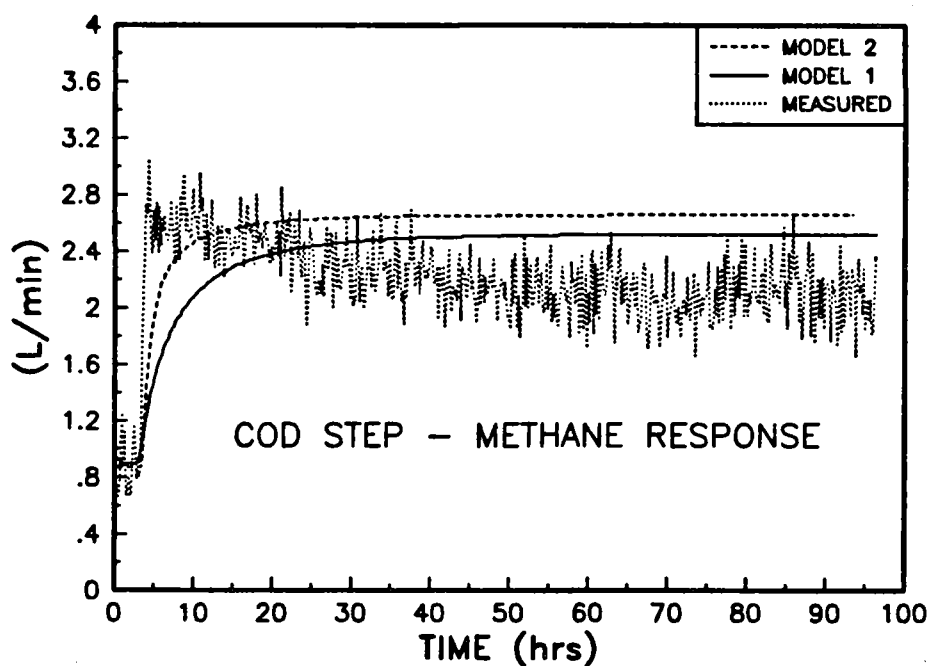


Figure 5.21 Measured and predicted response of methane production rate to concentration step #2 (Model 1 = 2 population model; Model 2 = 4 population model)

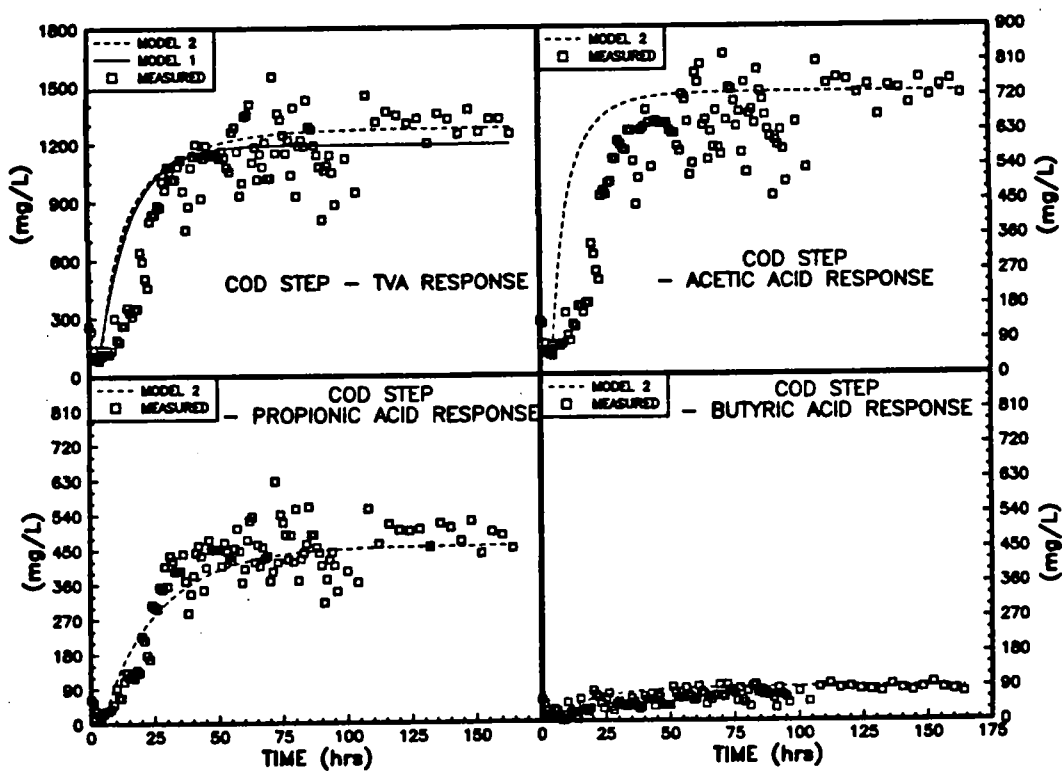


Figure 5.22 Measured and predicted responses of effluent volatile acid concentrations to concentration step #2 (Model 1 = 2 population model; Model 2 = 4 population model)



examination of mixing patterns in the HYBRID reactor was not conducted during this study. The profiles of substrate and product concentrations along the length of an upflow anaerobic sludge blanket (UASB) reactor operating at steady state were measured in a study by Sam-Soon et. al. (1987). The acetic acid concentration was observed to reach a maximum near the bottom of the reactor. However, the UASB was operated without recycle. Inert tracer studies conducted previously by Hall (1985), demonstrated that high rate anaerobic processes with and without effluent recycle most closely resembled well mixed reactors, although significant deviations from ideal behaviour were observed. Included among these deviations was the observation that a finite time to the peak of residence time distribution curves existed. This indicated that an inlet disturbance would not be propagated to the reactor outlet instantaneously. The result would be a lag in the observed reactor response to inlet perturbations.

The biofilm characteristics of the HYBRID reactor could also have contributed to the observed volatile acid response time lags. Concentration gradients in the biofilm could result in the bacteria responding to different concentrations of substrates and products than those indicated by measuring effluent concentrations. Evidence in the literature of the possible significance of this effect in the HYBRID reactor seems contradictory. Henze and Harremoës (1983), estimated that diffusion effects would be minimal in anaerobic biofilms less than 1 mm in thickness. Kennedy and Droste (1986), found no evidence of diffusion limitations in anaerobic biofilms up to 2.6 mm in thickness. Switzenbaum and Eimstad (1987), measured granule diameters in UASB's of 0.7 mm and biofilm thicknesses in anaerobic filters of 50 microns. Neither would appear to be in the range where biofilm diffusion would be limiting. In

contrast, Sam-Soon et. al. (1987), measured granule sizes in a UASB which ranged from 1 to 4 mm in diameter.

A more conclusive assessment of the effects of both the mixing and the biofilm characteristics on the dynamic response of high rate anaerobic reactors is needed to determine whether the observed lags are due to the physical characteristics of the system or are due to a biological response not adequately described by the model kinetics. This would require that future dynamic experimentation include mixing studies, measurements of biofilm thicknesses, and the measurement of substrate and product concentrations along the length of the reactor during transients.

The predicted response of gas phase hydrogen during feed step #3 and concentration step #2 are shown in Figures 5.23 and 5.24, respectively. In both cases, the time constant of the hydrogen response was less than 30 minutes. A rapid hydrogen response to changes in organic loading has been reported by Barnes et. al. (1984).

The second PRBS experiment was used as additional verification of the four population model gas response predictions. The feedrate forcing function and the process response during this model verification run are plotted in Figure 5.25. The transfer function portion of the time series model derived from the first PRBS run (Table 5.5) showed excellent agreement with the measured gas production rate. The parameter set for the four population model derived by fitting the predictions to feed step #3, were used in this verification run. Although the gain was slightly overpredicted and the predictions were offset from the measured values, the time constant of the predicted response showed excellent agreement with the measured response.

The major advantage of the four population model over the two population model appears to be in the more accurate predictions of the

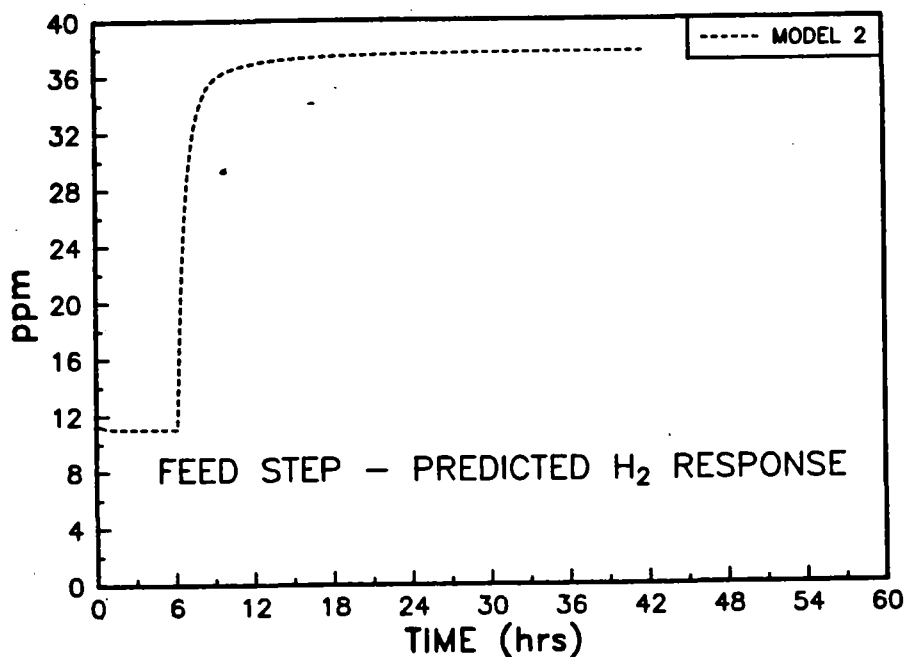


Figure 5.23 Predicted response of gas phase hydrogen concentration to feed step #3 (Model 2 = 4 population model)

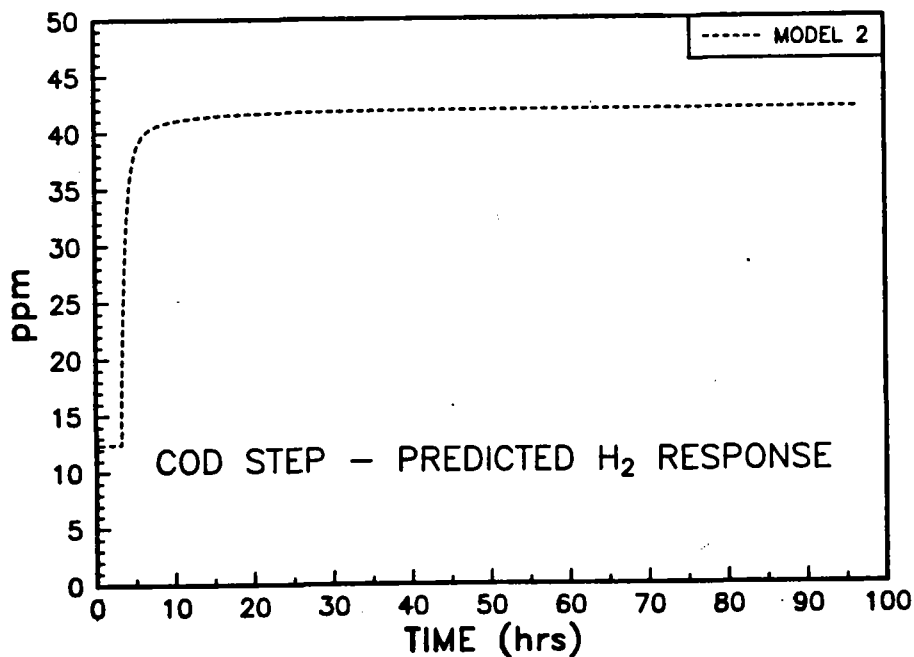


Figure 5.24 Predicted response of gas phase hydrogen concentration to concentration step #2 (Model 2 = 4 population model)

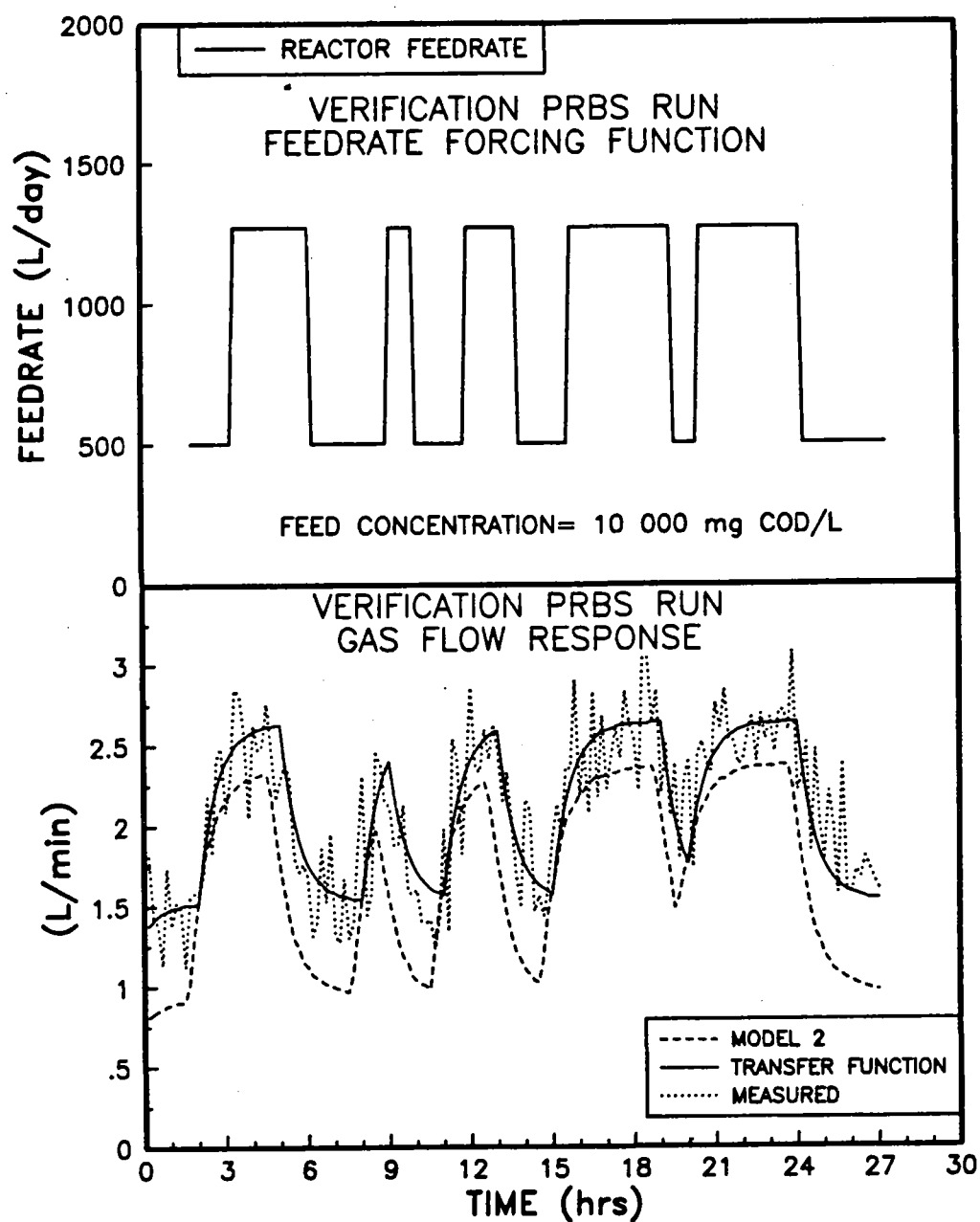


Figure 5.25 PRBS feedrate experiment used to verify 4 population model (Model 2) and transfer function model biogas predictions

dynamic characteristics of the gas response by the four population model. This increased accuracy results from the more detailed structure of the four population model. The prediction of methane flowrate by the four population model depends on the concentration of acetic acid and gas phase hydrogen. In the two population model, the predicted flowrate of methane depends on the total volatile acid concentration. Since the total volatile acid concentration response time constant is significantly longer than the time constant of the acetic acid response, the methane production rate time constant tends to be overpredicted by the two population model. However, more experiments are required to verify the relation between the responses of acetic acid and hydrogen, and the methane production rate response. These experiments would require a measurement of the concentration of the gas phase hydrogen concentration and a measurement of the concentration of acetic acid throughout the system during transient periods.

The advantages of the four population model need to be weighed against the disadvantage of increased model complexity. To make this assessment, a more detailed parameter identification study is required. If many of the parameters could be derived from stoichiometric considerations, the large number of parameters in the four population model would not be a serious limitation. However, if most of these parameters must be estimated from experimental data, the usefulness of the model in on-line control applications may be severely limited.

## 6. SUMMARY AND CONCLUSIONS

A pilot scale HYBRID reactor was operated under steady state and dynamic conditions using a pulp and paper mill effluent as a feedstock. An analysis of the reactor behaviour included mechanistic and empirical modelling of the process. The process input variables considered were influent concentration and feedrate. Output variables considered in the modelling exercise were effluent filtered COD, effluent volatile acid concentrations and methane production rates. The two mechanistic models evaluated were derived from two bacterial population, and four bacterial population assumptions. An empirical dynamic model for the single input-output pair of reactor feedrate and biogas flow response was developed from a time series analysis of one of the dynamic experiments. The pilot plant experiments and modelling led to the following conclusions

- 1) The methane production rate was found to be the most sensitive variable to changes in influent concentration or feedrate. A significant response was observed under all dynamic testing conditions studied, regardless of whether other output variables exhibited a significant response. The observed response was rapid, exhibiting a time constant in the range of 0.5 to 1.5 hours. Measurement of the methane production rate alone, however, was not found to be a good indicator of process efficiency.
- 2) The effluent propionic acid concentration was observed to be a sensitive indicator of process efficiency. However, obtaining on-line measurements of this variable may be difficult.
- 3) The two population and four population models were both able to describe the steady state behaviour of the variables studied under most operating conditions. However, neither model could adequately

predict the reduction in COD removal efficiency or the slow decline in the gas production rate observed during the most severe concentration step. The model inadequacies at this point were thought to be caused by an inhibition mechanism not described by either model.

- 4) Both mechanistic models were found to be adequate in describing most dynamic response characteristics of effluent volatile acid and FCOD concentrations following a step change in reactor feedrate or influent concentration, although the same model inadequacies discovered during steady state modelling were apparent.
- 5) The mechanistic models could not describe the time lags observed in the dynamic volatile acid responses. An assessment of the effects of mixing and biofilm characteristics on the dynamic response is needed to determine whether the observed lags were due to the physical characteristics of the reactor studied, or were due to a biological response not adequately described by the model kinetics.
- 6) The two population model was not able to simultaneously predict the correct dynamic response of the volatile acids and the gas flow. By considering individual volatile acid concentrations and the concentration of hydrogen in the gas phase, the four population model was able to correctly predict rapid changes in gas flow.
- 7) The complexity and the large number of parameters of the four population model could limit its application in on-line process control.

## 7. RECOMMENDATIONS

- 1) The carbon dioxide and hydrogen balances in the four population model should be verified experimentally.
- 2) Further experimentation should be carried out on a high rate anaerobic system in which the mixing and biofilm characteristics can be readily identified. Experimentation should include mixing studies, measurements of biofilm thicknesses, and the measurement of substrate and product concentrations along the length of the reactor during transients.
- 3) A detailed parameter estimation study involving both the two population and four population models should be conducted. The goal of this study would be to determine the number of parameters which need to be estimated from experimental data. If a large number of parameters calculated from theoretical considerations can be used successfully over a wide range of conditions, the goal of using the models in on-line applications would be more realistic.
- 4) Once an adequate model has been selected, it should be used off-line to evaluate options for process control and to assess the requirements for on-line sensors. It should be used on-line to provide estimates of important variables which cannot be measured.



## 8. REFERENCES

- Andrews, J. F., "Dynamic model of the anaerobic digestion process", ASCE J. San. Eng. Div., 95 (n.SA1), 95, 1969.
- Andrews, J. F. and S. P. Graef, "Dynamic modelling and simulation of the anaerobic digestion process", Advances in Chemistry Series, 105, (Edited by R. F. Gould), American Chemical Society, New York, 1971.
- Barnes, D., P. J. Bliss, B. Grauer, and K. Robins, "Pretreatment of high strength wastewater by an anaerobic fluidised bed process. Part II Response to organic load transients", Env. Tech. Letters, 6, 73-78, 1984.
- Bastin, G. and D. Dochain, "On-line estimation of microbial specific growth rates", Automatica, 22 (6), 705-709, 1986.
- Bastin, G., D. Dochain, M. Haest, M. Installe, and Ph. Opdenacker, "Modelling and adaptive control of a continuous anaerobic fermentation process", Proceedings of the 1st IFAC Workshop on Modelling and Control of Biotechnical Processes, Helsinki, Finland, August 17-19, 1982.
- Bauchop, T., and S. R. Eldsen, "The growth of microorganisms in relation to their energy supply", J. Gen. Microbiology, 23, 457-469, 1960.
- Beck, M. B., "Identification, estimation and control of biological wastewater treatment processes", IEE Proceedings, 133 (5), Pt. D, 1986.
- Beck, M. B., "Operational estimation and prediction of nitrification dynamics in the activated sludge process", Water Research, 15, 1313-1330, 1981.
- Beck, M. B. and P. C. Young, "Systematic identification of DO-BOD model structure", ASCE J. Env. Eng. Div., 99 (EE5), 909-927, 1976.

- Bellgardt, K. H., W. Kuhlmann, H. D. Meyer, K. Schugerl, M. Thoma, "Application of an extended Kalman filter for state estimation of a yeast fermentation", IEE Proceedings, 133 (5), Pt. D, 1986.
- Bolle, W. L., J. van Breugel, G. C. van Eybergen, N. W. F. Kossen and W. van Gils, "An integral dynamic model for the UASB reactor" Biotechnology and Bioengineering, 28, 1621-1636, 1986.
- Carr, A. D. and R. C. O'Donnell, "The dynamic behaviour of an anaerobic digester", Prog. Wat. Tech., 9, 727-738, 1977.
- Chalon, A., G. Bastin, and M. Installe, "Identification of a biomethanization process: A case study", 6th IFAC Symposium on Identification and System Parameter Estimation, Washington, June 7-11, 1982.
- Cheruy, A., L. Panzarella, and J. P. Denat, "Multimodel simulation and adaptive stochastic control of an activated sludge process", Proceedings of the 1st IFAC Workshop on Modelling and Control of Biotechnical Processes, Helsinki, Finland, August 17-19, 1982.
- Collins, A. S. and B. E. Gilliland, "Control of the anaerobic digestion process" ASCE J. San. Eng. Div., 100, (EE2), 487-506, 1977.
- Dochain, D. and G. Bastin, "Stable adaptive controllers for waste treatment by anaerobic digestion", Env. Tech. Letters, 6, 584-593, 1985.
- Dochain, D., G. Bastin, P. Renard, D. Poncelot, H. Naveau and E.-J. Nyns, "Computer control and monitoring of anaerobic wastewater treatment plants: Pilot scale applications", Proceedings of the EWPCA Conference on Anaerobic Wastewater Treatment, Amsterdam, Sept. 15-19, 1986.
- Eng, S. C., X. A. Fernandes and A. R. Paskins, "Biochemical effects of administering shock loads of sucrose to a laboratory-scale anaerobic (UASB) effluent treatment plant" Water Research, 20 (6), 789-794, 1986.

- Ghosh, S., and Pohland, F. G., "Kinetics of substrate assimilation and product formation in anaerobic digestion", Journal WPCF, **46**, 748-759, 1974.
- Graef, S. P. and J. F. Andrews, "Stability and control of anaerobic digestion", Journal WPCF, **46** (4), 666-683, 1974.
- Guilot, S. R. and L. van den Berg, "Dynamic performance of an anaerobic reactor combining an upflow sludge blanket and a filter for the treatment of sugar waste", Proceedings of the 39th Industrial Waste Conference, Purdue University, 1984.
- Halbert, D. J. and R. J. Wojtowicz, "The Modelling of an ANFLOW Municipal Waste-Treatment Unit", Oakridge National Laboratory Report ORNL/MIT-342, June, 1982.
- Hall, E. R., "Non-intrusive estimation of active volume in anaerobic reactors", Water Poll. Res. J. Canada, **20** (2), 44-54, 1985.
- Hall, E. R., C. F. Prong, P. D. Robson, and A. J. Chmelauskas, "Evaluation of anaerobic treatment for NSSC wastewater", 1986 Environmental Conference Proceedings, TAPPI PRESS, Atlanta, 207.
- Haime, A., E. Tiussa, and T. Tapani, "Dynamic modelling and control studies on the TAMAN process", Proceedings of the 1st IAWPRC Symposium on Forest Industry Wastewaters, Tampere, Finland, June 11-15, 1984.
- Harper, S. R. and F. G. Pohland, "Recent developments in hydrogen management during anaerobic biological wastewater treatment", Biotechnology and Bioengineering, **28**, 585-602, 1986.
- Henze, M. and P. Harremoes, "Anaerobic treatment of wastewater in fixed film reactors - A literature review", Wat. Sci Tech, **15**, 1-101, 1983.
- Heyes, R. H., and R. J. Hall, "Anaerobic digestion modelling - The role of  $H_2$ ", Biotechnology Letters, **3** (8), 431-436, 1981.

- Hill, D.T. and C. L. Barth, "A dynamic model for simulation of animal waste digestion", Journal WPCF, 49 (10), 2129-2143, 1977.
- Holmberg, A., "Modelling of the activated sludge process for microprocessor-based state estimation and control", Water Research, 16, 1233-1246, 1982.
- Holmberg, A. and J. Ranta, "Procedures for parameter and state estimation of microbial growth process models", Automatica, 18 (2), 125-145, 1982.
- Holmberg, U. and G. Olsson, "Simultaneous on-line estimation of oxygen transfer rate and respiration rate", Proceedings of the 1st IFAC Symposium on Modelling and Control of Biotechnological Processes, Noordwijkerhout, The Netherlands, Dec. 11-13, 1985.
- Jazwinski A. H., Stochastic Processes and Filtering Theory, Academic Press, New York, 1970.
- Jurgensen, S. L., M. M. Benjamin, and J. F. Ferguson, "Treatability of thermomechanical pulping process effluents with anaerobic biological reactors", 1985 Environmental Conference Proceedings, TAPPI PRESS, Atlanta, 83-92.
- Kalman, R. E., "A New Approach to Linear Filtering and Prediction Problems", Trans. ASME, J. Basic Eng., Series 82D, 35-45, 1960.
- Kennedy, K. J. and R. L. Droste, "Anaerobic fixed-film reactors treating carbohydrate wastewater", Water Research, 20 (6), 685-695, 1986.
- Kennedy, K. J., M. Muzar, and G. H. Copp, "Stability and Performance of Mesophilic Anaerobic Fixed-Film Reactors during Organic Overloading", Biotechnology and Bioengineering, 27, 86-93, 1985.
- McCarty, P. L., "Anaerobic waste treatment fundamentals. Part One : Chemistry and microbiology", Public Works, 107-112, September, 1964.

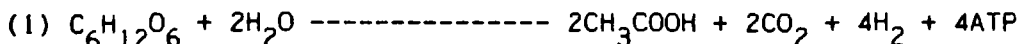
- McCarty, P. L. and D. P. Smith, "Anaerobic wastewater treatment", Environ. Sci. Technol., 20 (12), 1200-1206, 1982.
- McInerney, M. J., M. P. Bryant, and D. A. Stafford, "Metabolic stages and energetics of microbial anaerobic digestion", Anaerobic Digestion, Proc. of the 1st International Symposium on Anaerobic Digestion University College, Cardiff, Wales, September, 1979.
- Mosey, F. E., "Mathematical modelling of the anaerobic digestion process: regulatory mechanisms for the formation of short chain volatile acids from glucose", Wat. Sci. Tech., 15, 209-232, 1983.
- Olsson, G., "Control strategies for the activated sludge process, Comprehensive Biotechnology, M. Moo-Young (Ed.), Chapt. 65, 1107-1119, Pergamon (1985).
- Poduska, R. A. and J. F. Andrews, "Dynamics of nitrification in the activated sludge process", Journal WPCF, 47 (11), 1975.
- Pohland, F. G. and R. J. Engstrom, "High-rate digestion control, I. Fundamental concepts of acid-base equilibrium", Proceedings of the 19th Industrial Waste Conference, Purdue University, 1964.
- Pollock, M. J., Modelling and Control of Sustained Oscillations in the Emulsion Polymerization of Vinyl Acetate, Ph.D. Thesis, McMaster University (1983).
- Price, E. C., "The microbiology of anaerobic digestion", Biotechnology, Applications and Research, P. N. Cheremisinoff and R. P. Ouellette (Eds.), Technomic Publishing, Lancaster, Pennsylvania, 1985.
- Rozzi, A., "Modelling and control of anaerobic digestion processes", Trans Inst M C, 6 (3), 153-159, 1984.
- Rozzi, A., A. C. Di Pinto, and A. Brunetti, "Anaerobic process control by bicarbonate monitoring", Env. Tech. Letters, 6, 594-601, 1985.

- Rozzi, A., S. Merlini and R. Passino, "Development of a four population model of the anaerobic degradation of carbohydrates", Env. Tech. Letters, 6, 610-619, 1985.
- Sam-Soon, P., R. E. Loewenthal, P. L. Dold, and G. V. R. Marais, "Hypothesis for pelletisation in the Upflow Anaerobic Sludge Bed reactor", Water SA, 13 (2), 1987.
- Sinechal, X. J., M. J. Installe, and E. J. Nyns, "Differentiation between acetate and higher volatile acids in the modelling of the anaerobic biomethanation process", Biotechnology Letters, 1 (8), 309-314, 1979.
- Standard Methods for the Examination of Water and Wastewater, 15th Edition, Amer. Public Health Assoc., Washington, 1980.
- Stover, E. L., R. Gonzalez, and G. Gomathinayagam, "Shock load capabilities of anaerobic systems treating high strength wastewaters", Proceedings of the 40th Industrial Waste Conference, Purdue University, 1985.
- Svrcek, W. Y., R. F. Elliot, and J. E. Zajic, "The extended Kalman filter applied to a continuous culture model", Biotechnology and Bioengineering, 16, 827-846, 1974.
- Switzenbaum, M. S. and R. B. Eimstad, "Analysis of anaerobic biofilms", Env. Tech. Letters, 8 (1), 21-32, 1987.
- U.S. EPA, Process Design Manual for Sludge Treatment and Disposal September (1979).
- Van der Meer, R. R. and P. M. Heertjes, "Mathematical description of anaerobic treatment of wastewater in upflow reactors", Biotechnology and Bioengineering, 25, 2531-2556, 1986.
- Zeikus, J. G., "Microbial populations in digesters", Anaerobic Digestion, Proc. of the 1st International Symposium on Anaerobic Digestion, University College, Cardiff, Wales, September, 1979.

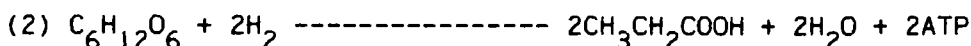
# APPENDIX I

## Example of Calculation of Four Population Model Yield Coefficients From ATP Production

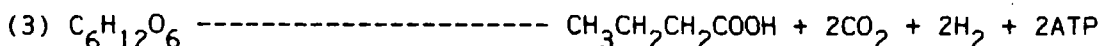
The following chemical reactions summarize the yield of ATP and therefore biomass (assuming 10 g biomass formed per mole of ATP produced) from the bacterial conversion of glucose to acetic, propionic and butyric acids, respectively (Mosey, 1983).



20 mg biomass formed per mmole acetic acid formed directly from glucose



10 mg biomass formed per mmole propionic acid formed from glucose



20 mg biomass formed per mmole butyric acid formed from glucose

From this information, the yield parameters are calculated directly as follows:

$$\begin{aligned} \text{KGA} &= \frac{1 \text{ mmole acetic}}{20 \text{ mg biomass}} \times 60 \frac{\text{mg acetic}}{\text{mmole acetic}} \\ &= 3 \text{ mg acetic from glucose/mg acid former biomass} \end{aligned}$$

$$\begin{aligned} \text{KGP} &= \frac{74}{10} \\ &= 7.4 \text{ mg propionic from glucose/mg acid former biomass} \end{aligned}$$

$$\begin{aligned} \text{KGB} &= \frac{88}{20} \\ &= 4.4 \text{ mg butyric from glucose/mg acid former biomass} \end{aligned}$$

Neglecting the uptake of substrate as a carbon source, the yield parameters in the soluble organics (glucose) mass balance are calculated as follows:

$$\begin{aligned} \text{KAC} &= \frac{1 \text{ mg biomass}}{\text{KGA} \text{ mg acetic}} \times \frac{1 \text{ mmole glucose}}{180 \text{ mg glucose}} \times 2 \frac{\text{mmole acetic}}{\text{mmole glucose}} \\ &\quad \times 60 \frac{\text{mg acetic}}{\text{mmole acetic}} \end{aligned}$$

= 0.22 mg acid formers/mg glucose to acetic acid

$$\text{KPR} = \frac{1}{\text{KGP}} \times \frac{1}{180} \times 2 \times 74$$

= 0.11 mg acid formers/mg glucose to propionic acid

$$\text{KBT} = \frac{1}{\text{KGB}} \times \frac{1}{180} \times 1 \times 88$$

= 0.11 mg acid formers/mg glucose to butyric acid



APPENDIX II: COMPUTER LISTING OF TWO POPULATION MODEL

DO=LONG-DY,ARG=COMMON/24/810,OPT=1,BOUND=FIXED,DB=187-38/-SL7-ER7=189-20MD/-ST,-27,PL=58C01-  
FTNS,I=DSENS,L=LIST.

```

1  PROGRAM DSSENS
2  IMPLICIT REAL (A-Z)
3  INTEGER N,N08,IER,K,I,SC,J,METH,MITER,INDEX,STIME,IMK(10)
4  INTEGER SENSFL
5  DIMENSION Y(10),WK(171),SCRAT(13,1156),RMAX(13),SCHANG(3)
6  DIMENSION TCONST(13),GAIN(3,13),AVHI(13)
7  EXTERNAL FCN,FCNJ
8
9  COMMON /A1/ PMAX,KM,SMAX,KAS,KXS1,FI,V,VAI,KHAX,SI,KXS,MR1,SR1
10 COMMON /A2/ RF,V2,II,MR2,SR2
11
12 *****VARIABLE DICTIONARY*****
13
14 VARIABLE      DESCRIPTION      UNITS
15
16 SI            CONCENTRATION SOLUBLE ORGANICS IN FEED      MG/L
17 VAI           CONCENTRATION VOLATILE ACIDS IN FEED        MG/L
18 II            CONCENTRATION INERTS IN FEED                MG/L
19
20 RF            RECYCLE RATE                                L/D
21
22 SO            REACTOR 1 INFLUENT SOLUBLE ORGANICS          MG/L
23 VAO           REACTOR 1 INFLUENT VOLATILE ACIDS            MG/L
24 IO            REACTOR 1 INFLUENT INERTS                    MG/L
25
26 HMAX          METHANOGEN MAXIMUM SPECIFIC GROWTH RATE      1/DAY
27 KM            METHANOGEN SATURATION CONSTANT              MG/L
28 SMAX          ACID FORMER MAXIMUM SPECIFIC GROWTH RATE      1/DAY
29 KAS           ACID FORMER SATURATION CONSTANT              MG/L
30 KXS           ACID FORMER YIELD COEFFICIENT                MG/MG
31 KXS1          METHANOGEN YIELD COEFFICIENT                 MG/MG
32 KHAX          VOLATILE ACID YIELD COEFFICIENT              MG/MG
33 MR1           REACTOR 1 SPECIFIC GROWTH RATE METHANOGENS  1/DAY
34 SR1           REACTOR 1 SPECIFIC GROWTH RATE ACID FORMERS  1/DAY
35 MR2           REACTOR 2 SPECIFIC GROWTH RATE METHANOGENS  1/DAY
36 SR2           REACTOR 2 SPECIFIC GROWTH RATE ACID FORMERS  1/DAY
37
38 V             REACTOR 1 VOLUME
39 V2            REACTOR 2 VOLUME
40
41 QCH4          REACTOR 1 METHANE PRODUCTION
42 QCH42         TOTAL 2 METHANE PRODUCTION
43 SV            STANDARD VOLUME OF 1 MOLE OF GAS
44
45 Y(1)          REACTOR 1 METHANOGENIC CONCENTRATION          MG/L
46 Y(2)          REACTOR 1 EFFLUENT VOLATILE ACIDS             MG/L
47 Y(3)          REACTOR 1 EFFLUENT SOLUBLE ORGANICS           MG/L
48 Y(4)          REACTOR 1 ACID FORMERS CONCENTRATION          MG/L
49 Y(5)          REACTOR 1 EFFLUENT INERTS                     MG/L
50 Y(6)          REACTOR 2 METHANOGENIC CONCENTRATION          MG/L
51 Y(7)          REACTOR 2 EFFLUENT VOLATILE ACIDS             MG/L
52 Y(8)          REACTOR 2 EFFLUENT SOLUBLE ORGANICS           MG/L
53 Y(9)          REACTOR 2 ACID FORMER CONCENTRATION           MG/L
54 Y(10)         REACTOR 2 EFFLUENT INERT CONCENTRATION        MG/L
55
56 *****
57 SIMDAT: INPUT FILE OF PARAMETERS AND INITIAL CONDITIONS
58 SIMSIM: OUTPUT FILE FOR TABULAR DATA
59 SIMPLT: OUTPUT FILE FOR PLOTS
60
61 OPEN(UNIT=3,FILE='SIMDAT',STATUS='OLD')
62 OPEN(UNIT=7,FILE='SIMSIM',STATUS='NEW')
63 OPEN(UNIT=6,FILE='SIMPLT',STATUS='NEW')
64 OPEN(UNIT=5,FILE='SIM2',STATUS='NEW')
65
66 READ INPUT FILE
67
68 READ(3,*)HMAX,KM,SMAX,KAS,KXS1,FI,V,VAI,KHAX,SI,KXS,KCH4
69 READ(3,*)RF,V2,II,SENSFL
70 READ(3,*)N08,N0B,SV,SCHANG(1),SCHANG(2),SCHANG(3),STIME
71 READ(3,*)Y(1),Y(2),Y(3),Y(4),Y(5)
72 READ(3,*)Y(6),Y(7),Y(8),Y(9),Y(10)
73 SC=13
74 T=0.0
75 TT=5.0/1440.0
76 WRITE(7,*)HMAX,KM,SMAX,KAS,KXS1,FI,V,VAI,KHAX,SI,KXS,KCH4

```

PROGRAM DSENS

74/810 OPT=1,ROUND= A/ S/ M/-D,-DS

FTN 5.1+670

87/11/26. 1

```

76      WRITE(7,*)RF,V2,II,SENSFL
77      WRITE(7,*)XMW,NDB,SV,SCCHANGE(1),SCCHANGE(2),SCCHANGE(3),STIME
78      WRITE(7,*)Y(1),Y(2),Y(3),Y(4),Y(5)
79      WRITE(7,*)Y(6),Y(7),Y(8),Y(9),Y(10)
80
81      * SET UP PARAMETERS FOR INTEGRATION ROUTINE
82      *
83      N=10
84      TOL=1.0E-09
85      H=1.0E-10
86      METH=1
87      MITER=0
88      INDEX=1
89      * SOLVE MODEL
90      *
91      DO 10 K=1,NDB
92          TEND=T+IT
93          CALL DGEAR(N,FCN,FCNJ,T,H,Y,TEND,TOL,METH,MITER,INDEX,
94                  *      IWK,WK,IER)
95          * CALCULATE GAS FLOW
96          *
97          QCH4=KCH4*SV*V*MR1*Y(1)/XMW
98          QCH42=QCH4+KCH4*SV*V2*MR2*Y(6)/XMW
99          *
100         * STORE RESULTS IN SCRATCH MATRIX
101         *
102         SCRAT(1,K)=TEND
103         SCRAT(2,K)=Y(2)
104         SCRAT(3,K)=Y(3)
105         SCRAT(4,K)=QCH4
106         SCRAT(5,K)=Y(5)
107         SCRAT(6,K)=Y(7)
108         SCRAT(7,K)=Y(8)
109         SCRAT(8,K)=Y(10)
110         SCRAT(9,K)=QCH42
111         SCRAT(10,K)=Y(10)+Y(8)
112         SCRAT(11,K)=Y(3) + Y(5) +1.07*Y(2)
113         SCRAT(12,K)=II+SI
114         SCRAT(13,K)=FI
115         *
116         * CALCULATE INFLUENT CONCENTRATION FOR NEXT INTERVAL
117         *
118         IF(K.EQ. STIME)THEN
119             II=II/(SI+II) * SCCHANGE(1) + II
120             SI=II/(SI+II)*SCCHANGE(1) + SI
121             VAI=SCCHANGE(2) + VAI
122             FI=SCCHANGE(3) + FI
123         ENDIF
124         CONTINUE
125         IF(SENSFL.EQ. 1)THEN
126             *
127             CALL GTCONST(STIME,TT,SC,NDB,SCRAT,TCONST,GAIN,AVHI,SCCHANGE)
128             *
129             * OUTPUT RESULTS
130             *
131             WRITE(7,100)
132             FORMAT(2X,'', VARIABLE',2X,'GA1', GA2, GA3',2X,
133                   *      TIME CONSTANT',2X,' AVERAGE')
134             DO 15 J=2,11
135                 TCONST(J)=TCONST(J)*24
136                 WRITE(7,150)J,GAIN(1,J),GAIN(2,J),GAIN(3,J),TCONST(J),AVHI(J)
137                 FORMAT(113,3(1X,F7.4),2(2X,F13.2))
138             CONTINUE
139             ENDOF
140             *
141             * IF THIS IS A SENSITIVITY ANALYSIS RUN (SENSFL=1), DO NOT PRINT TABULAR DATA
142             * OR PLOT RESULTS
143             *
144             IF(SENSFL.EQ. 1)GOTO 40
145             *
146             * TABULAR DATA PRINT STATEMENTS
147             *
148             WRITE(7,200)
149             FORMAT(6X,'VOL ACIDS(MG/L)',1X,' COD(MG/L)',1X,'GAS(L/D)',
150                   *      4X,'INERTS',3X,'2ND STAGE VAI')
151             DO 20 K=1,NDB

```

PROGRAM DSENS 74/810 OPT=1,ROUND= A/ S/ M/-0,-DS FTM 5.1+670

87/11/26. 1

```

153      WRITE(7,300)(SCRAT(J,K),J=1,6)
154      FORMAT(F6.2,5(2X,F8.2))
155      CONTINUE
156      WRITE(7,400)
157      FORMAT(1X,'2ND ST COD',3X,'2NDST IN',3X,'TOTAL GAS',3X,
158      *COD+INERTS (2)',2X,'COD+INERTS (1)')
159      DO 30 K=1,NDB
160      WRITE(7,500)(SCRAT(J,K),J=7,11)
161      FORMAT(5(2X,F8.2))
162      CONTINUE
163      *
164      * PLOT RESULTS
165      *
166      * CALL RPLT(NDB,SC,SCRAT,RMAX)
167      *
168      *
169      *
170      * DO 50 K=1,NDB
171      *
172      *      G=SCRAT(4,K)/1440
173      *      WRITE(5,1500)SCRAT(1,K),SCRAT(12,K),SCRAT(13,K),SCRAT(2,K),
174      *      *      G,SCRAT(11,K)
175      *      FORMAT(F6.2,5(2X,F8.2))
176      *      CONTINUE
177      *      CONTINUE
178      *
179      * STOP
180      * END

```

SUBROUTINE FCN(N,T,Y,YPRIME)  
 DH=PCN(7)=DT,ARG=COMMON,74/810 OPT=1,ROUND=F,4(S,M/-D,-DS,FIN=1097)MD/-ST,-87/11/26001  
 FTN5,I=DSNS,L=LIST.

```

1  SUBROUTINE FCN(N,T,Y,YPRIME)
2  IMPLICIT REAL(A-Z)
3  INTEGER N
4  DIMENSION Y(N),YPRIME(N)
5
6  COMMON /A1/MHAX,KH,SMAX,KAS,KXS1,FI,V,VAI,KHAX,SI,KXS,MR1,SR1
7  COMMON /A2/RF,V2,II,MR2,SR2
8
9  *****RECYCLE EQUATIONS*****
10
11  F=FI+RF
12  VAO=(VAI*FI+Y(7)*RF)/(FI+RF)
13  SO=(SI*FI+Y(8)*RF)/(FI+RF)
14  IO=(II*FI+Y(10)*RF)/(FI+RF)
15
16  *****FIRST STAGE EQUATIONS*****
17
18  * SPECIFIC GROWTH RATE, METHANOGENS
19  * MR1=MMAX/(1+KH/Y(2))
20  * SPECIFIC GROWTH RATE, ACIDOGENS
21  * SR1=SMAX/(1+KAS/Y(3))
22  * ORGANISM BALANCE, METHANOGENS
23  * YPRIME(1)=0.0
24  * VA BALANCE
25  * YPRIME(2)=-MR1*Y(1)/KXS1+F/V*(VAO-Y(2))+SR1*KHAX*Y(4)
26  * COD BALANCE
27  * YPRIME(3)=F/V*(SO-Y(3))-SR1*Y(4)/KXS
28  * ORGANISM BALANCE, ACIDOGENS
29  * YPRIME(4)=0.0
30  * INERT BALANCE
31  * YPRIME(5)=F/V*(IO-Y(5))
32
33  *****SECOND STAGE EQUATIONS*****
34
35  * SPECIFIC GROWTH RATE, METHANOGENS
36  * MR2=MMAX/(1+KH/Y(7))
37  * SPECIFIC GROWTH RATE, ACIDOGENS
38  * SR2=SMAX/(1+KAS/Y(8))
39  * ORGANISM BALANCE, METHANOGENS
40  * YPRIME(6)=0.0
41  * VA BALANCE
42  * YPRIME(7)=-MR2*Y(6)/KXS1+F/V2*(Y(2)-Y(7))+SR2*KHAX*Y(9)
43  * COD BALANCE
44  * YPRIME(8)=F/V2*(Y(3)-Y(8))-SR2*Y(9)/KXS
45  * ORGANISM BALANCE, ACIDOGENS
46  * YPRIME(9)=0.0
47  * INERT BALANCE
48  * YPRIME(10)=F/V2*(Y(5)-Y(10))
49
50
51
52
53
54
55
56
57
58
59
60
61
62
63
64
65
66
67
68
69
70
71
72
73
74
75

```

SUBROUTINE FCN

74/810 OPT=1,ROUND= A/ S/ M/-D,-DS

FTN 5.1+670

87/11/26. 1

76  
77  
78\*  
RETURN  
END

```

SUBROUTINE FCNJ              74/810 OPT=1,ROUND=A/S/M/-D/-DS      FTN 5.1+670
DO=-LONG/-DT,ARG=-COMMON/-FIXED,CS=USER/-FIXED,DB=-TB/-SB/-SL/-ER/-ID/-PMD/-ST,-AL,PL=5000 1.
FTN5,I=DSENS,L=LIST.

```

# FINANCIAL

```

SUBROUTINE FCNJ(N,X,Y,PD)
INTEGER N
REAL Y(N),PD(N,N),X
RETURN
END

```

SUBROUTINE RPLT 74/810 OPT=1,ROUND= A/ S/ M/-D,-DS FTM 5.1+670 87/11/20.1  
 DO=-LONG/-DT,ARG=-COMMON/-FIXED,CS= USER/-FIXED,OB=-TB/-SB/-SL/-ER/-ID/-PMD/-ST,-AL,PL=5000  
 FTM5,I=CSENS,L=LIST.

```

1  SUBROUTINE RPLT(NOB,SC,SCRAT,RMAX)
2  *
3  *
4  IMPLICIT REAL(A-Z)
5  INTEGER SC,I,J,K,NOB
6  DIMENSION SCRAT(SC,NOB),RMAX(SC)
7  *
8  DO 10 I=1,SC
9    RMAX(I)=0.0
10   CONTINUE
11   DO 30 I=1,SC
12     DO 20 J=1,NOB
13       IF (SCRAT(I,J).GT. RMAX(I)) THEN
14         RMAX(I)=1.2*SCRAT(I,J)
15       ENDIF
16     CONTINUE
17   CONTINUE
18   *
19   CALL SCALES(0.,NOB,0.,RMAX(2))
20   DO 40 K=1,NOB
21     CALL PLOTPT(SCRAT(1,K),SCRAT(2,K),2)
22   CONTINUE
23   CALL OUTPLT
24   WRITE(6,150)
25   FORMAT(////,20X,' EFF VOLATILE ACIDS(MG/L)')
26   CALL SCALES(0.,NOB,0.,RMAX(3))
27   DO 50 K=1,NOB
28     CALL PLOTPT(SCRAT(1,K),SCRAT(3,K),2)
29   CONTINUE
30   CALL OUTPLT
31   WRITE(6,160)
32   FORMAT(////,20X,'EFF COD(MG/L)')
33   CALL SCALES(0.,NOB,0.,RMAX(4))
34   DO 60 K=1,NOB
35     CALL PLOTPT(SCRAT(1,K),SCRAT(4,K),2)
36   CONTINUE
37   CALL OUTPLT
38   WRITE(6,170)
39   FORMAT(////,20X,'GAS PRODUCTION(L/D)')
40   *
41   CALL SCALES(0.,NOB,0.,RMAX(5))
42   DO 70 K=1,NOB
43     CALL PLOTPT(SCRAT(1,K),SCRAT(5,K),2)
44   CONTINUE
45   CALL OUTPLT
46   WRITE(6,180)
47   FORMAT(////,20X,'FIRST STAGE INERTS')
48   *
49   CALL SCALES(0.,NOB,0.,RMAX(6))
50   DO 80 K=1,NOB
51     CALL PLOTPT(SCRAT(1,K),SCRAT(6,K),2)
52   CONTINUE
53   CALL OUTPLT
54   WRITE(6,190)
55   FORMAT(////,20X,'2ND STAGE VOLATILE ACIDS')
56   *
57   CALL SCALES(0.,NOB,0.,RMAX(7))
58   DO 90 K=1,NOB
59     CALL PLOTPT(SCRAT(1,K),SCRAT(7,K),2)
60   CONTINUE
61   CALL OUTPLT
62   WRITE(6,200)
63   FORMAT(////,20X,'2ND STAGE COD')
64   *
65   CALL SCALES(0.,NOB,0.,RMAX(8))
66   DO 100 K=1,NOB
67     CALL PLOTPT(SCRAT(1,K),SCRAT(8,K),2)
68   CONTINUE
69   CALL OUTPLT
70   WRITE(6,210)
71   FORMAT(////,20X,'2ND STAGE INERTS')
72   *
73   CALL SCALES(0.,NOB,0.,RMAX(9))
74   DO 101 K=1,NOB
75     CALL PLOTPT(SCRAT(1,K),SCRAT(9,K),2)

```

SUBROUTINE RPLT

74/810 OPT=1,ROUND= A/ S/ M/-D,-DS

FTN 5.1+67J

87/11/26. 1

```
76      101  CONTINUE
77          CALL OUTPLT
78          WRITE(6,220)
79      220  FORMAT(////,20X,'TOTAL GAS PRODUCTION')
80          *
81          CALL SCALES(0.,NOB,0.,RMAX(10))
82          DO 102 K=1,NOB
83              CALL PLOTPT(SCRAT(1,K),SCRAT(10,K),2)
84      102  CONTINUE
85          CALL OUTPLT
86          WRITE(6,230)
87      230  FORMAT(////,20X,'INERTS + COD IN 2ND STAGE EFFLUENT')
88          *
89          CALL SCALES(0.,NOB,0.,RMAX(11))
90          DO 103 K=1,NOB
91              CALL PLOTPT(SCRAT(1,K),SCRAT(11,K),2)
92      103  CONTINUE
93          CALL OUTPLT
94          WRITE(6,240)
95      240  FORMAT(////,20X,'COD + INERTS (REACTOR 1)')
96          *
97          RETURN
98          END
```



SUBROUTINE GTCONST, TIME, TT, SC, NOB, SCRAT, TCONST, GAIN, AVHI,  
DO=-LONG/DT, ARG=-COMMON/FIXED, CS=USER/FIXED, DB=-P87-SB/-SL/-ER7=1D978 PMD/-ST,-87,PL46800<sup>13</sup>  
FTN5,I=DSNS,L=LIST.

```

*      SUBROUTINE GTCONST(TIME,TT,SC,NOB,SCRAT,TCONST,GAIN,AVHI,
*                          SCHANGE)
*      IMPLICIT REAL(A-Z)
*      INTEGER TIME,NOB,J,K,KK,SC,NAV,TLO,THI,I
*      DIMENSION SCRAT(SC,NOB),SUMLO(20),SUMHI(20),AVLO(20),AVHI(SC)
*      DIMENSION DIFF(20),TVALUE(20),TCONST(SC),GAIN(3,SC),SCHANG(3)
*
*      NAV=10
*      TLO=TIME-NAV
*      THI=NOB-NAV
*
*      DO 10 J=1,SC
*          SUMLO(J)=0.0
*          SUMHI(J)=0.0
*      CONTINUE
*
*      DO 20 J=2,SC
*          DO 30 K=TLO,TIME
*              SUMLO(J)=SCRAT(J,K)+SUMLO(J)
*          CONTINUE
*          DO 40 K=THI,NOB
*              SUMHI(J)=SCRAT(J,K)+SUMHI(J)
*          CONTINUE
*          AVLO(J)=SUMLO(J)/(NAV+1)
*          AVHI(J)=SUMHI(J)/(NAV+1)
*          DIFF(J)=AVHI(J)-AVLO(J)
*          TVALUE(J)=0.632*DIFF(J)+AVLO(J)
*
*      SEARCH FOR DATA POINT NEAR TIME CONSTANT
*      FIRST OPTION IS FOR STEP UP, SECOND FOR STEP DOWN
*
*      IF(TVALUE(J).GT.AVLO(J))THEN
*          DO 50 K=TIME,NOB
*              IF(SCRAT(J,K).LT.TVALUE(J))KK=K
*          CONTINUE
*      ELSE
*          DO 60 K=TIME,NOB
*              IF(SCRAT(J,K).GT.TVALUE(J))KK=K
*          CONTINUE
*      ENDIF
*
*      TCONST(J)=TT*(KK-TIME)
*      DO 70 I=1,3
*          IF(SCHANG(I).NE.0)THEN
*              GAIN(I,J)=DIFF(J)/SCHANG(I)
*          ELSE
*              GAIN(I,J)=0.0
*          ENDIF
*      CONTINUE
*      RETURN
*      END

```

APPENDIX III: COMPUTER LISTING OF FOUR POPULATION MODEL

PROGRAM AN4EQ 74/810 OPT=1,ROUND= A/ S/ M/-D,-DS FTN 5.1.670 87/11/88  
 DO=-LONG/-DT,ARG=-COMMON/-FIXED,CS= USER/-FIXED,DE=-TB/-SB/-SL/-ER/-ID/-PMD/-ST,-AL,PL=500J  
 FTN5,I=AN4SENS,L=LIST.

```

PROGRAM AN4EQ(INPUT,OUTPUT,TAPE1=INPUT,TAPE2=OUTPUT)
*****
SIMULATION OF A COMPLETELY MIXED ANAEROBIC REACTOR WITH 4 BACTERIAL
GROUPS PRESENT.
PROGRAMMED BY : R.M.JONES
LAST MODIFIED : OCTOBER 3, 1987
*****
IMPLICIT REAL (A-Z)
INTEGER ST,NFAC,K1,KTEST,FCOUNT,NSTEP
INTEGER N,N03,I,J,K,IER,SC,METH,MITER,INDEX,IWK(14)
DIMENSION SCRAT(29,1156),PMAX(29),Y(14),WK(350)
DIMENSION VAA(1000),FCA(1000),CD2M(1000),PHM(1000)
DIMENSION R1(1000),R2(1000),R3(1000),R4(1000),R5(1000),R6(1000)
DIMENSION SFAC(100),PFAC(100),AFAC(100),FFAC(100)
DIMENSION SCHANGE(5),TCONST(29),GAIN(5,29),AVHI(29),AVLO(29)
CHARACTER DNAME(28)*7,MEASR*7
EXTERNAL FCN,FCNJ
COMMON /A1/GMAX,KSG,PMAX,KSP,BMAX,KS8,MMAX,KSM,MHMAX,KSH
COMMON /B1/KAC,KPR,KBT,KGP,KPRA,KGB,K8TA,KGA,KPA,KBA,KAM,KHA
COMMON /B2/KH8,KHP,KCH4H
COMMON /C1/KH8A,K4PA,K4CM,KC02GA,KC02GB,KC02A,KC02H,KCH4A
COMMON /D1/AFB,PA8,BAB,MA8,MHB
COMMON /E1/KH2,KLA,KHCO2,CACO2
COMMON /F1/V,VG,PT,SV,RS
COMMON /G1/SP,KP,BI,RT
COMMON /H1/F,SD,ACO,PRO,BTO,ZO,ZB,CTO,HC03D,ID
COMMON /I1/HC03,P4,FC,GR,PPR,BR,MR,MHR,PCO2
COMMON /GEAR/ DUM4Y(49),SDUM4Y(4),IDUM4Y(38)

WRITE(2,*)'OUTPUT FOR KALPAN FILTER?'
READ(1,*) (A7) MEASR
OPEN(UNIT=3,FILE='AN4INP',STATUS='OLD')
OPEN(UNIT=4,FILE='ONAMF',STATUS='OLD')
OPEN(UNIT=5,FILE='SIM',STATUS='NEW')
OPEN(UNIT=7,FILE='FSIM1',STATUS='NEW')
OPEN(UNIT=6,FILE='FLOT',STATUS='NEW')

READ IN PARAMETERS AND INITIAL CONDITIONS FROM FILE "AN4INP"
*****BIOLOGICAL PARAMETERS*****
1. GROWTH EQUATION
READ(3,*)GMAX,KSG,PMAX,KSP,BMAX,KS8,MMAX,KSM,MHMAX,KSH
2. YIELDS
READ(3,*)KAC,KPR,KBT,KGP,KPRA,KGB,K8TA,KGA,KPA,KBA,KAM,KHA
READ(3,*)KH8A,K4PA,K4CM,KC02GA,KC02GB,KC02A,KC02H,KCH4A
READ(3,*)KH8,KHP,KCH4H
3. BACTERIAL CONCENTRATIONS
READ(3,*)AFB,PA8,BAB,MA8,MHB
*****PHYSICAL PARAMETERS*****
1. EQUILIBRIUM PARAMETERS
READ(3,*)KH2,KLA,KHCO2,CACO2
2. REACTOR PHYSICAL CHARACTERISTICS
READ(3,*)V,VG,PT,SV,RS,TEMP
3. CONTROLLER PARAMETERS
READ(3,*)SP,KP,BI,RT
4. INFLUENT CONDITIONS
READ(3,*)F,SD,ACO,PRO,BTO,ZO,ZB,CTO,HC03D,ID
*****SIMULATION RUN PARAMETERS*****

```

PROGRAM AN4EQ

74/810 OPT=1,ROUND= A/ S/ M/-D,-OS

FTN 5.1+670

87/11/25.

```

76      READ(3,*)NOB,TT,N,SC,TOL,H,METH,MITER,INDEX,PULSE,FAC,SENSFL
77      READ(3,*)SCHANG(1),FPUL,SCHANG(2),NSTEP,SCHANG(3)
78      READ(3,*)SCHANG(4),SCHANG(5)
79      READ(3,*)PNDS,RNDFC,RNDF,RNDZ,RNDCJ2,RNDPH
80
81      ***STATE INITIAL CONDITIONS*****
82
83      READ(3,*)Y(1),Y(2),Y(3),Y(4),Y(5),Y(6),Y(7),Y(8)
84
85      READ(3,*)Y(9),Y(10),Y(11),Y(12),Y(13),Y(14)
86
87      ***FACTORIAL EXPERIMENT*****
88
89      READ(3,*)ST,NFAC
90      K1=ST
91      IF (ST.GT.0) THEN
92          DO 1 J=1,NFAC
93              READ(3,*)SFAC(J),PFAC(J),AFAC(J),FFAC(J)
94          CONTINUE
95          1
96          SO1=SO
97          PRO1=PRO
98          ACO1=ACO
99          F1=F
100         FCOUNT=1
101         ENDDIF
102
103         *
104         * CALCULATE SELECTED PARAMETERS FROM STOICHIOMETRY
105         *
106         KPA=60/(KPRA*74)
107         KBA=(2*60)/(KSTA*88)
108         K4BA=2/(K8TA*38)
109         KHPA=3/(KPRA*74)
110
111         *
112         * OUTPUT DATA READ IN FROM "AN4INP"
113         *
114         WRITE(7,150)
115         150
116         FORMAT(11,"INPUT DATA")
117         WRITE(7,*)GMAX,KSG,PMAX,KSP,BMAX,KSB,MMAX,KSM,11MAX,KSH
118         WRITE(7,*)KAC,KPR,KBT,KGP,KPRA,KGB,KBTB,KGA,KPA,KBA,KAM,K4A
119         WRITE(7,*)KHBA,KHPA,KHC4,KC2GA,KC2G3,KC2A,KC2H,KC4A
120         WRITE(7,*)K4R,K4P,KC4H
121         WRITE(7,*)AFB,PAB,BA3,MAB,M4B
122         WRITE(7,*)KH2,KLA,KHCO2,CACO2
123         WRITE(7,*)V,VG,PT,SV,RS,TEMP
124         WRITE(7,*)SP,KP,BI,RT
125         WRITE(7,*)F,SO,ACO,PRO,BTO,ZO,ZB,CIO,HCO3O,IO
126         WRITE(7,*)NOB,TT,N,SC,TOL,H,METH,MITER,INDEX,PULSE,FAC
127         WRITE(7,*)SCHANG(1),FPUL,SCHANG(2),NSTEP,SCHANG(3)
128         WRITE(7,*)SCHANG(4),SCHANG(5)
129         WRITE(7,*)RNDZ,RNDFC,RNDF,RNDZ,RNDCJ2,RNDPH
130         WRITE(7,*)Y(1),Y(2),Y(3),Y(4),Y(5),Y(6),Y(7),Y(8)
131         WRITE(7,*)Y(9),Y(10),Y(11),Y(12),Y(13)
132         DO 2 J=1,NFAC
133             WRITE(7,*)SFAC(J),PFAC(J),AFAC(J)
134         CONTINUE
135         2
136
137         *
138         * READ IN OUTPUT NAMES FROM FILE "ONAME"
139         *
140         READ(4,*)(ONAM(J),J=1,28)
141
142         *
143         * GENERATE REQUIRE WHITE NOISE SEQUENCES
144         *
145         DSEED1 = 12345
146         CALL GGNML(DSEED1,NOB,R1)
147         DSEED2=6789
148         CALL GGNML(DSEED2,NOB,R2)
149         DSEED3=54321
150         CALL GGNML(DSEED3,NOB,R3)
151         DSEED4=65913
152         CALL GGNML(DSEED4,NOB,R4)
153         DSEED5=55555
154         CALL GGNML(DSEED5,NOB,R5)
155         DSEED6=19467
156         CALL GGNML(DSEED6,NOB,R6)
157
158         *
159         * INITIALIZE CUMULATIVE SUMS(TIME STEP,CUMULATIVE CAUSTIC,ETC.)

```

PROGPAM AN4EQ

74/810 DPT=1,ROUND= A/ S/ M/-D,-DS

FTN 5.1+670

87/11/26.

```

153      *
154      T=0.0
155      TT=TT/1440
156      FC=0.0
157      FSUM=0.0
158      IN=0
159      PH=SP
160      FM=F
161      ZOI=ZO
162      *
163      TEMPERATURE CORRECTIONS
164      *
165      KHC02 = KHC02 * (1.019617)**(38-TEMP)
166      CAC02 = CAC02 * (1.017310291)**(TEMP-25)
167      *
168      *****
169      *
170      ****SOLVE MODEL FOR NOB SAMPLING INTERVALS*****
171      *
172      DO 10 K=1,NOB
173      *
174      INCREMENT TIME STEP
175      *
176      TEND = T + TT
177      *
178      PH CONTROL
179      *
180      ER = SP - PH
181      IN = TT/RT * (ER + IN)
182      FC = KP * (ER + IN) + BI
183      *
184      IF (FC .LT. 0.0 .OR. F .EQ. 0.0) FC=0.0
185      *
186      FCA(K) = FC
187      *
188      CALCULATE PROCESS FORCING FUNCTIONS FOR THIS INTERVAL
189      *
190      IF (PULSE .EQ. 0) GO TO 6
191      *
192      PULSE EXPERIMENT
193      *
194      F=0.0
195      IF (PULSE .NE. 0) P=1/PULSE
196      IF (MOD(NINT(TEND*FAC),NINT(P*FAC)) .EQ. 0) F=FPUL
197      *
198      6
199      *
200      CONTINUE
201      *
202      STEP TESTS
203      GO TO 75
204      *
205      IF (SCHANG(1) .NE. 0 .AND. K .EQ. NSTEP) F=F+SCHANG(1)
206      IF (SCHANG(2) .NE. 0 .AND. K .EQ. NSTEP) THEN
207          CCOI=IO+SO
208          IC=IO/CCOI*SCHANG(2) + IO
209          SC=SO/CCOI*SCHANG(2) + SO
210      *
211      ENDIF
212      IF (SCHANG(3) .NE. 0 .AND. K .EQ. NSTEP) ACO=ACO+SCHANG(3)
213      IF (SCHANG(4) .NE. 0 .AND. K .EQ. NSTEP) PRO=PRO+SCHANG(4)
214      IF (SCHANG(5) .NE. 0 .AND. K .EQ. NSTEP) BTO=BTO+SCHANG(5)
215      *
216      STOCHASTIC INPUTS
217      *
218      SO = SO + R1(K) * RNDS
219      IF (SO .LT. 0) SO=0
220      FC = FC + P2(K) * RNOFC
221      IF (FC .LT. 0.0 .OR. F .EQ. 0.0) FC = 0.0
222      F = F + R3(K) * RNDF
223      IF (F .LT. 20) F=20
224      IF (F .GT. 250) F=250
225      ZO = ZO + R4(K) * RNDZ
226      IF (ZO .LT. 0) ZO=0
227      *
228      FACTORIAL EXPERIMENTS
229      *
230      KTEST=K-K1
231      IF (KTEST .EQ. 0 .AND. FCOUNT .LE. NFAC) THEN
232          SO=SFAC(FCOUNT) + SO1
233          PRO=PFAC(FCOUNT) + PRO1
234          ACO=AFAC(FCOUNT) + ACC1
235          F=FFAC(FCOUNT) + F1
236          FCOUNT=FCOUNT+1

```

11111

11111



```

07      GAIN(4,J),GAIN(5,J),TCONST(J),AVL(J),AV-H(J)
08      1600  FORMAT(16,5(1X,F7.4),2X,F5.1,2(2X,F9.1))
09      15    CONTINUE
10      ENDIF
11      *
12      * IF THIS IS A SENSITIVITY ANALYSIS RUN (SENSFL=1), DO NOT PRINT TABULAR DATA
13      * OR PLOT RESULTS
14      *
15      IF(SENSFL.EQ.1)GOTO 70
16      WRITE(7,100)
17      100    FORMAT('1','OUTPUT DATA')
18      WRITE(7,200)
19      200    FORMAT(1,12X,'INFLUENT DATA',20X,'EFFLUENT DATA')
20      WRITE(7,300)(DNAM(J),J=1,7)
21      300    FORMAT(7(2X,A8))
22      DO 20 K = 1,NOB
23      WRITE(7,400)(SCRAT(J,K),J=1,7)
24      400    FORMAT(7(2X,F8.2))
25      CONTINUE
26      WRITE(7,500)
27      500    FORMAT('1')
28      WRITE(7,600)(DNAM(J),J=8,14)
29      600    FORMAT(7(2X,A8))
30      DO 30 K = 1,NOB
31      WRITE(7,700)(SCRAT(J,K),J=8,14)
32      700    FORMAT(7(2X,F8.2))
33      CONTINUE
34      WRITE(7,800)
35      800    FORMAT('1')
36      WRITE(7,900)(DNAM(J),J=15,21)
37      900    FORMAT(7(2X,A8))
38      DO 40 K = 1,NOB
39      WRITE(7,1000)(SCRAT(J,K),J=15,21)
40      1000   FORMAT(7(2X,F8.2))
41      CONTINUE
42      WRITE(7,1100)
43      1100   FORMAT('1')
44      WRITE(7,1200)(DNAM(J),J=22,28)
45      1200   FORMAT(7(2X,A8))
46      DO 50 K=1,NOB
47      WRITE(7,1300)(SCRAT(J,K),J=22,28)
48      1300   FORMAT(7(2X,F8.2))
49      CONTINUE
50      *
51      * PLOT RESULTS
52      *
53      CALL RPLT(NOB,SC,SCRAT,FMAX,DNAM)
54      *
55      * OUTPUT MEASUREMENTS
56      *
57      DO 60 K=1,NOB
58      WRITE(5,1400)SCRAT(1,K),SCRAT(27,K),SCRAT(4,K),SCRAT(15,K),
59      *          CO2M(K),SCRAT(14,K),SCRAT(29,K),TEMP
60      C=SCRAT(28,K)+SCRAT(29,K)
61      G=SCRAT(11,K)/(1440*0.56)
62      TT1=SCRAT(1,K)*24
63      WRITE(5,1400)TT1,SCRAT(9,K),SCRAT(6,K),SCRAT(7,K),
64      *          SCRAT(29,K),G,C
65      1400   FORMAT(7(1X,F8.2))
66      60    CONTINUE
67      70    CONTINUE
68      *
69      STOP
70      END

```

SUBROUTINE FCN  
DO=LONG/-DT,ARG=-COMMON/-FIXED,CS=USER7-FIXED,DB=-P87-SB/-SL/-ER7-ID7-PMD/-ST,-A7,PL=300,1:  
FTN5,I=AN4SENS,L=LIST.  
74/810 DPT=1,ROUND=A/S/M/-P87-DS FTN 5:1+672  

```

SUBROUTINE FCN(N,T,Y,YPRIME)
IMPLICIT REAL (A-Z)
INTEGER N,JJ
DIMENSION Y(N),YPRIME(N)
COMMON /A1/GMAX,KSQ,PMAX,KSP,BMAX,KS8,YMAX,KS4,MHMAX,KS4
COMMON /B1/KAC,KPR,KBT,KGP,KPRA,KGB,KBT4,KGA,KPA,KBA,KAM,KHA
COMMON /R2/KH8,K4P,KCH4H
COMMON /C1/KH8A,K4PA,K4CH,KC02GA,KC02GB,KC02A,KC02H,KCH4A
COMMON /D1/AFB,PAB,BAB,MAB,M4B
COMMON /E1/KH2,KLA,KHC02,CAC02
COMMON /F1/V,VG,PT,SV,RS
COMMON /G1/SP,KP,B1,RT
COMMON /H1/F,S,ACQ,PRJ,BTO,ZO,ZB,CTO,HC03O,IO
COMMON /I1/HC03,PH,FC,GR,PRR,8R,MR,MHR,PC02

```

\*\*\*\*\*BICARBONATE ALKALINITY (MMOLE/L)\*\*\*\*\*

```
HCC3 = Y(6) - Y(2)/74 - Y(3)/88 - Y(4)/60
IF(HCC3 .LT. 0.0)HCC3=0.0
```

\*\*\*\*\*  
\*\*\*\*\*P4\*\*\*\*\*

```
IF(HC03.GT.0.0)THEN
  HY=CAC02*Y(7)/HC03
  IF(HY.GT.0.0)THEN
    PH=-ALOG10(HY)
  ENDIF
ENDIF
```

```
ER = SP-PH
IN = Y(8)
FC = KP*(ER+IN)+BI
IF (FC.LT. 0.0 .OR. F.EQ. 0.0)FC=0.0
```

\*\*\*\*\*GROWTH RATE OF ACID FORMERS\*\*\*\*\*

$$GR = GMAX * Y(1) * Y(9) / (KSG + Y(1))$$

\*\*\*\*\*GROWTH RATES OF ACETOGENIC BACTERIA\*\*\*\*\*

## PROPIONIC ACID BACTERIA

```
PRR = PMAX*Y(2)*Y(10)/(KSP + Y(2))
```

## BUTYRIC ACID BACTERIA

$$BR = BMAX * Y(3) * Y(11) / (KSB + Y(3))$$

\*  
\*\*\*\*\*GROWTH RATE OF ACETOCLASTIC METHANE BACTERIA\*\*\*\*\*

$$MR = MMAX * Y(4) * Y(12) / (KSM + Y(4))$$

\*\*\*\*\*GROWTH RATE OF H2-UTILIZING METHANE BACTERIA\*\*\*\*\*

$$MHR = MHMAX * Y(5) * Y(13) / (KSH + Y(5))$$

\*  
\*\*\*\*\*CARBON DIOXIDE PARTIAL PRESSURE\*\*\*\*\*

$$PCO2 = Y(7)/KHCO2$$

\*  
\*\*\*\*\*MOLAR GAS FLOW RATES\*\*\*\*\*

$$QM = (KCH_4A * MR + KCH_4I * MHR) / (1 - PCO_2 / PT)$$

$$QMC O_2 = PCO_2 / PT * QM$$

\*\*\*\*\*HYDROGEN REGULATION FUNCTIONS\*\*\*\*\*

```
RF1H = 1/(1 + 1500*Y(5))
RF2H = 1500*Y(5)/(1 + 1500*Y(5))
```

\*\*\*\*\*MASS BALANCES\*\*\*\*\*

✱

112213



SUBROUTINE FCN

74/810 OPT=1,ROUND= A/ S/ M/-D,-DS

FTN 5.1+670

37/11/26. 1

```

75      *      SOLUBLE ORGANICS BALANCE (MG/L)
76      *
77      *      YPRIME(1) = F/V*(SO-Y(1))-(1/KAC)*GR*(RF1H**2)*(1-2*RF2H)
78      *      +-(1/KPR)*GR*RF1H*RF2H-(1/KBT)*GR*(RF1H**2)*RF2H
79      *
80      *      PROPIONIC ACID BALANCE (MG/L)
81      *
82      *      YPRIME(2) = F/V*(PRO-Y(2)) + KGP*GR*RF1H*RF2H - (1/KPRA)
83      *      **PRR*RF1H
84      *
85      *      BUTYRIC ACID BALANCE (MG/L)
86      *
87      *      YPRIME(3) = F/V*(BTD-Y(3)) + KGB*GR*(RF1H**2)*RF2H -
88      *      +(1/KBTA)*GR*RF1H
89      *
90      *      ACETIC ACID BALANCE (MG/L)
91      *
92      *      YPRIME(4) = F/V*(ACD-Y(4)) + KGA*GR*(RF1H**2)*(1-2*RF2H)
93      *      ++KPA*PRR*RF1H + KBA*BR*RF1H - MR/KAM
94      *
95      *      HYDROGEN BALANCE (ATM PARTIAL PRESSURE)
96      *
97      *      YPRIME(5) = (1/KH2)*(-Y(5)/PT*(OH)/V
98      *      ++KHPA*PRR*RF1H + KHBA*BR*RF1H - KHP*GR*RF1H*RF2H
99      *      +- MHR/KHCM + KHB*GR*(RF1H**2)*RF2H + KHA*GR*(RF1H**2)
100     *      **((1-2*RF2H))
101     *
102     *      CATION BALANCE (MMOLE/L)
103     *
104     *      YPRIME(6) = F/V*(ZO-Y(6)) + ZB/V*FC
105     *
106     *      DISSOLVED CARBON DIOXIDE BALANCE (MMOLE/L)
107     *
108     *      YPRIME(7) = F/V*(CTO-Y(7)) + KCG2GA*GR*(RF1H**2)*(1-2*RF2H)
109     *      ++KCO2GB*GR*(RF1H**2)*RF2H + MR*KCO2A - MHR/KCO2H + F/V*
110     *      +(HCO3D-HCC3)+YPRIME(2)/74 + YPRIME(3)/88+YPRIME(4)/60-YPRIME(6)
111     *      +-OMCO2
112     *
113     *      PH CONTROLLER INTEGRAL ACTION
114     *
115     *      YPRIME(8) = ER/RT
116     *
117     *      BACTERIA MASS BALANCES
118     *
119     *      TWO CASES-1:CONSTANT SRT 2:CONSTANT BIOMASS INVENTORY(RS=C FLAG)
120     *
121     *      IF (RS .GT. 0)THEN
122     *
123     *      CASE 1:
124     *
125     *      ACID FORMERS BALANCE
126     *
127     *      YPRIME(9) = GR - 1/RS*Y(9)
128     *
129     *      PROPIONIC ACID BACTERIA
130     *
131     *      YPRIME(10) = PRR - 1/RS*Y(10)
132     *
133     *      BUTYRIC ACID BACTERIA
134     *
135     *      YPRIME(11) = BR - 1/RS*Y(11)
136     *
137     *      ACETOCCLASTIC METHANE FORMERS
138     *
139     *      YPRIME(12) = MR - 1/RS*Y(12)
140     *
141     *      H2-UTILIZING METHANE FORMERS
142     *
143     *      YPRIME(13) = MHR - 1/RS*Y(13)
144     *
145     *      ELSE
146     *
147     *      CASE 2:
148     *
149     *      DO 5 JJ=9,13
150     *      YPRIME(JJ)=0.0
151     *
152     *

```

SUBROUTINE FCN

74/810 OPT=1,ROUND= A/ S/ M/-D,-DS

FTN 5.1+670

37/11/26. 1

```

153     *      CONTINUE
154     *
155     *      ENDIF
156     *
157     *      INERT BALANCE
158     *
159     *      YPRIME(14) = F/V*(IO-Y(14))
160     *
161     *
162     *      RETURN
163     *      END

```

```

SUBROUTINE FCNJ 74/810 OPT=1,ROUND=A/S/M/D,DS FTM 5.1+673 87/1/26
DD=-LONG/-OT,ARG=-COMMON/-FIXED,CS=USER/-FIXED,DB=-TB/-SB/-SL/-ER/-ID/-PD/-ST,-AL,PL=500
FTN5,I=AN4SENS,L=LIST.

```

1  
2  
3  
4  
5  
6

```

*
SUBROUTINE FCNJ(N,X,Y,PD)
INTEGER N
REAL Y(N),PD(N,N),X
RETURN
END

```

SUBROUTINE RPLT 74/810 OPT=1,ROUND=A/S/M/-D,DS FIN 5-1+970  
 CC=-LONG/-DT,APG=-COMMON/-FIXED,CS=USER7-FIXED,DB=-187-SB/-SL/-ER7-ID7-PMD/-ST,-AL,PL=5000  
 FTNS,I=AN4SENS,L=LIST.

```

1      *
2      SUBROUTINE RPLT(NOB,SC,SCRAT,RMAX,DNAM)
3      IMPLICIT REAL (A-Z)
4      INTEGER SC,I,J,K,NOB
5      DIMENSION SCRAT(SC,NOB),RMAX(SC)
6      CHARACTER DNAM(SC)*7
7
8      *
9      *
10     *
11     *
12     *
13     *
14     *
15     *
16     *
17     *
18     *
19     *
20     *
21     *
22     *
23     *
24     *
25     *
26     *
27     *
28     *
29     *
30     *
31     *
32     *
33     *
34     *

```

FIND THE MAXIMUM VALUES OF THE RESULTS

```

DO 10 I=1,SC
  RMAX(I)=0.0
  CONTINUE
DO 30 I=1,SC
  DO 20 J=1,NOB
    IF(SCRAT(I,J).GT.RMAX(I))THEN
      RMAX(I)=1.2*SCRAT(I,J)
    ENDIF
  CONTINUE
CONTINUE

```

PLOT THE RESULTS

```

DO 40 I=2,SC
  CALL SCALES(0.,NOB,0.,RMAX(I))
  DO 50 J=1,NOB
    CALL PLOTPT(SCRAT(I,J),SCRAT(I,J),2)
  CONTINUE
  CALL OUTPLT
  WRITE(6,100)DNAM(I)
  FORMAT(///,20X,A8)
CONTINUE

```

RETURN  
END

SUBROUTINE GTCONST 74/810 OPT=1,ROUND=-46 S/M/-0.1-DSB/-SL/-ER7-1D7-PMD/-ST,-AL,PL=5000  
 DB=LONG/-DT,ARG=-COMMON/-FIXED,CS=USER/-FIXED,DB=-0.37-DSB/-SL/-ER7-1D7-PMD/-ST,-AL,PL=5000  
 FTN5,I=AN4SENS,L=LIST.

```

1      SUBROUTINE GTCONST(NSTEP,TT,SC,NDB,SCRAT,TCONST,GAIN,AVHI,
2      AVLO,SCCHANGE)
3      *
4      IMPLICIT REAL(A-Z)
5      INTEGER NSTEP,NDB,J,K,KK,SC,NAV,TLO,THI,I
6      DIMENSION SCRAT(SC,NDB),SUMLO(30),SUMHI(30),AVLO(SC),AVHI(SC)
7      DIMENSION DIFF(30),TVALUE(30),TCONST(SC),GAIN(5,SC),SCCHANGE(5)
8      *
9      NAV=10
10     TLO=NSTEP-NAV
11     THI=NDB-NAV
12     *
13     DO 10 J=1,SC
14       SUMLO(J)=0.0
15       SUMHI(J)=0.0
16     CONTINUE
17     *
18     DO 20 J=5,SC
19       DO 30 K=TLO,NSTEP
20         SUMLO(J)=SCRAT(J,K)+SUMLO(J)
21       CONTINUE
22       DO 40 K=THI,NDB
23         SUMHI(J)=SCRAT(J,K)+SUMHI(J)
24       CONTINUE
25       AVLO(J)=SUMLO(J)/(NAV+1)
26       AVHI(J)=SUMHI(J)/(NAV+1)
27       DIFF(J)=AVHI(J)-AVLO(J)
28       TVALUE(J)=0.632*DIFF(J)+AVLO(J)
29     *
30     *
31     * SEARCH FOR DATA POINT NEAR TIME CONSTANT
32     * FIRST OPTION IS FOR STEP UP, SECOND FOR STEP DOWN
33     *
34     KK=NSTEP
35     IF(TVALUE(J).GT.AVLO(J))THEN
36       DO 50 K=NSTEP,NDB
37         IF(SCRAT(J,K).LT.TVALUE(J))KK=K
38       CONTINUE
39     ELSE
40       DO 60 K=NSTEP,NDB
41         IF(SCRAT(J,K).GT.TVALUE(J))KK=K
42       CONTINUE
43     ENDIF
44     *
45     TCONST(J)=TT*(KK-NSTEP)
46     DO 70 I=1,5
47       IF(SCCHANGE(I).NE.0)THEN
48         GAIN(I,J)=DIFF(J)/SCCHANGE(I)
49       ELSE
50         GAIN(I,J)=0.0
51       ENDIF
52     CONTINUE
53     CONTINUE
54     RETURN
55     END
56
57
58
59
60
61
62
63
64
65
66
67
68
69
70
71
72
73
74
75
76
77
78
79
80
81
82
83
84
85
86
87
88
89
90
91
92
93
94
95
96
97
98
99

```

APPENDIX IV

MODELLING NOMENCLATURE

TABLE IV-1: TWO POPULATION MODEL NOMENCLATURE

SYMBOL	DESCRIPTION	UNITS
S	Concentration of biodegradable soluble organics in the effluent	mg/L
S <sub>o</sub>	Concentration of biodegradable soluble organics in the influent	mg/L
F	Reactor feedrate	L/d
V	Reactor volume	L
KXS	Acid-former yield coefficient	mg/mg
SR	Growth rate of acid-formers	mg/L.d
S <sub>MAX</sub>	Maximum specific growth rate of acid-formers	1/day
KAS	Acid-former saturation constant	mg/L
AF	Reactor concentration of acid-formers	mg/L
VA	Effluent concentration of volatile acids	mg/L
VA <sub>o</sub>	Influent concentration of volatile acids	mg/L
KHAX	Volatile acid yield coefficient	mg/L
KXS <sub>I</sub>	Methanogen yield coefficient	mg/mg
MR	Growth rate of methanogens	mg/L.d
M <sub>MAX</sub>	Maximum specific growth rate of methanogens	1/day
MF	Reactor concentration of methanogens	mg/L
KM	Methanogen saturation constant	mg/L
QCH <sub>4</sub>	Methane production rate	L/d
KCH <sub>4</sub>	Methane yield coefficient	mmole/mg
SV	Volume of 1 mmole of ideal gas at 1 atm and 35 °C	L
I	Concentration of non-biodegradable material in the effluent	mg/L
I <sub>o</sub>	Concentration of non-biodegradable material in the influent	mg/L

TABLE IV-2: FOUR POPULATION MODEL NOMENCLATURE

SYMBOL	DESCRIPTION	UNITS
G	Concentration of soluble organics in the effluent	mg/L
G <sub>o</sub>	Concentration of soluble organics in the influent	mg/L
F	Reactor feedrate	L/d
V	Reactor volume	L
KAC	Acid-former yield coefficient (soluble organics to acetic step)	mg/mg
KPR	Acid-former yield coefficient (soluble organics to propionic step)	mg/mg
KBT	Acid-former yield coefficient (soluble organics to butyric step)	mg/mg
GR	Unregulated growth rate of acid-formers	mg/L.d
RFAC	Hydrogen regulation function (soluble organics to acetic step)	
RFPR	Hydrogen regulation function (soluble organics to propionic step)	
RFBT	Hydrogen regulation function (soluble organics to butyric step)	
GMAX	Unregulated maximum specific growth rate of acid-formers	1/day
KSG	Acid-former saturation constant	mg/L
AF	Reactor concentration of acid-formers	mg/L
PH <sub>2</sub>	Partial pressure of hydrogen in the reactor gas phase	atm
P	Effluent concentration of propionic acid	mg/L
P <sub>o</sub>	Influent concentration of propionic acid	mg/L
KGP	Propionic acid yield coefficient	mg/mg
KPRA	Propionic acid utilizing acetogenic bacteria yield coefficient	mg/mg

TABLE IV-2: FOUR POPULATION MODEL NOMENCLATURE (Continued)

SYMBOL	DESCRIPTION	UNITS
PRR	Unregulated growth rate of propionic acid utilizing acetogenic bacteria	mg/L.d
RFPA	Hydrogen regulation function (propionic to acetic step)	
PMAX	Maximum unregulated specific growth rate of propionic acid utilizing acetogens	1/day
PA	Reactor concentration of propionic acid utilizing acetogens	mg/L
KSP	Propionic acid utilizing acetogen saturation constant	mg/L
B	Effluent concentration of butyric acid	mg/L
Bo	Influent concentration of butyric acid	mg/L
KGB	Butyric acid yield coefficient	mg/mg
KBTA	Butyric acid utilizing acetogen yield coefficient	mg/mg
RFBTA	Hydrogen regulation function (butyric to acetic step)	
BR	Unregulated growth rate of butyric acid utilizing acetogens	mg/L.d
BMAX	Maximum specific unregulated growth rate of butyric acid utilizing acetogens	1/day
KSB	Butyric acid utilizing acetogen saturation constant	mg/L
BA	Reactor concentration of butyric acid utilizing acetogens	mg/L
A	Effluent concentration of acetic acid	mg/L
Ao	Influent concentration of acetic acid	mg/L
KGA	acetic acid yield coefficient (soluble organics to acetic step)	mg/mg
KPA	acetic acid yield coefficient (propionic to acetic step)	mg/mg



TABLE IV-2: FOUR POPULATION MODEL NOMENCLATURE (Continued)

SYMBOL	DESCRIPTION	UNITS
KBA	acetic acid yield coefficient (butyric to acetic step)	mg/mg
KAM	Aceticlastic methanogen yield coefficient	mg/mg
MR	Aceticlastic methanogen growth rate	mg/L.d
MMAX	Aceticlastic methanogen maximum specific growth rate	1/day
KSM	Aceticlastic methanogen saturation constant	mg/L
AMF	Reactor concentration of aceticlastic methanogens	mg/L
KH2	Henry's law constant for hydrogen	mmole/atm.L
KHPA	Hydrogen yield coefficient (propionic to acetic step)	mmole/mg
KHBA	Hydrogen yield coefficient (butyric to acetic step)	mmole/mg
KHP	Hydrogen yield coefficient (soluble organics to propionic step)	mmole/mg
KHB	Hydrogen yield coefficient (soluble organics to butyric step)	mmole/mg
KHA	Hydrogen yield coefficient (soluble organics to acetic step)	mmole/mg
KHCM	Hydrogen utilizing methanogen yield coefficient	mg/mmole
MHR	Hydrogen utilizing methanogen growth rate	mg/L.d
MHMAX	Maximum specific growth rate of hydrogen utilizing methanogens	1/day
HMF	Reactor concentration of hydrogen utilizing methanogens	mg/L
KSH	Hydrogen utilizing methanogen saturation constant	mg/L
PT	Total gas phase pressure	atm

TABLE IV-2: FOUR POPULATION MODEL NOMENCLATURE (Continued)

SYMBOL	DESCRIPTION	UNITS
QM	Total molar gas flowrate ( $\text{CH}_4 + \text{CO}_2$ )	mmole/L.d
KCH4A	Methane yield coefficient (aceticiastic methane production)	mmole/mg
KCH4H	Methane yield coefficient (methane production from hydrogen)	mmole/mg
PCO2	Carbon dioxide partial pressure	atm
KHCO2	Henry's law constant for carbon dioxide	mmole/L.atm
$\text{H}^+$	Effluent hydrogen ion concentration	mmole/L
$\text{CO}_2\text{d}$	Effluent dissolved carbon dioxide concentration	mmole/L
$\text{CO}_2\text{do}$	Influent dissolved carbon dioxide concentration	mmole/L
$\text{HCO}_3^-$	Effluent bicarbonate concentration	mmole/L
$\text{HCO}_3^-_o$	Influent concentration of bicarbonate	mmole/L
KH2CO3	Bicarbonate equilibrium constant	
TVA	Effluent total molar volatile acid concentration	mmole/L
Z	Effluent net cation concentration	mmole/L
$Z_o$	Influent net cation concentration	mmole/L
Fc	Addition rate of strong base for pH control	L/d
ZB	Concentration of strong base for pH control	mmole/L
$\text{QMCO}_2$	molar gas flow rate of $\text{CO}_2$	mmole/d
KCO2GA	$\text{CO}_2$ yield coefficient (soluble organics to acetic step)	mmole/mg
KCO2GB	$\text{CO}_2$ yield coefficient (soluble organics to butyric step)	mmole/mg
KCO2A	$\text{CO}_2$ yield coefficient (acetic to methane step)	mmole/mg

TABLE IV-2: FOUR POPULATION MODEL NOMENCLATURE (Continued)

SYMBOL	DESCRIPTION	UNITS
KCO <sub>2</sub> H	Hydrogen utilizing methanogen yield coefficient	mg/mmole
I	Effluent concentration of soluble non-biodegradable material	mg/L
I <sub>0</sub>	Influent concentration of soluble non-biodegradable material	mg/L
QC <sub>02</sub>	Volumetric production rate of CO <sub>2</sub>	L/d
QCH <sub>4</sub>	Volumetric production rate of CH <sub>4</sub>	L/d



# **Library, Canada Centre for Inland Waters**

**867 Lakeshore Road  
Burlington, Ontario  
L7R 4A6**

**Tel: (905) 336-4982**

**Fax: (905) 336-4428**